SEX-DETERMINATION AND WNT PATHWAYS REGULATE DEVELOPMENTAL MUSCLE REMODELING IN *C. elegans*

A Dissertation

by

XIN CHEN

Submitted to the Office of Graduate and Professional Studies of
Texas A&M University
in partial fulfillment of the requirements for the degree of

DOCTOR OF PHILOSOPHY

Chair of Committee,	L. Rene Garcia
Committee Members,	Paul Hardin
	Wayne Versaw
	Vlad Panin
Head of Department,	Tom McKnight

December 2016

Major Subject: Biology

ABSTRACT

In response to altered physiological demands, cardiac muscles remodel their muscle mass and contractile properties to sustain muscle performance. However, dramatic alterations of the sarcomere structure are rarely observed in mammalian models. I studied the *C. elegans* anal depressor development in males and hermaphrodites, to address how a differentiated muscle cell sex-specifically remodels to achieve sarcomere rearrangement and functional alterations. In both larval males and hermaphrodites, the anal depressor muscle possesses a dorsal-ventrally oriented sarcomere. The contraction of the muscle cell facilitates defecation behavior. However in adult males, the anal depressor reorganizes its sarcomere and becomes a copulation muscle. To identify the cytoskeletal alteration events, as well as the sex-determination mechanism that contribute to the sarcomere rearrangement, I used YFP:actin to monitor, and mutant analysis, laser-ablation and transgenic feminization to perturb the cell's morphological dynamics. In young larva, the muscle of both sexes has similar sarcomere morphology. However later in L4, the male extrinsic sex mechanism promotes formation of a ventral slit, demarcating the sarcomere into anterior and posterior half. The male intrinsic sex determination mechanism then promotes the disassembly of sarcomere. Finally, the anterior domain establishes a novel ventral attachment to the sex muscles, and reassembles an anterior-posteriorly oriented sarcomere.

To identify the signaling pathways that are sex-differentially activated to promote sarcomere disassembly, I first examined a series of Wnt-canonical mutants. *egl-*

20, *lin-44*, *lin-17* and *bar-1* mutants possess sarcomere disassembly defects. However, the incomplete penetrance of the Wnt mutants suggests the involvement of parallel mechanisms. Through forward genetics, I isolated a nonsense mutation in *egl-8*/phospholipase C-β, which potentially perturbs the calcium signaling in the anal depressor. Mutant analysis of *goa-1*/G_{α}, *itr-1*/IP_3R, and *unc-68*/RyR suggests the positive role of Wnt-calcium pathway in regulating the sarcomere disassembly process. By monitoring the calcium dynamics in the anal depressor, I found that the calcium signaling is active during L4 development, to activate a group of proteases (*clp-6*/Calpain) and phosphatase (*tax-6*/Calcineurin). Monitoring BAR-1 activity in the anal depressor suggests an active role of β-catenin signaling during early development. Therefore, Wnt-β-catenin and Wnt-calcium pathway function during different development stages to regulate anal depressor remodeling.

ACKNOWLEDGEMENTS

I would like to thank my advisor Dr. Rene Garcia. His support and guidance helped me to resolve the tough problems that I met in my project. He also helped me to develop the ability to think logically and creatively. His enthusiasm towards science and his capability to deal with the difficulties set a good example for me to follow in my future career life.

I would also like to thank my committee members: Dr. Paul Hardin, Dr. Wayne Versaw, and Dr. Vlad Panin have offered me valuable suggestions about my research. My lab mates have given me a lot of help on my research: I would like to thank Dr. Liusuo Zhang, Dr. Brigitte LeBoeuf, Dr. Changhon Jee, Dr. Paola Correa, Dr. Xiaoyan Guo, Jimmy Goncalves, Yufeng Wan, and Dr. Daisy Gualberto for sharing their research experience and ideas with me.

I would like to thank my friends Shian Liu, Yi Sun, Tianxin Liu, Xiangyu Shi, and Yi Xue. Time spent with my friends has made the life of a graduate student to be more joyful. Special thanks go to Guoqiang Yin, Xinying Zhou, Xin Li, Tao Han, Robbi and Pam for their help and encouragement.

Finally, I would like to thank my parents for their love and support. Although we are in different countries, my parents have paid a lot of attention on my life in the States. They feel very happy about the progress that I made in my research. Their encouragement has motivated me to go through the tough times and do better research.

CONTRIBUTORS AND FUNDING SOURCES

Contributors

This work was supervised by a dissertation committee consisting of Professor Rene Garcia (advisor) of the Department of Biology, Professor Paul Hardin of the Department of Biology, Professor Wayne Versaw of the Department of Biology, and Professor Vlad Panin of the Department of Biochemistry and Biophysics.

All work for the dissertation was completed by the student, under the advisement of Rene Garcia of the Department of Biology.

Funding Sources

This work was made possible by funding from Howard Hughes Medical Institute.

NOMENCLATURE

BAR-1	*C. elegans* homologue of β-catenin
CFP	cyan fluorescent protein
CLP-6	*C. elegans* homologue of calpain
CNB-1	*C. elegans* homologue of calcineurin B
EGL-8	*C. elegans* homologue of phospholipase C-β
EGL-19	*C. elegans* homologue of voltage-gated calcium channel
EGL-20	*C. elegans* homologue of Wnt ligand
EXP-1	*C. elegans* homologue of excitatory GABA receptor
GOA-1	*C. elegans* homologue of G_{α}
lf	loss of function
LIN-17	*C. elegans* homologue of Frizzled
LIN-44	*C. elegans* homologue of Wnt ligand
MAB-5	homeodomain transcription factor
RyR	ryanodine receptor
TAX-6	*C. elegans* homologue of calcineurin A
UNC-68	*C. elegans* homologue of ryanodine receptor
YFP	yellow fluorescent protein

TABLE OF CONTENTS

Page

ABSTRACT ii

ACKNOWLEDGEMENTS iv

CONTRIBUTORS AND FUNDING SOURCES v

NOMENCLATURE vi

TABLE OF CONTENTS vii

LIST OF FIGURES x

LIST OF TABLES xiv

CHAPTER I INTRODUCTION 1

- Capability of a fully-differentiated muscle cell to regenerate 1
- Heart regeneration 2
- Mammalian cardiogenesis 4
- Wnt signaling regulates cardiogenesis in mammalian cells 6
- The biphasic role of Wnt signaling in cardiogenesis 7
- The interaction between BMP signaling and Wnt signaling in regulating cardiogenesis 8
- Wnt signaling in regulating *isl1*$^{+}$ progenitor renewal and differentiation 9
- Wnt-Ca^{2+} pathway: ligands efficiency and crosstalk with other Wnt pathways 11
- Ca^{2+} homestasis in vertebrate skeletal muscle 13
- Wnt signaling in *C. elegans* 14
- Sex determination and sexual dimorphism 17
- Dissertation objectives: 21

CHAPTER II EXPERIMENTAL PROCEDURES 24

- Strains 24
- Plasmids construction 25
- Generate transgenic mutant lines 38

Page

Imaging 39
Measurement of the dorsal width of the anal depressor attachment 40
3D reconstruction 40
Measurement of the area of the anal depressor posterior domain ... 41
SNP mapping 41
RNAi assay 42
Calcium imaging 42
Monitoring BAR-1 levels in the anal depressor 43
Mating potency assay 43
Arecoline drug test 44
Assessment of mating behaviors 44
Laser ablation 44
Determining the defecation efficiency 46

CHAPTER III THE SEXUALLY DIMORPHIC DEVELOPMENT OF THE ANAL DEPRESSOR IS CONTROLLED BY CELL-AUTONOMOUS AND NON-AUTONOMOUS SEX DETERMINATION MECHANISMS 47

The male anal depressor is distinct from the hermaphrodite anal depressor early from after L1 stage. 47
The majority of the male remodeling events are controlled cell-autonomously by the male sex determination mechanism. 55
Feminizing the anal depressor compromises male mating behavior. 59
Overexpressing FEM-3 in the larval hermaphrodite anal depressor induces male-like growth dynamics. 63
The anterior movement of the male anal depressor requires the developing male sex muscle cells. 66
A masculinized M lineage is sufficient to induce anterior movement in the hermaphrodite anal depressor. 76
The male endogenous pathway and exogenous signaling function additively to regulate the anterior movement process 78
Defecation behavior does not require the male anal depressor during the L4 stage. 79
Chapter III summary 84

CHAPTER IV WNT SIGNALING REGULATES DEVELOPMENT OF THE MALE ANAL DEPRESSOR 86

The sarcomere disassembly during L4 larval stage is controlled by the Wnt signaling pathway 86

Page

Determining the site of action of Wnt-canonical pathway 96
Mutagenesis to identify parallel pathways that co-regulate anal depressor development 101
Determine the site of action of Wnt-calcium pathway 109
Ca^{2+} responsive proteins promote sarcomere disassembly 111
Behavior calcium regulates sarcomere disassembly 114
Determine the relationship between the Wnt-β-catenin pathway and Wnt-calcium pathway 116
Determine what Wnts are involved in regulating β-catenin and calcium pathway 122
The role of Wnt-PCP pathway in regulating anal depressor development 125
Chapter IV summary 127

CHAPTER V THE SYMMETRICAL DEVELOPMENT OF THE ANAL DEPRESSOR REQUIRES WNT SIGNALING IN BOTH THE MALE AND THE HERMAPHRODITE 128

The symmetrical development of anal depressor is maintained through Wnt signaling 128
LIN-44 is the Wnt ligand to maintain the symmetry of the anal depressor 133
Chapter V summary 133

CHAPTER VI SUMMARY OF EXPERIMENTS AND DISCUSSION 134

Summary of experimental results 134
Discussion 135
Future Experiments 143

REFERENCES 148

APPENDIX A 163

Supplementary Tables 163

LIST OF FIGURES

Page

Figure 1. Morphological changes of the hermaphrodite anal depressor. 49

Figure 2. Growth dynamics of the hermaphrodite anal depressor.. 50

Figure 3. Morphological changes of the male anal depressor. 52

Figure 4. Growth dynamics of the male anal depressor. 53

Figure 5. Feminizing the male anal depressor. 57

Figure 6. Quantification of the dorsal width of feminized anal depressor. 58

Figure 7. Feminization of the anal depressor causes multiple mating defects. 60

Figure 8. Masculinizing the hermaphrodite anal depressor. 63

Figure 9. Masculinization repressed the dorsal expansion of the hermaphrodite anal depressor. 65

Figure 10. The spicule cells and proctodeum cells do not regulate the anterior movement of the anal depressor. 67

Figure 11. Compromising the male sex muscle activity affects the L4 development of the anal depressor. 69

Figure 12. The anal depressor has anterior migration defects and sarcomere disassembly defects when the sex muscle morphogenesis is compromised. 70

Figure 13. *mab-5* does not confer defects to the dorsal growth of the male anal depressor during early larval development. 71

Figure 14. Cell-autonomous expression of *mab-5* did not rescue the anal depressor defects of *mab-5* mutants. 74

Figure 15. Masculinization of the hermaphrodite sex muscles is able to induce slit formation in the anal depressor. 77

Page

Figure 16. The male sex determination pathway and exogenous signals from the male sex muscles function additively to regulate the male anal depressor's anterior movement. 79

Figure 17. The male anal depressor retracts the muscle arm from the pre-anal ganglion at the L3 larval stage. 80

Figure 18. Defecation does not rely on the reorganizing anal depressor during L4 development. 82

Figure 19. The male anal depressor reorganizes the sarcomere during L4 development. 87

Figure 20. Wnt mutants possess anal depressor sarcomere disassembly defects..... 89

Figure 21. Quantification and classification of the anal depressor defects of Wnt mutants. 91

Figure 22. Frizzled mutants possess anal depressor disassembly defects. 93

Figure 23. β-catenin mutants have anal depressor disassembly defects. 95

Figure 24. Expression profile of Wnt and Frizzled during different developmental stages. 97

Figure 25. Cell-specific rescue of *egl-20* expression from the anal depressor rescued the sarcomere disassembly defects. 99

Figure 26. *bar-1* is expressed from the anal depressor during larval development. . 100

Figure 27. *rg441* mutant males possess anal depressor sarcomere disassembly defects. 102

Figure 28. Diagram of EGL-8 isoforms and location of *rg441*. 104

Figure 29. The anal depressor defects in *rg441* males were rescued using *egl-8* genomic DNA. 105

Figure 30. *goa-1* mutants possess anal depressor sarcomere disassembly defects. .. 106

Page

Figure 31. Quantification and classification of the anal depressor defects of *itr-1* and *unc-68* mutants. 108

Figure 32. *egl-8* expression pattern in the male tail. 109

Figure 33. Calcium dynamics in the anal depressor during midL4-L4 molt transition time. 111

Figure 34. Ca^{2+} responsive proteins regulate sarcomere disassembly in the anal depressor. 112

Figure 35. Quantification and classification of the anal depressor defects of *egl-19* and *exp-1* mutants. 115

Figure 36. BAR-1 signaling in the anal depressor at different larval stages. 117

Figure 37. Heat-shock induced BAR-1 signaling disrupt the remodeling of the male anal depressor. 119

Figure 38. Quantification and classification of the anal depressor defects of *lit-1* RNAi mutants. 121

Figure 39. *egl-20(lf)* mutant males have decreased level of BAR-1 signaling in the anal depressor. 123

Figure 40. Calcium dynamics in the anal depressor during midL4-L4 molt transition time in *egl-20(n585)* mutant males. 124

Figure 41. Attempts of using heat-shock-induced *egl-20* expression to rescue the anal depressor defects in *egl-20(lf)* mutant males. 125

Figure 42. Quantification and classification of the anal depressor defects of *lin-18* and *rho-1* RNAi mutants. 126

Figure 43. The *lin-17(lf)* mutants have asymmetrical anal depressor development. 129

Figure 44. Quantification of asymmetrical developmental defects of *lin-17(lf)* mutants. 131

Page

Figure 45. Growth dynamics of expanded left attachment in *lin-17(lf)* hermaphrodites and males. 132

Figure 46. Model of Wnt signaling pathways regulating different remodeling events in the male anal depressor. 136

LIST OF TABLES

Page

Table 1. Percentages of animals that have muscle arm extended into the pre-anal ganglion. 81

Table 2. Mutation in *egl-8* contributes to the anal depressor defects. 104

CHAPTER I

INTRODUCTION*

Capability of a fully-differentiated muscle cell to regenerate

Diseases-induced heart injury requires the cardiac muscles to regenerate to compensate for the loss of muscle fibers. However, the regeneration capability is limited to certain cardiac systems, like zebrafish cardiac muscles. To activate the regeneration potential of a human heart, illuminating the muscle remodeling mechanisms utilized in those model systems is both necessary and required.

The cardiac muscles can adopt different muscle remodeling mechanisms to respond to diseases-induced heart injury. They can become hypertrophied to expand the size of the sarcomere. They can also generate novel cardiomyocytes from either the progenitor cells, or from the pre-existing cardiomyocytes. The remodeled muscle cells undergo cellular processes that are also involved in cardiogenesis. Therefore studying cardiogenesis pathways helps to develop and improve heart regeneration therapies.

Wnt signaling has been shown to regulate different aspects of cardiogenesis in the vertebrate system. Therefore it might also play a role in regulating cardiac muscle regeneration. Due to the conservation of the Wnt signaling pathway, the easily-manipulated body structure and the well-controlled muscle remodeling process in

---

*Portions of this chapter are reprinted from Chen, X. and Rene Garcia, L. (2015) Developmental alterations of the *C. elegans* male anal depressor morphology and function require sex-specific cell autonomous and cell non-autonomous interactions. Developmental Biology 398, 24-43.

worms, we used *C. elegans* to study muscle regeneration. The sexually dimorphic development of the *C. elegans* muscle cells indicates that the sex determination mechanisms act upstream of the muscle remodeling pathway to regulate muscle remodeling. Therefore, the muscle remodeling events occurring in *C. elegans* are under tight control, which sheds lights on how to develop more reliable therapy for heart regeneration.

Heart regeneration

In rat and zebrafish, cardiac muscles can regenerate to compensate for the loss of the muscle fibers. Heart regeneration can occur by either the proliferation of the myocardial progenitors, or the proliferation of the fully-differentiated cardiomyocytes. The latter has been shown to be intriguing, because it might involve the process of cell dedifferentiation.

Recent studies found that cardiomyocytes in adult heart can proliferate to repair heart injury. Neuregulin1 (NRG1) is the agonist for the RTK of the EGF receptor family (Erb4). In mice, NRG1/Erb4 signaling was found to be vital for cardiomyocyte generation (Gassmann et al., 1995; Lee et al., 1995). Differentiated rat cardiomyocytes can proliferate and generate novel muscle fibers under induction conditions. Conditional knockout of ErbB4 in the differentiated cardiomyocytes abolished their ability to proliferate during postnatal development. And overexpression of ErbB4 in the differentiated cardiomyocytes also increase the proliferate potential of those cells (Bersell et al., 2009). NRG1 stimulates the differentiated cardiomyocytes to reenter cell

cycle, generate new cardiomyocytes to compensate for the loss of muscle fibers after myocardial infarction.

Other studies suggest that dedifferentiation occurs before the cardiomyocytes can proliferate (Jopling et al., 2010). After amputation, the differentiated zebrafish cardiomyocytes reenter cell cycle and undergo DNA duplication. Those cardiomyocytes do not show regression within the cardiac lineage, since no earlier marker expression was detected in those proliferating cells. However, they did show levels of dedifferentiation. Those cardiomyocytes detach from each other, the sarcomeric filaments are disorganized and the transverse and longitudinal sarcomeric structures were absent. Inhibition of plk1, which is a regulator of cell cycle progression, leads to reduced heart regeneration after amputation.

During zebrafish heart regeneration, the cardiomyocytes did not upregulate the expression levels of the early cardiac markers, like Nkx2.5 and Tbx5. Expression of those genes are observed during early embryonic heart development. However, msxB and msxC, plus notch1b and deltaC are found to increase their expression levels dramatically in the regenerating myocardium (Raya et al., 2003). Those genes are not expressed during embryonic heart development. This indicates that heart regeneration in zebrafish may adopt a genetic program that is completely different from heart development.

Cardiac progenitors also contribute to heart regeneration in zebrafish (Lepilina et al., 2006). After amputation, undifferentiated cardiomyocytes start to appear at the apical edge of regeneration region. Those cardiomyocytes are not derived from the pre-existing

cardiomyocytes, since no dedifferentiation process was detected. Therefore, those newly differentiated cardiomyocytes are derived from the progenitor cells. The cardiac markers of the embryonic cardiogenesis are also detected around the apical edge of the regenerative tissue during the heart regeneration process. The heart epidermis generate an epithelial layer that envelopes the wound after heart injury. This epithelial layer also invades into the myocardium to generate the vasculature structure that promotes regeneration. To investigate the importance of heart epidermis in heart regeneration, they inhibited Fgf signaling, which is essential for the invasive and enveloping activity of the epidermis. They found that the inhibition of the Fgf signaling compromised the regeneration capability of the heart, indicating the importance of epidermis in heart regeneration.

Although the remodeling mechanisms are diversified, they all involve some common cellular processes: sarcomere disassembly, production of new sarcomeric proteins, and synthesis of a new sarcomere. Those cellular events also occur during the process of heart formation. Therefore, illuminating the signaling network that controls cardiogenesis also benefits heart regeneration research.

Mammalian cardiogenesis

The generation of a mammalian heart involves specification of the precardiac mesoderm, formation of the heart tube and generation of heart chambers. The initiation of heart marker genes expression marks different developmental stages of cardiogenesis, and also serves as the impetus to drive the heart formation process. During gastrulation, cells derived from the primitive streak give rise to the precardiac mesoderm (Garcia-

Martinez and Schoenwolf, 1993; Tam et al., 1997). Those cardiac progenitors undergo cell migration, turn on early myocardial markers, and form the epithelium of cardiac crescent (Tam et al., 1997). The cardiac crescent then fuses at the midline to form the early heart tube. The tube then undergoes the looping process and expands the myocardium. The heart is finally shaped by the formation of cardiac chambers.

MESP1 (mesoderm posterior 1) and MESP2 (mesoderm posterior 2) are the two earliest cardiac markers for the cardiac progenitors, which are detected from the cardiac crescent. BMPs and FGFs then activate downstream myocardial regulators, such as *NKX2-5*(NK2 transcription factor related, locus 5) and *GATA4*(GATA-binding protein 4) (Brand, 2003). WNT signaling has been shown to exert a repressive effect (Brand, 2003).

NKX2-5 then activates *Hand1* (heart and neural crest derivatives expressed transcript 1), which marks the left ventricle (Yamagishi et al., 2001). TBX5 also promotes *Hand1* expression and represses *Hand2* expression, therefore promoting left-ventricle specification and repressing the fate specification of other regions (Takeuchi et al., 2003; Waldo et al., 2001). The right ventricle was specified by *Hand2* expression (Srivastava et al., 1995; Srivastava et al., 1997). TBX1 upregulates Fgf signaling (Fgf8 and Fgf10) in the second heart field, which is essential for cell proliferation (Waldo et al., 2001). ISL1 promotes cell migration, cell proliferation and cell maintenance in the second heart field (Cai et al., 2003).

Wnt signaling regulates cardiogenesis in mammalian cells

Among the signaling pathways that regulate heart formation, Wnt signaling has been shown to regulate different aspects of cardiogenesis. The role of the Wnt pathway differs depending on the context of the signaling events. During early heart induction process, Wnt signaling exerts repressive effect on the formation of the precardiac mesoderm.

In *Xenopus*, the cardiogenic mesoderm is derived from the dorsoanterior mesoderm. The Spemann organizer and the dorsoanterior endoderm function as the signaling center for heart induction in the dorsoanterior mesoderm (Schultheiss et al., 1995). In chick embryos, the anterior endoderm can differentiate into heart muscles, whereas posterior endoderm differentiates into blood and vessels. Expression of *crescent* from the anterior endoderm helps to antagonize Wnt8c and Wnt3a derived from the posterior tissues, and promote heart tissue formation (Marvin et al., 2001).

Wnt antagonists were also shown to have heart induction effects on noncardiogenic tissues. The noncardiogenic ventral marginal zone (VMZ) explants, which is derived from the *Xenopus* embryos, was induced to beating hearts by exposure to the Spemann organizer and dorsoanterior endoderm (Schneider and Mercola, 2001). Injecting Wnt antagonists *dkk-1* or *crescent* mRNA into the VMZ explants was able to induce early heart markers, such as Nkx2.5 and Tbx5, as well as cardiomyocyte-specific contractile proteins like TnIc and MHCα. Similarly, the posterior lateral plate mesoderm (PLP) explants starts to express several cardiac genes, including Nkx-2.5, vMHC, aMHC, and GATA-4 when it was infected with RCAS viruses encoding *crescent*

(Marvin et al., 2001). On the other hand, Wnt dramatically reduced the Nkx-2.5 expression level if it is ectopically expressed in the chick embryo fibroblasts. This suggests that the expression of Wnts inhibits the cardiac markers expression and differentiation into muscles.

However, other studies revealed a positive role of Wnt signaling in regulating heart muscle formation. Wnt11 is the only *Xenopus* Wnt gene whose expression pattern shows correlation with cardiac specification. Knocking down Wnt11 expression conferred defects to heart development. And ectopic expression of Wnt11 in the embryonic explants induces the formation of cardiac structures. The heart induction activity of Wnt11 is not mediated by β-catenin, but through protein kinase C and JNK (Pandur et al., 2002). Therefore non-canonical Wnt pathway functions to promote cardiogenesis.

The role of canonical Wnt pathway in heart muscle formation was also tested in mouse embryos (Lickert et al., 2002). Conditional deletion of β-catenin in the endoderm of the mouse embryo leads to the cell fate change of the posterior endodermal cells. Instead of giving rise to cells of the hindgut, the presumptive endodermal cells give rise to ectopic precardic mesoderm and eventually generate cardiac structures in the posterior embryo. Therefore, unlike non-canonical pathway, the Wnt-canonical pathway negatively regulates cardiogenesis.

The biphasic role of Wnt signaling in cardiogenesis

Studies using zebrafish and mouse ES cells show that Wnt signaling plays biphasic role in regulating cardiogenesis (Naito et al., 2006; Ueno et al., 2007). During

zebrafish embryonic development, Wnt signaling represses anterior lateral mesodermal fates and promotes posterior lateral mesodermal fate. Activation of the Wnt pathway by heat shock induced Wnt8 had different effects on cardiac development, depending on the time when the signaling was induced. Heat shock before gastrulation promotes heart marker expression, but heat shock after gastrulation represses heart marker expression (Ueno et al., 2007).

Heart induction experiments done in the mouse ES cells generated similar results: Treatment of Wnt3A during early development promotes cardiogenesis, whereas treatment during late development stage represses cardiogenesis (Naito et al., 2006; Ueno et al., 2007).

Study of the transcriptional activity of Wnt3A target genes shows that Wnt-signaling also induces a negative-feedback loop besides heart inducing activity. Wnt antagonist Dkk-1 and Wnt11 transcripts are increased after Wnt3A treatment (Ueno et al., 2007). It supports the conclusion that Wnt signaling plays a biphasic role in heart inducing activity. Therefore the system generates this negative-feedback mechanism to allow later cardiogenesis events to occur.

The interaction between BMP signaling and Wnt signaling in regulating cardiogenesis

BMP signaling has been shown to promote cardiogenesis in many model systems (Frasch, 1995; Monzen et al., 1999; Schultheiss et al., 1997; Zhang and Bradley, 1996). BMP inhibitor treatment at late ES cell differentiation stage causes decreased expression level of heart markers (Naito et al., 2006). Ectopic Wnt signaling induced at this stage

reduced BMP expression level, whereas addition of BMP4 restored the Wnt3A-inhibited heart induction activity. Therefore, Wnt-β-catenin signaling represses late-stage cardiac development by antagonizing BMP activity.

Wnt signaling in regulating *isl1*$^+$ progenitor renewal and differentiation

The Wnt pathway also regulates the maintenance of the pluripotency as well as proliferation capabilities of the cardiovascular progenitor cells. The Multipotent *isl1*$^+$ cardiovascular progenitors (MICPs) can generate three major cell types in the heart: cardiac, smooth muscle and endothelial cells (Moretti et al., 2006). *In vivo* studies indicate the *isl1*$^+$ cardiovascular progenitors contribute to over two thirds cells of embryonic heart, and to all three major cell types in almost all the cardiovascular compartments (Cai et al., 2003; Laugwitz et al., 2005).

Cardiac mesenchymal cells (CMC) provide the microenviroment to maintain multipotency and to promote renewal of the *isl*$^+$ cardiovascular progenitors. Studies show that Wnt-β-catenin signaling derived from the CMCs promote *isl*$^+$ cells proliferation, but inhibits their prespecification and differentiation (Qyang et al., 2007). *In vitro* studies show that Wnt-3a, which is a well-established ligand for the Wnt-β-catenin pathway (Logan and Nusse, 2004), inhibits the prespecification of MICPs from embryoid bodies. But it promotes MICPs proliferation after cell fate specification. The role of the Wnt-β-catenin pathway is also supported by *in vivo* studies: Introducing constitutively active β-catenin into the *isl*$^+$ cells causes the expansion of the second heart field; ectopic activation of Wnt-β-catenin signaling in the anterior heart field (AHF) also blocks the differentiation of *isl*$^+$ cells in the outflow tract (OFT); conditional knockout β-

catenin in the AHF reduces the proliferation rate of the *isl*$^{+}$ progenitors in the OFT (Qyang et al., 2007); and conditional deletion of β-catenin in the *isl*$^{+}$ progenitors results in decreased expression level of *isl1*, reduced proliferation rate of *isl*$^{+}$ cells and increased level of apoptosis (Lin et al., 2007).

β-catenin was also found to be stabilized in all heart chambers and in the outflow tract derived from the SHF during later embryonic stage. Deletion of β-catenin in the SHF progenitors before cardiac differentiation resulted in the loss of right ventricle (Ai et al., 2007; Kwon et al., 2007). The initial commitment markers (Isl) and migration markers (Fgf10) are not affected by conditional deletion of β-catenin. However, stabilization of β-catenin in the SHF progenitors leads to enlarged right ventricle segment, expanded SHF progenitor pool and increased number of mitotic cells (Ai et al., 2007). *In vivo* studies, using a conditional allele of β-catenin that was inactivated in the SHF progenitors after cardiac differentiation, show reduction in ventricular size, and ventricular wall thickness. This was resulted from reduction in proliferation activity of the progenitors and decreased level of differentiation (indicated by decreased level of expression of cardiogenesis markers, BMP4, hand2, Mef2c, etc).

Therefore, heart formation in the vertebrate system requires the participation of the Wnt canonical pathway, as well as the Wnt non-canonical pathway. The diversified roles that the Wnt signaling pathways play during cardiogenesis can be attributed to the altered signaling context. They can also be attributed to the distinct effectors activated by different Wnt pathways. The complexity of the signaling components as well as the

interaction between different Wnt pathways confers Wnt signaling the capability to regulate complicated biological processes.

Wnt-Ca^{2+} pathway: ligands efficiency and crosstalk with other Wnt pathways

In model systems like *Xenopus* and zebrafish, the Wnt ligands preferentially activate one Wnt pathway rather than others. The antagonistic effects of those Wnt ligands indicate that the signaling pathways that they activate are mutually inhibitive. Identifying the signaling components that mediate the crosstalk helps to illuminate the interactions between different Wnt pathways.

Overexpression of Wnt ligands had different effects on the development of *Xenopus* embryos. And some Wnts have been found to mutually inhibit the activity of each other. Overexpression of XWnt-8 induces ectopic dorsal mesoderm in *Xenopus* embryos (Christian et al., 1992). This effect can be mimicked by inhibiting the PI cycle using Li^+ (Cooke et al., 1989; Slack et al., 1988). Li^+ functions as a PI cycle inhibitor (Busa and Gimlich, 1989), however, it has also been found to inhibit GSK-3 activity (Klein and Melton, 1996). This indicates XWnt-8 activity may function to activate the canonical beta-catenin pathway, and to inhibit PI cycle. On the other hand, overexpression of XWnt-5A perturbs convergent extension movement, and downregulates the induction of *goosecoid* expression by XWnt-8. XWnt-5A may function to activate PI cycle activity, since overstimulation of PI cycle using serotonin type 1c receptor would have the same effects as XWnt-5A on blastula-stage embryos (Ault et al., 1996). To verify that XWnt-5A suppresses the XWnt-8-induced *goosecoid* expression through upregulating Ca^{2+} levels, XWnt-5A was injected into zebrafish

embryos and Ca^{2+} dynamics in the enveloping layer of the early blastula was monitored. Compared to the control injection, XWnt-5A induced higher Ca^{2+} frequency (Slusarski et al., 1997b), confirming the role of PI cycle and Ca^{2+} influx downstream of XWnt-5A to suppress the activity of XWnt-8.

How does XWnt-5A initiate Ca^{2+} transients? Some Frizzled receptors have been reported to have a seven transmembrane topology that is similar to the G-protein coupled receptors (GPCR) (Chan et al., 1992; Wang et al., 1996); therefore, Frizzled may function as a GPCR to activate G-protein mediated signaling and activate Ca^{2+} influx. Rat frizzled-2 (Rfz-2) and XWnt-5A has been found to induce Ca^{2+} release when ectopically expressed in the zebrafish embryo (Slusarski et al., 1997a). PTX, which is the $G_{o/i}$ inhibitor, was able to block the Ca^{2+} increase induced by Rfz-2. Inhibiting the activity of $G_{\beta\gamma}$ units using α-transducin also blocked Rfz-2-induced Ca^{2+} increase. This proves that Rfz-2 induces the Ca^{2+} change in the zebrafish embryo through activating the $G_{o/i}$ - $G_{\beta\gamma}$ - phosphatidylinositol pathway.

Different Wnt ligands have differential ability to translocate PKC to the cell membrane. XWntXWnt-5A, Rfz2, Mfz3, Mfz4 or Mfz6 were able to induce the activation of PKC much more efficiently compared to XWntXWnt-8, Rfz1, Mfz7 or Mfz8 (Sheldahl et al., 1999). The activation of PKC requires the activation of $G_{q\alpha}$ and $G_{\beta\gamma}$, since using PTX (G_{α} inhibitor) or expressing $G_{o/i}$ (inhibits $G_{\beta\gamma}$ activity) would block the activation of PKC.

PKC also plays important roles in cross-talk between different Wnt pathways. Wingless has been shown to inactivate GSK-3β (Cook et al., 1996). The inhibition of

GSK-3β activity by Wg is not suppressed by inhibition of PI3 kinase or p42/p44 MAP kinase cascade. However, the PKC inhibitor Ro31-8220 was able to block the inhibition of GSK-3 activity. It indicates that Wg signals through PKC to phosphorylate GSK-3 and therefore inhibits its activity.

Ca^{2+} homestasis in vertebrate skeletal muscle

Besides regulating muscle development via the Wnt-calcium pathway, the role of calcium signaling in regulating muscle physiology is well established. The sarcoplasmic reticulum plays important roles in regulating Ca^{2+} levels in the cytoplasm. In order for skeletal muscle to contract, cytoplasmic Ca^{2+} levels must be rhythmically upregulated and downregulated to facilitate contractile protein interaction. The upregulation of cytoplasmic Ca^{2+} was achieved through a series of events: a stimulation signal, transmission of the signal by altering membrane potential, activation of the voltage-gated Ca^{2+} channels, activation of the RyR on the sarcoplasmic reticulum (SR), and eventually Ca^{2+} efflux from the SR into the cytoplasm. During the relaxation cycle, Ca^{2+} needs to be removed from the cytoplasm, by Ca^{2+} uptake into the SR. The channels that facilitate the processes are mainly the Na+/ Ca^{2+} exchanger (NCX), and the Ca^{2+} ATPase in the SR (SERCA) (Dirksen, 2009).

Mitochondria promotes Ca^{2+} removal activity of the SR (Allen et al., 2008). Within the mammalian skeletal muscles, mitochondria are located close to the Ca^{2+} releasing unit (CRU). CRU consists of T-tubule membrane and sarcoplasmic reticulum terminal cisternae, which contains the RyR responding to Ca^{2+} levels changes and releasing Ca^{2+} from the SR (Melzer et al., 1995). Mitochondria have been found to

sequester Ca^{2+} during Ca^{2+} oscillations in cardiac myocytes, neurons and many other cell types (Duchen, 1999). But because of the low affinity of the Ca^{2+} transporter located on the mitochondria, the role of mitochondria Ca^{2+} uptake during contraction-relaxation cycle may not be significant. Mitochondria may only function as a sensor of the cytoplasmic Ca^{2+} homeostasis.

However, mitochondria may play an indirect role in promoting the Ca^{2+} uptake function of the Ca^{2+} ATPase in the SR. Although ATP is required to promote sarcomere protein contraction, around 80% of the ATP consumed is to facilitate SERCA's reuptake of Ca^{2+} from the cytoplasm (Allen et al., 2008). Therefore malfunction of the mitochondria may lead to failure of the SR to be refilled with Ca^{2+} and block the contraction-relaxation cycle.

Therefore, proper function of the muscle cells requires behavior-activated calcium signaling. The generation of rhythmic calcium influx requires the coordination of different cellular compartments. The involvement of those cellular compartments in regulating developmental calcium signaling is unknown. But the conserved function of ER and mitochondria predicts that the Wnt-calcium pathway utilizes the same system to modulate calcium signaling.

Wnt signaling in *C. elegans*

The Wnt signaling network was shown to be conserved among *C. elegans* and the vertebrates. The worms have the corresponding homologs for different components of the Wnt pathways. The biological output of the Wnt pathways is also conservative. In

C. elegans, Wnt signaling pathways have been found to promote cell fate specification, and regulate cell migration and cell polarity.

Wnt signaling and vulva induction

Wnt signaling has been shown to activate the expression of the hox gene *lin-39* in the six vulva precursor cells (VPCs) (Eisenmann et al., 1998). *lin-39* maintains the competency of the VPCs to respond to the vulva induction signals from the EGF signaling pathway. *lin-39* loss-of-function mutants show loss of VPCs and the P3.p to P8.p fused with the hypodermal syncytium. *lin-39* expression domain was expanded in a *pry-1* mutant (Maloof et al., 1999), indicating that *pry-1* negatively regulates the Wnt pathway. Also *pry-1* mutant has the multi-vulva phenotype, and this phenotype is not suppressed by *let-23*/RTK or *let-60*/Raf loss of function mutations (Gleason et al., 2002). This indicates that Wnt and RTK/Ras pathway may play redundant roles in regulating 1° and 2° vulva fate.

Wnt signaling and cell migration

In the hermaphrodites, the Q neuroblast gives rise to two descendants, QL and QR. The migratory neuroblasts (QL on the left and QR on the right) initially have similar anterior-posterior positions. Each of the neuroblasts gives rise to three neurons and two cells that undergo apoptosis (Sulston and White, 1980). However, the migration direction of the mother cell and their daughters are distinct between the QL and QR lineage. The QL cell and its descendants migrate posteriorly towards the tail. The QR lineage migrates anteriorly, towards the head. The difference in migration is specified by the differential activation of *mab-5* expression in the QL cell. In *mab-5* (lf) mutants, both

QL and QR cells migrate anteriorly (Chalfie et al., 1981; Kenyon, 1986). The activation of *mab-5* in the QL lineage is mediated by a canonical Wnt pathway, which involves BAR-1/β-catenin being relieved from the degradation by the APC destruction complex, and positively regulating the transcriptional activity of POP-1/TCF.

The migration of Q lineage cells are in response to EGL-20/Wnt (Whangbo and Kenyon, 1999). Egl-20 has been shown to activate *mab-5* expression in the QL cell, which is required for either maintain stationary or migrate posteriorly. Altering the expression domain of *egl-20* from tail to head did not switch the migration pattern of QL and QR. Instead, the QL and QR cells displayed doseage-dependent response to EGL-20, in which the lower level of EGL-20 promotes anterior migration, and higher levels of EGL-20 promotes posterior migration.

Different β-catenin proteins have different functions in *C. elegans*

C. elegans has three β-catenin homologs, including *bar-1*, *wrm-1* and *hmp-2*. The three β-catenin proteins have different functions in *C. elegans*. BAR-1 and WRM-1 function downstream of the Wnt signaling. However, only BAR-1 interacts with POP-1/TCF to function in a canonical Wnt pathway (Korswagen et al., 2000). WRM-1 binds to the NLK/TAK complex to inhibit POP-1 transcriptional activity, and therefore functions in a non-canonical pathway (Rocheleau et al., 1999; Shin et al., 1999). HMP-2 is localized to the adherens junctions and interacts with HMR-1/cadherin and HMP-1/α-catenin (Korswagen et al., 2000). Therefore, it functions to consolidate the actin cytoskeleton.

The non-canonical Wnt pathway in *C. elegans*

The EMS cell division is regulated by MOM-2/Wnt pathway. The MOM-2/Wnt pathway promotes E cell fate in one of the daughter cell, the other daughter cell will not be affected by the pathway and becomes MS cell. If any of the pathway components are mutated, the two daughter cells will all become MS cell. However, different from the canonical Wnt pathway discovered from flies and vertebrates, mutating the POP-1/TCF has the opposite effect to mutating WRM-1/β-catenin, indicating WRM-1/β-catenin is inhibiting POP-1/TCF activity (Lin et al., 1998; Lin et al., 1995). Another difference is that SGG-1/GSK3β and APC-related protein APR-1 promotes the WRM-1/β-catenin function (Rocheleau et al., 1997; Schlesinger et al., 1999). The inhibition of POP-1/TCF activity is achieved by the collaboration of MOM-2/Wnt pathway with a parallel MAPK pathway. The MAPK pathway activates MOM-4/TAK1 and LIT-1/NLK, which activate and form complex with WRM-1/β-catenin to phosphorylate POP-1 and inhibit its activity (Rocheleau et al., 1999; Shin et al., 1999). The vertebrate homologs for NLK and TAK may have similar functions, to phosphorylate and inhibit the binding of β-catenin/TCF-4 complex to DNA (Ishitani et al., 1999).

Sex determination and sexual dimorphism

C. elegans serves as a good model system to study muscle remodeling, not only because of the conservation of the Wnt signaling pathway, but also because of the well-controlled muscle remodeling process. In *C. elegans*, some of the muscle cells are developmentally-remodeled in the males. In those cells, muscle remodeling is under the control of specific developmental programs, and therefore rarely proceeds beyond limit.

Among those developmental programs, the sex determination mechanisms act in higher hierarchy to activate the muscle remodeling pathways. This is because the muscle cells are remodeled in a sex-specific manner.

The developmental mechanisms that transform genotypic sex into sexual dimorphic structures vary between species. In some species, the sex determination mechanism induces sex differential hormone signaling, which in turn exert effects on the morphogenesis of sex specific structures. In mammals, the *Sry* gene is expressed from the Y chromosome. The SRY protein induces testis development (Koopman et al., 1991) and the testicular hormones promote the masculinization of the embryo (Can et al., 1998; Eddy et al., 1996; Imbeaud et al., 1996). In other species, a hierarchy of sex determination molecules acts in conjunction with hormone signaling to contribute to the sexual dimorphic development. How the sex determination signal is transformed into cellular events to promote sexually dimorphic development has been studied thoroughly in *C. elegans*. In *C. elegans*, the activities of the sex determination proteins are sex-regulated (de Bono et al., 1995; Hodgkin, 1987; Hodgkin, 1988). The activity level of those proteins triggers sex differential cellular events, which lead to the morphogenesis of sex-specific structures.

C. elegans naturally exists as either a hermaphrodite or a male, which are morphologically and behaviorally different. The sexual dimorphism can arise from cells that are derived from sex-specific cell divisions, migration, differentiation, and apoptosis events. It also arises from sex common cells, which superficially look similar between the two sexes, but display different functional properties (Lee and Portman, 2007;

Mowrey et al., 2014; Reiner and Thomas, 1995; White and Jorgensen, 2012; White et al., 2007).

The initial sex determination signal comes from the sex chromosome/autosome ratio (X:A), with X:A=0.5 determining the male fate, and X:A=1 determining the female fate. Depending on the chromosome/autosome ratio, a cascade of sex determination proteins differentially interacts with each other to regulate the activity of the terminal regulator, TRA-1 (de Bono et al., 1995; Hodgkin, 1987; Hodgkin, 1988). In the hermaphrodites, TRA-1 is active, whereas in the male, the TRA-1 activity is suppressed by the upstream male sex determination pathway proteins. TRA-1 functions as a transcription factor that enters the nucleus to promote hermaphrodite development and repress male development (Hodgkin, 1987; Hunter and Wood, 1990).

TRA-1 mediates sexual dimorphism through the activation or repression of critical regulators for cell metabolism, migration, or proliferation events. One of TRA-1's functions is to differentially activate the programmed apoptosis regulators in the males or the hermaphrodites. For example, the HSN neurons are egg-laying promoting neurons that exist only in the hermaphrodites. They are generated during embryonic development in both sexes, but die in the male (Sulston and Horvitz, 1977; Sulston et al., 1983). The female sex determination mechanism prevents apoptosis in the hermaphrodite HSNs by repressing the cell death activator gene, *egl-1* (Conradt and Horvitz, 1999). In contrast, to trigger the programmed cell death of the male specific CEM neurons in the hermaphrodites, TRA-1 functions to suppress the apoptosis inhibitor CEH-30 (Peden et al., 2007; Schwartz and Horvitz, 2007).

Cell fusion and migration can also be regulated differentially to promote sexually dimorphic development. This occurs in the development of the dimorphic tail. Before the L4 larval stage, both the hermaphrodites and males possess a tapered tail. However, during L4 development, the male tail tip cells fuse and migrate anterior-dorsally (Nguyen et al., 1999). As a result, the adult male tail has a blunt-ended shape. The DM protein, *dmd-3*, functions in the male tail to promote tail tip cell fusion and migration. The female sex determination pathway blocks the process by repressing the DMD-3 activity in the hermaphrodite tail. Transforming the female sex determination pathway into a male one will trigger tail tip retraction in the XX pseudomales (Mason et al., 2008). Therefore, the sex determination pathway plays an essential role in switching the tail remodeling program to be on in males and off in hermaphrodites.

Sexual dimorphic structures are more commonly generated by differential cell specification, followed by division, migration and differentiation. The B, F, U, Y and M cells display male-specific cell lineages, which give rise to the copulatory structures in the male tail. In both sexes, the B cell is born as a single cell in the tail region (Sulston et al., 1980a). During the L1 stage, the male B cell undergoes an asymmetrical cell division (Sulston et al., 1980a) and in later larval stages ultimately produces the spicules, spicule associated neurons, proctodeum and post cloacal sensillia neurons (Sulston et al., 1980a). In the hermaphrodites, the B cell remains as a single cell. The detailed mechanisms that promote the male B cell to enter the cell cycle and undergo differentiation has not been determined. In contrast, the M cell descendants undergo distinct cell divisions and migration in the two sexes, to produce the different

reproductive muscles. In the hermaphrodite, the M. vlpaa and M. vrpaa descendants of the M cell migrate to the vulva region and divide to give rise to the uterine and vulva muscles (Sulston and Horvitz, 1977). Whereas in the male, M.dlpaa, M. dlpap, M. drpaa, M. drpap, in addition to M. vlpaa and M. vrpaa, migrate to the tail region to produce the male-specific sex muscles (Sulston et al., 1980a).

Finally, gender common neurons and muscles can alter their morphology and/or function during the last stage of larval development to produce sexually distinctive cells in the adults. The alterations can be subtle, so that no obvious anatomical difference can be detected. For example, the modulation of the neural and muscular locomotion circuit activity contributes to the difference in locomotion behavior between the males and the hermaphrodites (Mowrey et al., 2014). Similarly, the functional difference in sensory neurons leads to the sexually distinctive olfactory and gustatory preference behaviors (Lee and Portman, 2007; White and Jorgensen, 2012; White et al., 2007). In contrast, the alterations can also be radical, so that the adult cells display a distinct morphology, as-well-as function. The male sphincter muscle and the anal depressor muscle follow this developmental path to generate the two sexually dimorphic muscle cells.

Dissertation objectives:

The main objective of this dissertation is to identify the sex determination mechanisms that govern the sexually dimorphic development of the anal depressor, and the signaling network that regulates the sarcomere disassembly process in the male.

Chapter II describes in detail the experimental procedures used to elucidate this dissertation objective. In this study, I used genetics, confocal imaging, laser ablation,

transgene manipulation, and calcium imaging to identify the signaling components that control the anal depressor development.

In Chapter III, I determined that both endogenous sex determination pathway and exogenous inductive signaling are involved in the sexually differential growth of the anal depressor. By illuminating the sarcomere structure of the muscle cell, I found that the male anal depressor undergoes dramatic changes during L4 development. Through feminization and masculinization assay, I found that early anterior growth of the anal depressor is controlled by the cell-autonomous sex determination pathway. However, the migration of the anterior domain and the sarcomere disassembly process are controlled by signaling derived from the sex muscles. The conclusion is supported by the M cell-ablation assay and analysis of *mab-5* mutants. Additionally, the morphological change of the male anal depressor is accompanied by functional transition. Laser ablation of the anal depressor does not affect defecation behavior after L4 development, indicating it does not function as a defecation muscle after being reorganized.

In Chapter IV, I described in detail the identification of genes and potential signaling pathways that regulate the sarcomere disassembly process in the male anal depressor. Analysis of the Wnt mutant phenotype and their expression pattern suggest that the Wnt-canonical signaling functions in the anal depressor to regulate sarcomere disassembly. Through EMS mutagenesis and mutant screening, I isolated a mutation that confers similar sarcomere disassembly defects. By SNP mapping and genome sequencing, I mapped the mutation to *egl-8*/PLC-β. Mutant analysis of *itr-1* and *unc-68* suggest that Wnt-calcium pathway also promote the disassembly of the sarcomere.

Calcium imaging and monitoring β-catenin levels in the anal depressor indicate that the Wnt-β-catenin signaling functions during earlier developmental stage, whereas the Wnt-calcium signaling is activated during L4 development to directly regulate sarcomere disassembly.

In Chapter V, I identified that *lin-44* and *lin-17* mutants have anal depressor asymmetry phenotype. This suggests that Wnt signaling is required for symmetrical development of the anal depressor in both the hermaphrodite and the male.

CHAPTER II

EXPERIMENTAL PROCEDURES*

Strains

C. elegans strains were cultured at 20°C and manipulated following standard protocols (Brenner, 1974). All strains contained *him-5(e1490)* on LG V (Hodgkin et al., 1979). I also used the following alleles in this study: *mab-5(e2088)* on LG III (Kenyon, 1986); *pha-1(e2123)* on LGIII (Schnabel and Schnabel, 1990); *lite-1(ce314)* on LG X (Edwards et al., 2008); *egl-20 (n585)* on LG IV*; lin-44 (n1792)* on LG I*; cwn-1(ok546)* on LG II*; lin-17(e620)* on LG I*; mig-1(e1787)* on LG I*; bar-1(ga80)* on LG X*; hmp-2(qm39)* on LG I*; egl-8 (n488)* on LG V*; goa-1(n1134)* on LG I*; gpa-16(it143)* on LG I*; gpa-14(pk347)* on LG I*; rrf-3(pk1426)* on LG II*; unc-68(r1158)* on LG V*; pkc-2(ok328)* on LG X*; tax-6(ok2065)*on LG IV*; cnb-1(jh103)* on LG V*; clp-6(ok1779)* on LG IV*; egl-19(n582)* on LG IV*; exp-1(ox276)* on LG II.

The *rg441* allele described in this study was isolated from an EMS screen that selected for males that have anal depressor sarcomere disassembly defects. The strain CG912, which carries the integrated transgene *rg*Is*3* [P*lev-11*:Dsred; P*lev-11*:G-CaMP] was mutagenized to generate mutant lines. The *rg441* strain was identified and outcrossed three times to eliminate background mutations. Whole genome sequencing

---

* Portions of this chapter are reprinted from Chen, X. and Rene Garcia, L. (2015) Developmental alterations of the *C. elegans* male anal depressor morphology and function require sex-specific cell autonomous and cell non-autonomous interactions. Developmental Biology 398, 24-43.

was conducted by BGI Americas Corporation and the *rg441* allele was found to be located within *egl-8* locus on LG V. The *rg441* mutation changed the wild type sequence CTTGAC**C**AAT to the mutant sequence CTTGAC**T**AAT (Gln to Ochre).

Plasmids construction

Plasmid for anal depressor visualization

To drive the expression of fluorescent proteins in the anal depressor, I used the transgenic array *rg*Ex*430* [P*lev-11*: G-CaMP; P*lev-11*: mDsRed] (Guo et al., 2012). To maintain a stable transgene expression level, *rg*Ex*430* [P*lev-11*: G-CaMP; P*lev-11*: mDsRed] was integrated into the strain CG912 using a UV irradiation-based method (Mello et al., 1991). The *pha-1(e2123)* and *lite-1(ce314)* mutations contained within CG912 were eliminated by outcrossing with *him-5(e1490)* males before integration. The integrated line was outcrossed 5 times to reduce background mutations.

To visualize the actin filaments, I fused the YFP coding sequence to the N terminus of the actin genomic sequence (Guo et al., 2012). To generate pXG31, pXG30 (the gateway ccdB cassette: YFP::actin) was recombined with pLR21 (Reiner et al., 2006), which contains the *unc-103*E promoter. pXG31 was injected at 50 ng/µL together with 150 ng/µL of pUC18 into *him-5(e1490)* hermaphrodites to make the transgene *rg*Ex*497* [P*unc-103E*: YFP::actin] (Guo et al., 2012).

To drive the YFP::actin expression using the *exp-1* promoter, I PCR-amplified the 3.6 kb *exp-1* sequence upstream of the ATG (Beg and Jorgensen, 2003). The primer pair used to amplify the *exp-1* promoter was: 5'-GGGGACCACTTTGTACAAGAAAGCTGGGTATTCTGGTCGATGCTGTGCTTGC

CCATGGCT -3’ and 5’-

GGGGACAAGTTTGTACAAAAAAGCAGGCTCACGGAGCGGAGGACGATTTTG

GAGATTAAC -3’.The primer pair contains Invitrogen Gateway ATTB sites.

To generate the entry vector pXC15, I recombined the *exp-1* promoter sequence into the ATTP-containing donor vector pDG15 (Reiner et al., 2006) using BP clonase (Invitrogen, Carlsbad, CA). pXC15 was then recombined with the destination vector pXG30 using LR clonase (Invitrogen) to generate pXC8. pXC8 was injected at 50 ng/µL, together with pBX1 (100 ng/µL) and pUC18 (50ng/µL) into *pha-1(e2123); him-5(e1490); lite-1(ce314)* adult hermaphrodites.

***tra-2* feminizing plasmid construction**

The pEntry 1-2-*tra-2*(IC) (Mowrey et al., 2014), which contains the 1084 bp of the *tra-2* intracellular fragment coding sequence, was a gift from Kelli Fagan and Dr. Douglas Portman from the University of Rochester, New York.

The *tra-2* intracellular fragment was PCR-amplified from pEntry 1-2-*tra-2*-(IC) using the primer pair:

5’-

GAGGATCTCGCCACCATGGAATTCTCAATCAAACGATCATCTCCTCCCTGCC

G -3’

and 5’-

GCCAATCCCGGCCGCTTAAACCTCTGGGTCTGATAGGTCGCCTTCCCGT -3’.

These two primers contain homology to the sequences that flank the G-CaMP3 in pLR279 (the gateway *ccdB* cassette: G-CaMP3::SL2:::DsRed) (Correa et al., 2012).

The primer pair: 5'-GACCCAGAGGTTTAAGCGGCCGGGATTGGCCAAAGG -3' and 5'-GATTGAGAATTCCATGGTGGCGAGATCCTCTAGATCAACC -3' was used to linearize and remove the G-CaMP coding sequence in pLR279. The two primers contain homology to the 5' and 3' sequence of the *tra-2*-(IC) sequence, respectively. The *tra-2*-(IC) fragment was ligated into the SL2:DsRed plasmid backbone using the In-Fusion Dry-Down PCR Cloning Kit (Clontech, Mountain View, CA) to make pXC14 (the gateway *ccdB* cassette: *tra-2* (IC)::SL2:::DsRed). Using LR clonase, pXC14 was recombined with pXC15 to generate pXC16. To visualize both the cytoplasm and the sarcomere structure of the feminized anal depressor, pXC16 (50 ng/µL) was co-injected with pXG31 (40 ng/µL), pBX1 (100 ng/µL) and pUC18 (10 ng/µL) into *pha-1(e2123)*; *him-5(e1490); lite-1(ce314)* adult hermaphrodites.

***fem-3* masculinizing plasmid construction**

The pEntry 1-2 *fem*-(+) SL2 mCherry (Mowrey et al., 2014), which contains the 1165 bp of the *fem-3* cDNA sequence, was a gift from Kelli Fagan and Dr. Douglas Portman from the University of Rochester, New York. The *fem-3* cDNA sequence was PCR-amplified from pEntry 1-2-*fem-3* SL2 mCherry using the primer pair 5'-GAGGATCTCGCCACCATGGAGGTGGATCCGGGTTCAGATGATGTAGAAGC -3' and 5'-GCCAATCCCGGCCGCATCGTTTCCTGGAGCAATCAGTAGCATAAACATTCAT AATCCGAA -3'. These two primers contain homology to the sequences that flank the G-CaMP3 coding sequence in pLR279. The primer pair

5’-GCTCCAGGAAACGATGCGGCCGGGATTGGCCAAAGG -3’ and 5’-CGGATCCACCTCCATGGTGGCGAGATCCTCTAGATCAACC -3’ was used to linearize pLR279 and remove the G-CaMP coding sequence. The two primers contain homology to the 5’ and 3’ sequence of the *fem-3* cDNA sequence, respectively. The *fem-3* cDNA was ligated into the SL2:DsRed plasmid backbone using the In-Fusion Dry-Down PCR Cloning Kit to make pXC26 (the gateway *ccdB* cassette:*fem-3* cDNA::SL2:::DsRed). Using LR clonase, pXC26 was recombined with pXC15 to generate pXC29. To visualize both the cytoplasm and the sarcomere structure of the masculinized anal depressor, pXC29 (50 ng/µL) was co-injected with pXG31 (40ng/µL), pBX1 (100 ng/µL) and pUC18 (10 ng/µL) into *pha-1(e2123)*; *him-5(e1490); lite-1(ce314)* adult hermaphrodites.

Cloning the *hlh-8* promoter

~5.9 kb sequence upstream of the *hlh-8* ATG was PCR-amplified using the pair 5’-GGGGACAAGTTTGTACAAAAAAGCAGGCTGCCGCTCGAGGACTTTGAAAATCGCAA -3’ and 5’-GGGGACCACTTTGTACAAGAAAGCTGGGTACTGTGAAAATCATATTTGAAATCGGTCAGT-3’. This promoter region contains *cis*-acting elements that drive expression in the M lineage and the coelomocytes, but not in the anal depressor or any other defecation-associated muscles (Harfe et al., 1998). The primer pair contains Invitrogen Gateway ATTB sites. I recombined the *hlh-8* promoter sequence into the

ATTP-containing donor vector pDG15 (Reiner et al., 2006) using BP clonase to generate the entry vector pXC27.

***mab-5* rescuing plasmid construction**

The 376 bp *mab-5* cDNA sequence containing the 3rd to 5th exons was PCR amplified from the genomic DNA of the strain CF301 *mab-5(e2088); unc-31(e169); him-5(e1490); muIs9[hs-mab-5 +C14G10(unc-31^{+})]* (Salser et al., 1993). The primer pair used was: 5'-GAGGATCTCGCCACCATTCGCCTATAACCCACTTCAAGCAACATCTGC-3' and 5'-GCCAATCCCGGCCGCTCAAGAAGAATGTTGTTCATTTTGCTCATCTTGATTTGATTCT-3'. These two primers contain homology to the sequences that flank the G-CaMP3 coding sequence in pLR279 (Correa et al., 2012). The primer pair 5'-CAACATTCTTCTTGA GCGGCCGGGATTGGCCAAAGG-3' and 5'-GGGTTATAGGCGAATGGTGGCGAGATCCTCTAGATCAACC-3' was used to linearize pLR279 and remove the G-CaMP coding sequence. The two primers contain homology to the 5' and 3' sequence of the *mab-5* cDNA sequence (3rd to 5th exons), respectively. The *mab-5* cDNA sequence (3rd to 5th exons) was ligated into the SL2:DsRed plasmid backbone using the In-Fusion Dry-Down PCR Cloning Kit to make pXC25 [the gateway *ccdB* cassette:*mab-5* cDNA (3rd to 5th exons)::SL2:::DsRed].

The 496 bp *mab-5* genomic sequence ranging from the 1st exon to the 2nd exon (including the 1st intron) was PCR-amplified from the genomic DNA of *him-5(e1490)* strain. I used the primer pair 5'-

GAGGATCTCGCCACCATGAGCATGTATCCTGGATGGACAGGCGAC-3' and 5'-GGGTTATAGGCGAATGGATTTGATGAATTATCCATCCAACCGGCAGC-3'. These two primers contain homology to the pXC25 sequence flanking the *mab-5* cDNA sequence (3rd to 5th exons). pXC25 was linearized using the primer pair 5'-TAATTCATCAAATCCATTCGCCTATAACCCACTTCAAGCAACATC-3' and 5'-AGGATACATGCTCATGGTGGCGAGATCCTCTAGATCAACC-3'. The two primers contain homology to the 5' and 3' sequence of *mab-5* genomic sequence (1st to 2nd exon). The *mab-5* genomic sequence (1st to 2nd exon) was ligated into the pXC25 using the In-Fusion Dry-Down PCR Cloning Kit to make pXC28 [the gateway *ccdB* cassette:*mab-5* genomic sequence (1st to 2nd exon) + *mab-5* cDNA (3rd to 5th exons)::SL2:::DsRed]. Using LR clonase, pXC28 was recombined with pXC27 or pXC15 to generate pXC32 and pXC31, respectively. To visualize the anal depressor's sarcomere structure, pXC32 (70 ng/µL) or pXC31 (70 ng/µL) was co-injected with pXG31 (30 ng/µL) and pUC18 (100 ng/µL) into *mab-5 (e2088)/+; him-5 (e1490)* adult hermaphrodites. The F1 hermaphrodites that were *mab-5 (e2088)* homozygous and stably transmitted the transgene were kept.

Constructs for masculinization of the M lineage in the hermaphrodites

Using LR clonase, pXC26 was recombined with pXC27 to generate pXC30. To visualize the sarcomere structure of the anal depressor, pXC30 (70ng/µL) was co-injected with pXG31 (20ng/µL), pBX1 (100 ng/µL) and pUC18 (10ng/µL) into *pha-1 (e2123)*; *him-5 (e1490); lite-1 (ce314)* adult hermaphrodites.

Plasmid to examine the expression pattern of Wnt, Frizzled, β-catenin and Phospholipase C

The 7kb promoter region (Whangbo and Kenyon, 1999) of *egl-20* was cloned using the primers: 5'-GGGGACAAGTTTGTACAAAAAAGCAGGCTGCCTGTAATTGAATGAAAATTGCTTAATGAA-3' and 5'-GGGGACAAGTTTGTACAAAAAAGCAGGCTGCTTTGCACTTATTTTCAGCCTGGCATTGGC-3'. The primer set contains ATTB site, therefore the promoter region was recombined using BP clonase, into pDG15 to generate pXC33. To make pXC35 [P*egl-20*:Timer], pXC33 was recombined with pLR186 (a plasmid containing gateway destination ATTR cassette in front of pTimer) using LR clonase.

The 2.7kb promoter region of *lin-44* was cloned using the primers: 5'-GGGGACAAGTTTGTACAAAAAAGCAGGCTGCGTCGGATGGTCATATGCATGTCTTTCCGG-3' and 5'-GGGGACCACTTTGTACAAGAAAGCTGGGTAGCTGTGTCACCTCGAAAAGTGCGTTTCTT-3'. And the 6.5 kb promoter region of *lin-17* was cloned using the primer set: 5'-GGGGACAAGTTTGTACAAAAAAGCAGGCTGCAACCACCAGTTGATCTTGGAGAGGGAAAG-3' and 5'-GGGGACCACTTTGTACAAGAAAGCTGGGTATTTGGAGAAGGAGCCAGTCTCTCGAGGAGC-3'. Both primer sets have ATTB sites, and therefore the promoters of *lin-44* and *lin-17* were recombined into pDG15, using the BP clonase, to generate

pXC108 and pXC11, respectively. pXC108 and pXC11 were recombined with pGW322YFP (plasmid containing the gateway destination ATTR cassette in front of YFP), to make pXC110 [P*lin-44*:YFP] and pXC12 [P*lin-17*:YFP], respectively.

To examine the expression pattern of *lin-44*, pXC110 (50 ng/µL) was co-injected with pBX1 (50 ng/µL), and pUC18 (100 ng/µL) into *pha-1 (e2123)*; *him-5 (e1490); lite-1 (ce314)* adult hermaphrodites.

To examine the expression pattern of *lin-17*, pXC12 (50 ng/µL) was co-injected with pBX1 (50 ng/µL), and pUC18 (100 ng/µL) into *pha-1 (e2123)*; *him-5 (e1490); lite-1 (ce314)* adult hermaphrodites.

The 6.3 kb promoter region of *bar-1* was cloned using the primer set: 5'-GGGGACAAGTTTGTACAAAAAAGCAGGCTCAACGCTAAACCCAAATCATCGTTAAAACAT-3' and 5'-GGGGACCACTTTGTACAAGAAAGCTGGGTACCCAGTTTTCTGAAAAAAAAAGCCAAATA -3'. The primer set contains the ATTB site, therefore the promoter region was recombined using BP clonase, into pDG15 to generate pXC67. pXC67 was recombined with pGW322YFP to make pXC70 [Pbar-1:YFP]. The genomic sequence of *bar-1* from ATG to the 761 codon was PCR amplified using the primer set: 5'-TTTCAGAAAACTGGGATGGACCTGGATCCGAACCTAGTTATTAACCATGA-3' and 5'-TTCTCCTTTACTCATATCCAAGTACGTCTCGGGAGGTCCAATTGAGTATT-3'. The primers contain homology to the 3' end of bar-1 promoter region and 5' end of YFP. pXC70 [Pbar-1:YFP] was linearized using primes: 5'-

GAGACGTACTTGGATATGAGTAAAGGAGAAGAACTTTTCACTGGAGTTG-3' and 5'-CGGATCCAGGTCCATCCCAGTTTTCTGAAAAAAAAAGCCAAATATTTTTTTATGAAT-3'. The primer set contains homology to the 3' end and 5' end of cloned bar-1 genomic sequence, respectively. The bar-1 genomic region was infused with the linearized vector pXC70 [Pbar-1:YFP] using the In-Fusion Dry-Down PCR Cloning Kit to make pXC87 [Pbar-1: BAR-1::YFP].

pXC67[Pbar-1 in pDG15] was also recombined with pGW77C (plasmid containing gateway ATTR site in front of CFP) to make pXC93[Pbar-1:CFP].

To examine the expression pattern of *bar-1*, pXC87 (40 ng/µL) was co-injected with pXC93 (30 ng/µL), pBX1 (50 ng/µL), and pUC18 (80 ng/µL) into *pha-1 (e2123)*; *him-5 (e1490); lite-1 (ce314)* adult hermaphrodites.

The 3.0 kb promoter region of *egl-8* was PCR amplified using the primer set: 5'-GGGGACAAGTTTGTACAAAAAAGCAGGCTGCTTGACCAAAACCACGAGTTGCAGGCTA-3' and 5'-GGGGACCACTTTGTACAAGAAAGCTGGGTACTCTTCTTGCCGGTTACCAGGAAAA-3'. The primer set contains ATTB site, therefore was recombined into pDG15 using BP clonase, to make pXC36. pXC36 was recombined with pGW322YFP using LR clonase, to make pXC39 [P*egl-8*:YFP].

To examine the expression pattern of *egl-8*, pXC39 (50 ng/µL) was co-injected with pBX1 (50 ng/µL), and pUC18 (100 ng/µL) into *pha-1 (e2123)*; *him-5 (e1490); lite-1 (ce314)* adult hermaphrodites.

Plasmids for rescuing EGL-20 in *egl-20(n585)* mutants in time-specific or tissue-specific manner

2.3 kb of *egl-20* genomic sequence from ATG till last stop codon was PCR amplified using the primer set: 5'-GAGGATCTCGCCACC ATGCAATTTTTCATTTGCCTGATTTTTCTATTTGTTCTCCTCG-3' and 5'-GCCAATCCCGGCCGCTTATTTGCATGTATGTACTGCAACTTCTTCGGTACAAG -3'. These two primers contain homology to the sequences that flank the G-CaMP3 coding sequence in pLR279. The primer pair 5'-CAACATTCTTCTTGAGCGGCCGGGATTGGCCAAAGG-3' and 5'-GGGTTATAGGCGAATGGTGGCGAGATCCTCTAGATCAACC-3' was used to linearize pLR279 and remove the G-CaMP coding sequence. The two primers contain homology to the 3' and 5' sequence of the *egl-20* genomic sequence, respectively. The *egl-20* genomic sequence was ligated into the SL2:DsRed plasmid backbone using the In-Fusion Dry-Down PCR Cloning Kit to make pXC99 [the gateway *ccdB* cassette:*egl-20*::SL2:::DsRed].

pXC33 [Pegl-20 in pDG15], pBL172 [heat shock promoter in pDG15] and pBL348 [*aex-2* promoter recombined with pDG15] was recombined with pXC99 using LR clonase to make pXC100 [P*egl-20*:*egl-20*::SL2:::DsRed], pXC101 [*hsp-16*: *egl-20*::SL2:::DsRed], and pXC106 [P*aex-2*: *egl-20*::SL2:::DsRed], respectively.

To test the functionality of EGL-20 expressed from the transgene, pXC100 (50 ng/µL) was co-injected with pXC23 (50 ng/µL), pBX1 (50 ng/µL) and pUC18 (50 ng/µL) into *egl-20(n585); him-5(e1490)* adult hermaphrodites.

To test the timing of EGL-20 function, pXC101 (20 ng/µL) was co-injected with pXC8 (30 ng/µL), pBX1 (50 ng/µL), and pUC18 (100 ng/µL) into *egl-20(n585); pha-1(e2123)*; *him-5(e1490)* adult hermaphrodites.

To test the site of action of EGL-20, pXC106 (50 ng/µL) was co-injected with pXC23 [P*unc-103E*:YFP::actin(only exons)] (30 ng/µL), pBX1 (50 ng/µL), and pUC18 (70 ng/µL) into *egl-20(n585); pha-1(e2123)*; *him-5(e1490)* adult hermaphrodites.

***rg441* rescue constructs**

To amplify the genomic sequence of *egl-8,* I first cloned the genomic region from the 6th to the 11th exons using primer pair: 5'-GGGGACAAGTTTGTACAAAAAAGCAGGCTCAATGTGCACAGACGTGTTCTTCAAGGTGGG-3', 5'-GGGGACCACTTGTACAAGAAAGCTGGGTACCCACACCTTACGGGTTGCAGCCGAAAC. The primer pair contains ATTB sites, therefore can be recombined into pDG15 using BP clonase, to make pXC66. I also cloned the genomic region from the promoter region to the 6th exon using primer pair: GGAATATATCCTGTACCGCCTCCCACTTAAATTGGCGGCTCTTT, CACGTCTGTGCACATGGCCTTTCCGTGAGTGATAATGGGTTCTC; the primer pair contains homology to the 3' end of the 6th exons. I linearized pXC66 using primers: 5'-ACTCACGGAAAGGCCATGTGCACAGACGTGTTCTTCAAGGTGGGTATTTTGAACT-3', 5'-TTAAGTGGGAGGCGGTACAGGATATATTCCGCTTCCTCGCTCACTGACTCGC

T-3'. The PCR product of the promoter region to the 6th exons sequence was ligated into pXC66 using In-Fusion Dry-Down PCR Cloning Kit to make pXC71 (*egl-8* genomic sequence from promoter region to the 11th exons).

To amplify the *egl-8* genomic region from 12th exon to the 16th exon, I used the primer pair: 5'-GGCCCCAAATAATGACTACTTTGTGGTACAAGTTAGAGCGAGCTATCCAGGGGAGC-3', 5'-GAAGTTGTCCATATTCCTATCATTATTGACCAAATCTTGTGGCACTGGACTTCCAAT-3'. The primer pair contains ATTB sites, therefore can be recombined into pDG15 using BP clonase, to make pXC53. I also cloned the genomic region from 17th exon to the genomic requence that is 3.6 kb downstream of *egl-8* using the primer: 5'-GTCAATAATGATAGGGTCCGATCTCTCGTGAACACTCAAACCGGAGAATGGTC, 5'-GAAGTTGTCCATATTTAAAGACAACCCACCAGCAGGCGCCAAGTTGTGTCT -3'. The primers contain homology to the 3' end of the 16th exon. pXC53 was linearized using primers: 5'-GGTGGGTTGTCTTTAAATATGGACAACTTCTTCGCCCCCGTTTTCACCATGGGCAAATA -3', 5'-CACGAGAGATCGGACCCTATCATTATTGACCAAATCTTGTGGCACTGGACTTCCAAT-3'. The PCR product of the 17th exon to the downstream sequence was ligated into pXC53 using In-Fusion Dry-Down PCR Cloning Kit to make pXC54 (*egl-8*

genomic sequence from 12th exons till the 3.6 kb sequence downstream of *egl-8* in pDG15).

The exon sequences contained in pXC54 and pXC71 were sequenced. The insertion mutation contained within pXC54 was corrected by single site mutagenesis to make pXC78 (*egl-8* genomic sequence from 12th exons till the 3.6 kb sequence downstream of egl-8 in pDG15 with mutation corrected).

The *egl-8* genomic sequence from the promoter region till the 11th exon was linearized from pXC71 using primers: 5'-CCGCCTCCCACTTAAATTGGCGGCTCTTT-3', 5'-CCCACACCTTACGGGTTGCAGCCGAAAC-3'.

The *egl-8* genomic sequence from the 12th exons till the 3.6 kb sequence downstream of *egl-8* was linearized from pXC78 using primers: 5'-CTACTTTGTGGTACAAGTTAGAGCGAGCTATCCAGGGGAGC-3'; 5'-TAAAGACAACCCACCAGCAGGCGCCAAGTTGTGTCT-3'.

The intron region between the 11th and 12th exons was PCR amplified using primers: 5'-CAGGTTGCTTGAAACGATGGAATGCGATATTTTCT-3'; 5'-CTGCCCACCCTTGGTTCATAGTACTCACTAGTC-3'.

The three PCR products of *egl-8* genomic sequence were injected at 32.5 ng/µL (promoter region till 11th exon), 16.3 ng/µL (intron between 11th and 12th exon), 27.5 ng/µL (12th exon till downstream) together with pLR132 [P*lev-11*:DsRed] (20 ng/µL) and pUC18 (103 ng/µL) into *rg441* adult hermaphrodites. The injection concentration of the three PCR products was calculated so that their molecular ratio is close to 1:1:1.

Generate transgenic mutant lines

Crosses were set up between *him-5(e1490)* males that carry the transgene *rg*Ex*497* [P*unc-103E*: YFP::actin] males with mutant hermaphrodites to generate the following transgenic mutants lines:

*egl-20 (n585) him-5(e1490) rg*Ex*497* [P*unc-103E*: YFP::actin]*; lin-44 (n1792) him-5(e1490) rg*Ex*497* [P*unc-103E*: YFP::actin]*; cwn-1(ok546) him-5(e1490) rg*Ex*497* [P*unc-103E*: YFP::actin]*; lin-17(e620) him-5(e1490) rg*Ex*497* [P*unc-103E*: YFP::actin]*; mig-1(e1787) him-5(e1490) rg*Ex*497* [P*unc-103E*: YFP::actin]*; bar-1(ga80) him-5(e1490) rg*Ex*497* [P*unc-103E*: YFP::actin]*; hmp-2(qm39) him-5(e1490) rg*Ex*497* [P*unc-103E*: YFP::actin]*; egl-8 (rg441) him-5(e1490) rg*Ex*497* [P*unc-103E*: YFP::actin]; *egl-8 (n488) him-5(e1490) rg*Ex*497* [P*unc-103E*: YFP::actin]*; goa-1(n1134) him-5(e1490) rg*Ex*497* [P*unc-103E*: YFP::actin]*; gpa-16(it143) him-5(e1490) rg*Ex*497* [P*unc-103E*: YFP::actin]*; gpa-14(pk347) him-5(e1490) rg*Ex*497* [P*unc-103E*: YFP::actin]*; unc-68(r1158) him-5(e1490) rg*Ex*497* [P*unc-103E*: YFP::actin]*; pkc-2(ok328) him-5(e1490) rg*Ex*497* [P*unc-103E*: YFP::actin]*; tax-6(ok2065) him-5(e1490) rg*Ex*497* [P*unc-103E*: YFP::actin]*; cnb-1(jh103) him-5(e1490) rg*Ex*497* [P*unc-103E*: YFP::actin]*; clp-6(ok1779) him-5(e1490) rg*Ex*497* [P*unc-103E*: YFP::actin]*; egl-19(n582) him-5(e1490) rg*Ex*497* [P*unc-103E*: YFP::actin]*; exp-1(ox276) him-5(e1490) rg*Ex*497* [P*unc-103E*: YFP::actin]; *rrf-3 (pk1426) him-5(e1490) rg*Ex*497* [P*unc-103E*: YFP::actin].

Imaging

I identified the anal depressor morphology, related to a specific development age. The ages for the L1 to L3 hermaphrodites and males were determined by the length of the gonadal arm, and the position of the distal tip cells (hermaphrodite) or linker cell (male) (Antebi, 1997; Hedgecock et al., 1987). The ages for the L4 and adult hermaphrodites were determined by the developmental stage of the vulva (Sternberg and Horvitz, 1986). The ages for the L4 and adult males were determined by the position of tail tip cells (Nguyen et al., 1999; Sulston et al., 1980a).

To facilitate imaging, the worms were mounted on agar pads made from a melted agar solution (Sulston and Horvitz, 1977). The agar solution was made by adding sterile water to Difco Noble agar. The concentration of the agar pads for larval males and hermaphrodites was 3%. To immobilize the worm, NaN_3 was used and the concentrations were: 12 mM NaN_3 for L1-L2 males and L1-L2 hermaphrodites, and 24 mM NaN_3 for L3-L4 males and L3-adult hermaphrodites. 8% agar pads with polystyrene beads were used for adult males (Kim et al., 2013). NaN_3 was not used for the adult males, because it caused the adult males to protract their spicules. Cover slips were then put on the top of the worm. The worms were crushed so that they were lying on their lateral side. All the images were taken using an Olympus IX81 microscope (Olympus Corporation, Tokyo, Japan) fitted with a Yokogawa CSU-X1 Spinning Disk Unit (Andor Technology, CT, USA). The two outermost lateral sides of the worm tail were set up as the starting and ending z stack for optical sectioning. Series of confocal images were then collected from one lateral side of the worm tail to the other. For each animal, the

oblique images of the individual attachment (either the left or the right) of the anal depressor were overlaid together using the Corel Photo-Paint software (Version 13.0.0.739, Corel Corporation, Ottawa, Canada) to create a flattened image. The flattened images were used for measurements and analyses.

Measurement of the dorsal width of the anal depressor attachment

Measurements were conducted using the HCImage software (version 2.0.0.0., Hamamatsu, Bridgewater, NJ). The extended focus image of the individual attachment was used for the measurements. An image of the staged micro-meter was taken at each magnification. The scale bar was then calibrated based on the known distance on the calibration image.

3D reconstruction

To construct the 3D image shown in Figure 1A, 400 confocal images were taken of a hermaphrodite anal depressor expressing the transgene *rg*Ex*497* [P*unc-103*E: YFP::actin], from one lateral side to the other side. The stack of images was processed using the MetaMorph software (version 7.8.0.0., Molecular Devices, Sunnyvale, CA) to establish a 3D model. The 3D model was rotated to be at the lateral-transverse angle. The image was processed and the background (non-specific expression from the tail neurons) was removed.

To construct the 3D image shown in Figure 2J, 50 confocal images were taken of a male anal depressor expressing the transgene *rg*Is*3* [P*lev-11*: G-CaMP; P*lev-11*: mDsRed]. A 3D model was then reconstructed using the MetaMorph software.

Measurement of the area of the anal depressor posterior domain

Measurements were conducted using the MetaMorph software (version 7.8.0.0., Molecular Devices, Silicon Valley). For each animal, the oblique images of the left and right attachments of the anal depressor were overlaid together using the Corel Photo-Paint software (Version 13.0.0.739, Corel Corporation, Ottawa, Canada) to create a flattened image. The flattened images were used for measurements. The anal depressor region that was occupied by myofilaments was outlined and the area of the region was calculated as the number of pixels contained within. The area of non-disassembled region of both attachments were added together to represent the data point for each individual worm.

SNP mapping

Hawaiian males were crossed into *rg441* strain to produce F1 heterozygous hermaphrodites. The self-progeny of F1s were single picked. Among the F2s that give rise to a lot of males (indicating the genotype is homozygous for *him-5(e1490)*), none produced F3 males that are all wild type for *rg441* phenotype. This indicates that the mutation responsible for *rg441* phenotype is linked to *him-5*. From the F2 plates that are heterozygous for the *rg441* (1/4 of the F3 males have defective anal depressor), F4 hermaphrodites were single picked at L4 stage. Among the F4 plates picked, 16 plates were identified as homozygous for *rg441*, and 14 plates were identified as homozygous wild type. For each plate, worms were washed off and lysed to get the genomic DNA. Different SNP locus were PCR amplified and the identity was examined by restriction digestion (N2 allele or Hawaii allele) for the 16 *rg441* lines and 14 wild type lines. All

16 *rg441* lines have N2 allele and all 14 wild type lines have Hawaii allele for F36F12, which is located on the left end of chromosome V. This indicates the *rg441* mutation was located within that interval.

RNAi assay

rrf-3(pk1426) him-5(e1490) L4 hermaphrodites which carry the transgene *rg*Ex*497* [P*unc-103E*: YFP::actin] were fed with bacteria producing double-stranded RNAs to target the ORF of *lin-17, itr-1, lit-1, lin-18* and *rho-1*. Bacteria with the L4440 (control) or double-T7 vector including exons of target genes were grown and induced by IPTG using a standard protocol (Kamath et al., 2001). Carbenicillin was used at the concentration of 10 mg/mL to increase the level of plasmid maintenance, and therefore the effectiveness of RNAi. Exons of genes that were cloned into the double-T7 vector are: 6^{th} to 8^{th} exons of *lin-17*; 14-19^{th} exons of *itr-1*; 5^{th}-6^{th} exons of *lit-1*; 1^{st}-4^{th} exons of *lin-18*; 1^{st}-3^{rd} exons of *rho-1*. Males that display the corresponding mutant phenotype were picked for anal depressor imaging and defects detection.

Calcium imaging

Male at mid-L4 stage was put on agar pads which were made from 2.5% noble agar dissolved in S-basal solution. Abemectin was added to the agar solution to immobilize the worm. The final concentration is 0.25mg/mL. The G-CaMP and DsRed fluorescence signals at the male tail were recorded simultaneously using a Dual View Simultaneous Image splitter (Photometrics, AZ) and a Hamamatsu ImagEM Electron multiplier (EM) CCD camera, with the exposure time of 1 second. The worms were imaged using the 40X objective, and the imaging continued until the worm reached L4-

molt stage. The Ca^{2+} data was analyzed using the Hamamatsu SimplePCI (version 6.6.0.0) software and Microsoft Excel, as described previously (LeBoeuf et al., 2011).

Monitoring BAR-1 levels in the anal depressor

Images of the male tail were taken using an Olympus IX81 microscope (Olympus Corporation, Tokyo, Japan) fitted with a Yokogawa CSU-X1 Spinning Disk Unit (Andor Technology, CT, USA). Confocal images were then collected from one lateral side of the worm tail to the other as described in the imaging section. The images were taken sequentially at the excitation wavelength of 515nm for YFP and 445nm for CFP using fixed laser and camera settings. The data was analyzed using the Hamamatsu SimplePCI (version 6.6.0.0) software. Two ROIs outlining the anal depressor was drawn on the anal depressor itself (ROI 1), and the background (ROI 2). Total gray of the ROI was calculated for each stack. The total gray for all stacks were summed up for ROI 1 and ROI 2. The total fluorescence within the anal depressor was calculated as Total Gray $_{ROI\ 1}$ - Total Gray $_{ROI\ 2.}$ The total fluorescence of YFP was divided by the total fluorescence of CFP to represent the relative BAR-1 protein levels.

Mating potency assay

L4 males were isolated and picked to a NGM plate with *E.coli* the night before the mating potency assay. L4 *pha-1* hermaphrodites were also isolated and grown at 20 °C for one day before the mating potency assay. 10 µL of *E. coli* was spotted onto a NGM plate the night before the mating potency assay. On the next day, the mating potency assay was performed by picking one 1-day-old *pha-1* hermaphrodite and one 1-day-old male to a NGM plate (seeded with 10 ul of *E. coli)*. Two to three days later, the

males whose mating potency plate contained cross-progenies were scored as sexually potent (Correa et al., 2012; Guo et al., 2012; Liu et al., 2011).

Arecoline drug test

To assay arecoline-induced spicule protraction, I dissolved acecoline (Acrose organics, NJ) in distilled water to make a stock solution of 1 mM. 1 mL of the drug was added to a nine-well Pyrex titer dish. Three to five males were transferred to the drug bath. Then for 5 minutes, the males were observed under a stereomicroscope for spicule protraction. Males that had >50% of their spicules out for longer than 10 seconds were scored as positive. Drug baths were changed after 20 males were observed (Liu et al., 2007).

Assessment of mating behaviors

L4 males were isolated one day before the mating observation assay. The next day, I placed fifteen 2-day-old *unc-64*(*e246*) hermaphrodites on a 5-mm-diameter bacterial lawn for an hour. One 1-day-old male was then placed with the hermaphrodites. The male's behavior was recorded for no longer than ~ 5 minutes, using an Olympus BX51 microscope mounted with a digital camera. In the recordings, multiple mating behavioral criteria were then analyzed for each male. The E_{SI} (Efficiency of spicule insertion) was calculated as previously described (Correa et al., 2012; Guo et al., 2012; LeBoeuf et al., 2014; Liu et al., 2011).

Laser ablation

To eliminate the male copulatory structures, I conducted laser-ablation to damage their ancestor cells. To facilitate imaging of the anal depressor, the laser-ablation was

conducted on males that carried either *rg*Is*3* [P*lev-11*: G-CaMP; P*lev-11*: mDsRed] (B.a and B.p cell ablation, F and U cell ablation, and SM 1, 2 and 3 ablation) or both *rg*Is*3* and *rg*Ex*497* [P*unc-103*E: YFP::actin] (M cell ablation) transgenic arrays. The B.a and B.p ablations and F and U ablations were conducted at the late L1 stage. The M cell was ablated at the L1 stage. The SM 1, 2 and 3 cells were ablated either on the left or right side at the late L2-early L3 stage. The cells were identified based on previous cell lineage descriptions (Sulston et al., 1980a).

To determine if the abnormally formed male sex muscles are responsible for the additional posterior disassembly defects, I laser-ablated the M cell in L1 *mab-5(lf)* males. To facilitate imaging, I crossed *mab-5 (e2088)* hermaphrodites with CG997 (*him-5 rg*Ex*497* [P*unc-103*E: YFP::actin] males) to make the *mab-5 (e2088) rg*Ex*497* [P*unc-103*E: YFP::actin] transgenic line. The F2 hermaphrodites that gave rise to males with abnormal ray patterns were identified as *mab-5(e2088)* homozygotes (Kenyon, 1986).

The laser ablation was conducted using a Spectra-Physics VSL-337ND-S Nitrogen Laser (Mountain View, Ca) attached to an Olympus BX51 microscope. To immobilize the worm, a 2% agar pad with 10mM NaN_3 was used for L1 worms and a 3% agar pad with 24mM NaN_3 was used for L3 worms. Cell ablation was conducted following the standard protocol (Bargmann and Avery, 1995). The mock-ablated worms were operated under the same anesthetic conditions as the ablated worms, with the exception that no laser-ablation was performed. After the operation, the worm was transferred back onto NGM plates containing OP50. The worms were allowed to grow into the L4 stage and then imaged under the confocal microscope.

Determining the defecation efficiency

To identify if the anal depressor is required for defecation during L4 development, I laser-ablated the L1 male anal depressor nucleus. The strain that carries *rg*Is*3* [P*lev-11*: G-CaMP; P*lev-11*: mDsRed] was used to facilitate the identification of the anal depressor. After the laser-ablation, the worm was transferred back onto NGM plates containing OP50. After entering the L3 or L4 stage, the worms were imaged under the Zeiss Stemi SV11 dissecting microscope. During the imaging, the worms were allowed to crawl freely on OP50. The Simple PCI software (version 6.6.0.0., Hamamatsu, Bridgewater, NJ) was used to calculate the intestinal area. A region-of-interest (ROI) was placed on the intestinal lumen and the boundary of the ROI was adjusted, so that it was overlaid with the intestinal lumen boundary. The number of pixels that were encompassed within the ROI was measured by the software and used as indicator of the intestinal lumen area.

CHAPTER III

THE SEXUALLY DIMORPHIC DEVELOPMENT OF THE ANAL DEPRESSOR IS CONTROLLED BY CELL-AUTONOMOUS AND NON-AUTONOMOUS SEX DETERMINATION MECHANISMS*

The male anal depressor is distinct from the hermaphrodite anal depressor early from after L1 stage.

During the L4 larval stage, the male anal depressor muscle undergoes sex-specific remodification to change its function into an adult copulation muscle (Garcia et al., 2001; Jarrell et al., 2012; Reiner and Thomas, 1995; Sulston et al., 1980a). Prior to the obvious dimorphic remodeling, the larval male and hermaphrodite anal depressor are morphologically similar and do not exhibit obvious differences in function during defecation behavior. I first asked if the anal depressor of pre-L4 larval males and hermaphrodites is neuter, or does it undergo subtle dimorphic changes during early larval development.

To visualize the changes in the anal depressor's morphology and in particular, the sarcomere, I used the *unc-103E* and *exp-1* promoters to express YFP fused to the actin genomic sequence. In both sexes, the *unc-103E* promoter drives expression in the anal depressor, sex muscles and some head neurons (Gruninger et al., 2006). I used the

---

* Portions of this chapter are reprinted from Chen, X. and Rene Garcia, L. (2015) Developmental alterations of the *C. elegans* male anal depressor morphology and function require sex-specific cell autonomous and cell non-autonomous interactions. Developmental Biology 398, 24-43.

construct to monitor alterations in the neighbouring cells, in conjunction with changes in the anal depressor. However in some animals, sequences contained within the actin genomic sequence promoted sporadic expression in some tail neurons. To differentiate the anal depressor's morphological changes from the neighbouring sex muscle cells, I also used the *exp-1* promoter, which restricted YFP:actin expression to the anal depressor and the intestinal muscles of both sexes. Both promoters allowed us to visualize cytoplasmic structures throughout the male and hermaphrodite lifespan (Beg and Jorgensen, 2003; Gruninger et al., 2006). To obtain a complete image of the sarcomere structure, I took series of confocal images ranging from the left lateral side to the right; this is because the sarcomere is not completely parallel to the lateral side (Figure 1A). I then combined the stacks to assemble a flattened image of the cell's shape and the sarcomere (Figure 1A and 1B), so that parameters such as the sarcomere's length and width can be measured. I presented an image of a single side to represent the anal depressor morphology at each stage (Figure 1C-1G), since the left and right attachments of the male and hermaphrodite anal depressor were symmetrical throughout development (Figure 2B).

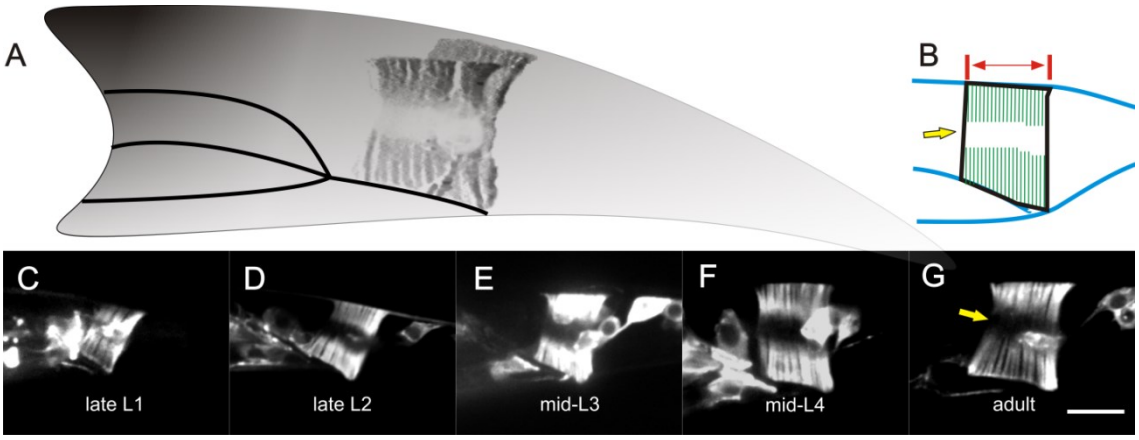

Figure 1. Morphological changes of the hermaphrodite anal depressor. (A) A 3D model of the adult hermaphrodite anal depressor. The anal depressor model was made from stacks of images taken from the left to the right lateral side. The images were reconstructed as a 3D image and rotated to be a lateral-transverse view. The anal depressor is an H-shaped cell with two attachments symmetrically positioned at the left and right side. The left and right attachments are attached to the dorsal hypodermis and ventrally attached to the rectum. (B) Cartoon for the hermaphrodite anal depressor viewed from the lateral side. The arrow indicates the H zone. The H zone is the gap between the two arrays of actin filaments (greenish blue lines) within a single sarcomere. The double arrows indicate the dorsal width that was measured in Figure 2. (C-G) Lateral views of the anal depressor in A: late L1 (C), late L2 (D), mid-L3 (E), mid-L4 (F) and an adult (G) stage hermaphrodite. All the animals expressed the transgene *rg*Ex*497* [P*unc-103*E:YFP::actin]. The arrow in G indicates the H zone. For each of the images shown, the fluorescent staining indicates the actin filaments. The dark band in between the two arrays of actin filaments indicates the H zone. Within a single sarcomere, the H zone is the myosin region that does not overlap with the actin filaments. All the images are positioned as the anterior to the left and ventral to the bottom. For all of the images, the scale bar represents 10μm.

As early as after the L1 stage, I observed a quantitive growth difference between the hermaphrodite and male anal depressor. The hermaphrodite anal depressor has been shown to maintain the sarcomere throughout the animal's lifespan (Thomas, 1990). As expected, I found that the hermaphrodite larva's sarcomere expanded both anterior-posteriorly and dorsal-ventrally (Figure 1C-1G). To quantify this change, I measured the rectangular anal depressor sarcomere's dorsal width, since the width determines how much of the rectum that the anal depressor can lift. I then compared this metric between

the different larval and adult stages. I found that for the hermaphrodite anal depressor, anterior-posterior expansion steadily occured throughout development (Figure 2A).

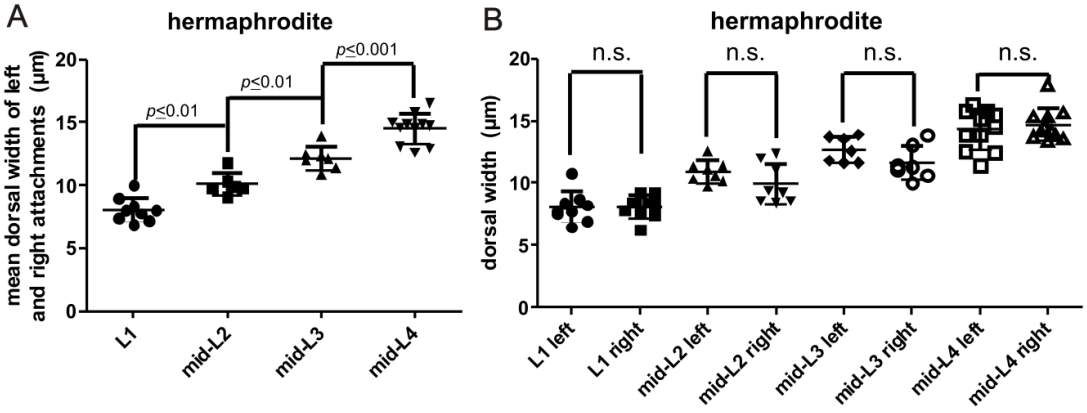

Figure 2. Growth dynamics of the hermaphrodite anal depressor. (A) Growth dynamics of the dorsal attachment of the anal depressor in hermaphrodites. Each dot is the mean value of the dorsal width of the left and right attachments of a single animal. Mean ± SD is indicated. The *p* value was calculated using one-way ANOVA with the Bonferroni's Multiple Comparison Test. (B) Comparisons of the dorsal width of the hermaphrodite anal depressor's left and right attachments at different larval stages. Mean ± SD is indicated. The *p* value was calculated using one-way ANOVA with the Bonferroni's Multiple Comparison Test (n.s. = not significant).

In contrast to the hermaphrodite, the male anal depressor displayed retarded growth dynamics. From L1 to mid-L3, the male anal depressor morphologically resembled the larval hermaphrodite anal depressor, maintaining the dorsal attachment on the dorsal hypodermis and the ventral attachment on the rectum (Figure 3A- 3C and 3A'- 3C'). But unlike the hermaphrodite muscle, I observed that the anal depressor growth was static between late L1 to mid-L2 stage. I measured some anterior-posterior growth during mid-L2 to mid-L3 stage (Figure 4B); however, the average expansion magnitude was much smaller compared to the hermaphrodite ($p<0.001$, unpaired t test) (Figure 2A and 4B). At every stage I measured, the male anal depressor was thinner than the hermaphrodite's (mid-L2, $p<0.01$; mid-L3, $p<0.0001$; early L4, $p<0.0001$; unpaired t test). After mid-L3, the dorsal width of the male anal depressor qualitatively decreased (Figure 4B). Therefore, sex differences in the anal depressor development occurs after L2 and persist throughout L1 to L3 stage animals.

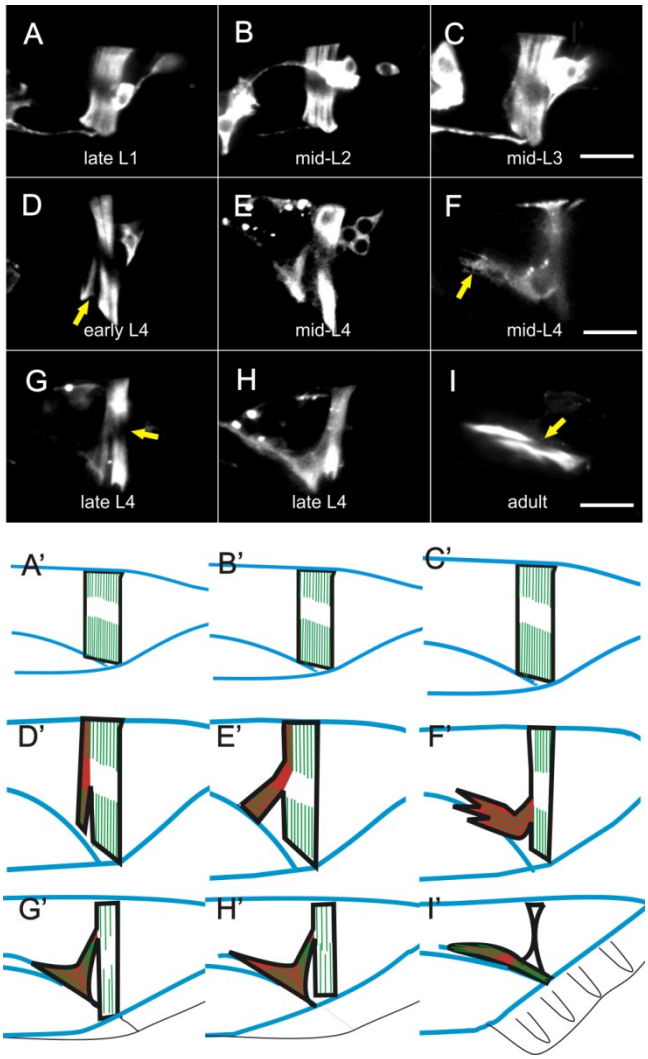

Figure 3. Morphological changes of the male anal depressor. (A-I) Lateral views of the male anal depressor at: late L1 (A), mid-L2 (B), mid-L3 (C), 37 hr early L4 (D), 40hr mid-L4 (E), 41hr mid-L4 (F), 42hr late L4 (G), 43hr late L4 (H) and adult (I) stage. The arrow in (D) indicates the ventral slit formed between the anterior and posterior domains. The arrow in (F) indicates that the actin filaments contained in the anterior domain are migrating dorsal-anteriorly in the mid-L4 stage male anal depressor. The arrow in (G) indicates a reduced H zone in the posterior domain. The arrow in (I) indicates the H zone in the newly-established sarcomere in the ventral attachment of the anterior domain. All the animals imaged carry the transgene *rg*Ex*497* [P*unc-103*E:YFP::actin] except (F) *rg*Ex*602* [P*exp-1*:YFP::actin]. (A'-I') Cartoons for the anal depressors in (A-I). The actin thin filaments that are contained within the sarcomere for L1 to L3 stages are indicated as greenish blue lines (A'-C'). For L4 and adult stages (D'-I'), the actin filaments contained within the anterior domain are highlighted with a red background; and the posterior domain background is uncolored. All the images are positioned as the anterior to the left and ventral to the bottom. For all of the images, the scale bar represents 10μm.

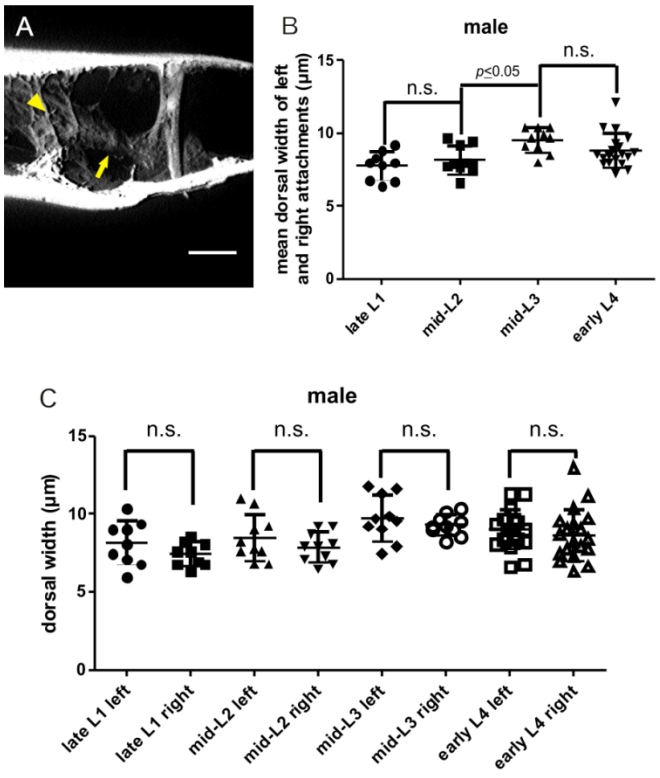

Figure 4. Growth dynamics of the male anal depressor. (A) A flatten 3D reconstructed stack of a fluorescing mid-L4 anal depressor and developing dorsal and ventral protractor muscles. The filopodia from the anterior domain of the anal depressor (arrow) is shown extending towards the dorsal protractor muscle cell, whose nuclei is indicated (arrow head). (B) Growth dynamics of the male anal depressor's dorsal attachment. Each dot is the mean value of the dorsal width of the left and right attachments for each animal. Mean $\pm$ SD is indicated. The *p* value was calculated using one-way ANOVA with the Bonferroni's Multiple Comparison Test (n.s. = not significant). (C) Comparisons of the dorsal width of the male anal depressor's left and right attachments at different larval stages. Mean $\pm$ SD is indicated. The *p* value was calculated using one-way ANOVA with the Bonferroni's Multiple Comparison Test (n.s. = not significant). (A) is positioned as the anterior to the left and ventral to the bottom.

During L4 development, the male anal depressor moves its ventral attachment to the spicule protractor muscles and reorganizes the sarcomere to run anterior-posteriorly. However, the details concerning cell interactions, timing, whether the sarcomere is disassembled and reassembled simultaneously or sequentially were unknown. To

address these questions, I identified the sarcomere reorganization events that occur during the L4 larval stage. During late L3 development, I observed that a ventral slit was formed at the ventral rectal attachment, demarcating the anal depressor into anterior and posterior domains (Figure 3D). At around 40 hr mid-L4, the anterior domain moved dorsal-anteriorly towards the developing dorsal spicule protractor muscles (Figure 3E and 4A). The trans-located anterior domain at this time (40 hr) maintained the sarcomere structure. The sarcomere in the posterior domain was still intact and was ventrally attached to the rectum. At around 41 hr (Figure 3F), the interface between the anal depressor's anterior domain and the dorsal protractor muscles expanded. The old sarcomere in the dorsal column of the anterior domain disassembled, and the actin filaments began to reform anterior-posteriorly (Figure 3F). At around 42 hr late L4 stage, the sarcomere contained within the posterior domain began to also disassemble and eventually, the posterior domain atrophied due to the reduction of actin filaments (Figure 3G and 3H). The actin filaments, which have been repositioned to the ventral part of the anterior domain, were reassembled to establish a novel anterior posterior-oriented sarcomere (Figure 3I). Therefore during the reorganization period in L4, only the anterior domain of the male anal depressor migrates from rectum to the spicule protractor muscles. The sarcomere disassembly occurs in a stepwise fashion, with anterior domain disassembling prior to the posterior domain.

The majority of the male remodeling events are controlled cell-autonomously by the male sex determination mechanism.

The similar morphology between the larval male and hermaphrodite anal depressor led us initially to believe that the early larval anal depressor was neuter. However, the differences in the anal depressor growth rate suggested that the male anal depressor development might be regulated earlier than the mid-late L3 stage. Previous studies showed that sexual dimorphic development can either be regulated by the innate sex determination mechanism (Conradt and Horvitz, 1999; Ross et al., 2005), or induced non-autonomously by communication with neighboring sex-specific cells (Hunter et al., 1999). To identify which aspect of the male anal depressor development was controlled by a cell autonomous mechanism, and which might be regulated by the neighboring male-specified cells, I transgenically expressed a feminizing factor in the anal depressor, and asked if and what male remodeling events were altered.

To transform the anal depressor's sexual identity, I expressed an intracellular fragment of TRA-2 in the male anal depressor using the *exp-1* promoter (Beg and Jorgensen, 2003). In the somatic cells of hermaphrodites, the X:A chromosome ratio regulates the sex determination pathway, so that TRA-2 is not inhibited by HER-1. Active TRA-2 suppresses the FEM proteins, which frees TRA-1 to enter the nucleus and promote hermaphrodite somatic development. In a male cell, the X:A ratio regulates the sex determination pathway in the opposite direction, so that TRA-2 is inhibited by HER-1. Active FEM proteins repress TRA-1 function and male development is specified (de Bono et al., 1995; Hodgkin, 1987; Kuwabara, 1996). The function of HER-1 to suppress

TRA-2 occurs through the transmembrane domain of TRA-2 (Hunter and Wood, 1992; Perry et al., 1993). TRA-2's intracellular carboxy terminal region (*tra-2* IC) is required to inhibit the FEM proteins (Kuwabara and Kimble, 1995). The intracellular domain of TRA-2 is insensitive to HER-1 inhibition, and thus overexpressing the truncated protein can constitutively inhibit the FEM proteins (Lum et al., 2000; Mowrey et al., 2014). In this way the male sex determination pathway can be converted into a female pathway.

I found that in transgenic *tra-2* IC-containing males, the larval anterior-posterior expansion was altered to resemble the hermaphrodite's muscle. The dorsal sarcomere of the feminized male anal depressor (Figure 5A-5D) was expanded more at the anterior-posterior orientation compared to wild-type males (Figure 3A-3E) at each larval stage; the kinetics of dorsal expansion were similar to the hermaphrodite anal depressor (Figure 6A-6C). This suggests that at least in wild-type males, the anal depressor's rate of dorsal expansion is cell autonomously promoted by the intrinsic sex determination pathway. However, in L3 to L4 larvae, the feminized anal depressor stopped dorsal expansion (Figure 6D). This could be due to incomplete feminization from the transgene or because of interactions with neighboring male cells, or lack of interactions with neighboring hermaphrodite cells. Nonetheless, the elevated level of dorsal expansion indicates that in wild-type males, the early regulation of the anal depressor's growth is cell autonomous and sex-intrinsic.

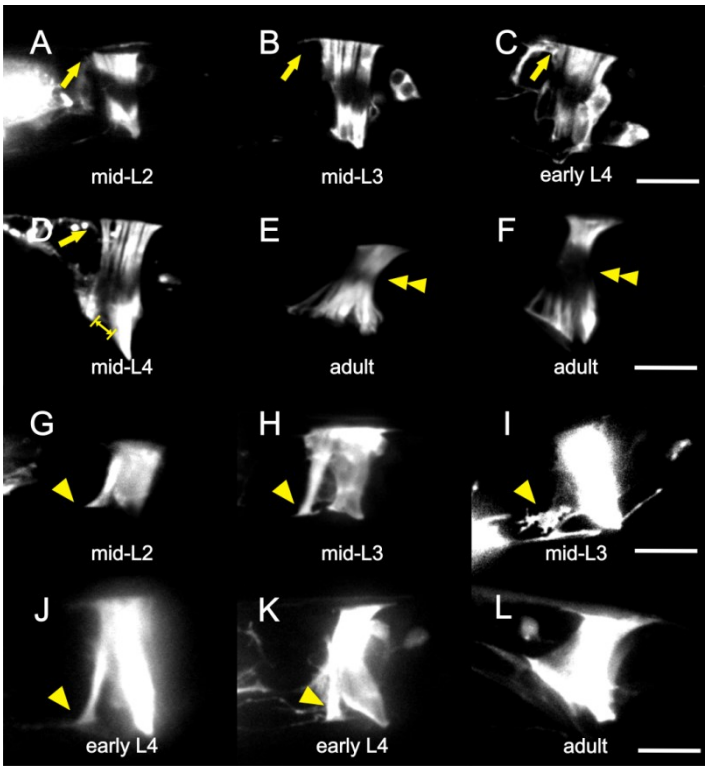

Figure 5. Feminizing the male anal depressor. (A-F) Lateral views of the anal depressor of: mid-L2 (A) and mid-L3 (B), 37 hr early L4 (C), 40 hr mid-L4 (D), and adult (E and F) stage males, which carry the transgene *rg*Ex*698* [P*exp-1*:*tra-2* (IC)::SL2:::DsRed; P*unc-103*E:YFP::actin]. The pictures were taken in the YFP emission channel. The arrows in (A-D) indicate the expanded anal depressor's dorsal attachments at different larval stages. The double arrows in D indicate the demarcation between the anal depressor's anterior and posterior domain. The double arrowheads in E and F indicate the vertically positioned H zone in both the adult anal depressor anterior and posterior domains. (G-L) Lateral views of the anal depressor of: mid-L2 (G), mid-L3 (H and I), 37 hr early L4 (J and K), and adult (L) males carrying the transgene *rg*Ex*698* [P*exp-1*:*tra-2* (IC)::SL2:::DsRed; P*unc-103*E:YFP::actin]. The pictures were taken in the DsRed emission channel. The arrowheads indicate either the ventral-anteriorly migrating filopodia extended from the anal depressor's ventral attachment (G, I and K), or the abnormal sarcomere ventral attachment that is extended into the pre-anal ganglion region (H and J). All the pictures are positioned as the anterior to the left and ventral to the bottom. In all of the images, the scale bar represents 10μm.

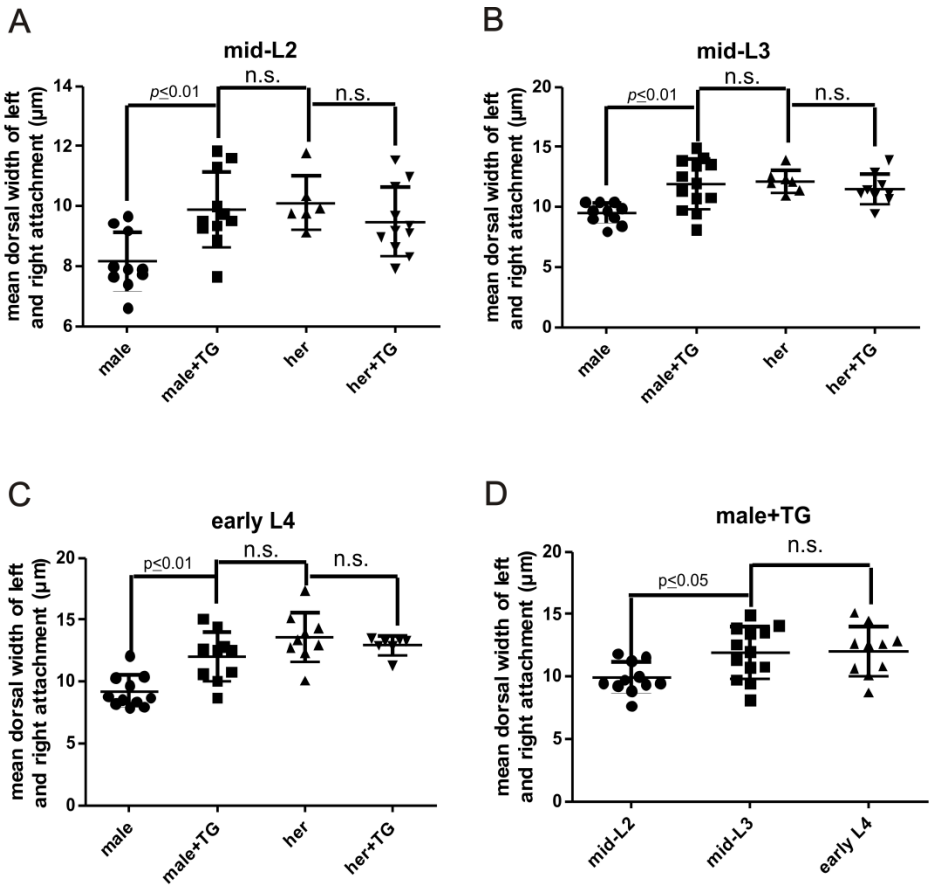

Figure 6. Quantification of the dorsal width of feminized anal depressor. (A-C) Mean comparisons of the anal depressor's dorsal width between the male wild-type anal depressor (male), wild-type male anal depressor expressing the transgene *rg*Ex*698* [P*exp-1*:*tra-2* (IC)::SL2:::DsRed; P*unc-103*E:YFP::actin] (male+TG), wild-type hermaphrodite anal depressor (her) and wild-type hermaphrodite anal depressor expressing the transgene *rg*Ex*698* [P*exp-1*:*tra-2* (IC)::SL2:::DsRed; P*unc-103*E:YFP::actin] (her+TG) at mid-L2 (A), mid-L3 (B) and early L4 (C) stages. Mean ± SD is indicated. The *p* value was calculated using one-way ANOVA with the Bonferroni's Multiple Comparison Test (n.s. = not significant). (D) Mean comparisons of the left and right dorsal width for the wild-type male anal depressor expressing the transgene *rg*Ex*698* [P*exp-1*:*tra-2* (IC)::SL2:::DsRed; P*unc-103*E:YFP::actin] at mid-L2, mid-L3 and early L4 stages. Mean ± SD is indicated. The *p* value was calculated using one-way ANOVA with the Bonferroni's Multiple Comparison Test (n.s. = not significant).

To rule out the possibility that the transgenic-induced dorsal expansion was unrelated to sex transformation, I also measured the dorsal expansion dynamics in the

transgenic hermaphrodite anal depressor. I found that the transgenic hermaphrodite anal depressor displayed wild-type dorsal growth (Figure 6A-6C). This observation supports the interpretation that the *tra-2* IC transgene artificially induced the dorsal expansion in the male's muscle.

Although the dorsal growth of the feminized male anal depressor resembled the hermaphrodite anal depressor during L1 to L3 stages, it partially displayed male morphogenesis aspects during L4 development. Like a wild-type male anal depressor, at mid-L4 stage (Figure 3E), the feminized male anal depressor demarcated an anterior and posterior domain and moved the anterior domain towards the developing spicule protractor muscles (Figure 5D). However, unlike the wild-type anal depressor, the dorsal-ventrally oriented sarcomere did not disassemble later in the L4 stage (Figure 5E and 5F). These observations suggest that the initiation of the wild-type male anal depressor's reorganization is influenced by external signals, but further morphological changes require the intrinsic masculine sex determination program.

Feminizing the anal depressor compromises male mating behavior.

We hypothesize that in adults, the male mating circuit requires a properly gender-specified anal depressor to function. If correct, then feminizing the anal depressor should interfere with copulation behavior. Therefore I conducted mating potency, arecoline drug test and mating observation assays to assess what specific behaviors were affected by feminizing the muscle (Garcia et al., 2001; Liu and Sternberg, 1995; Liu et al., 2011).

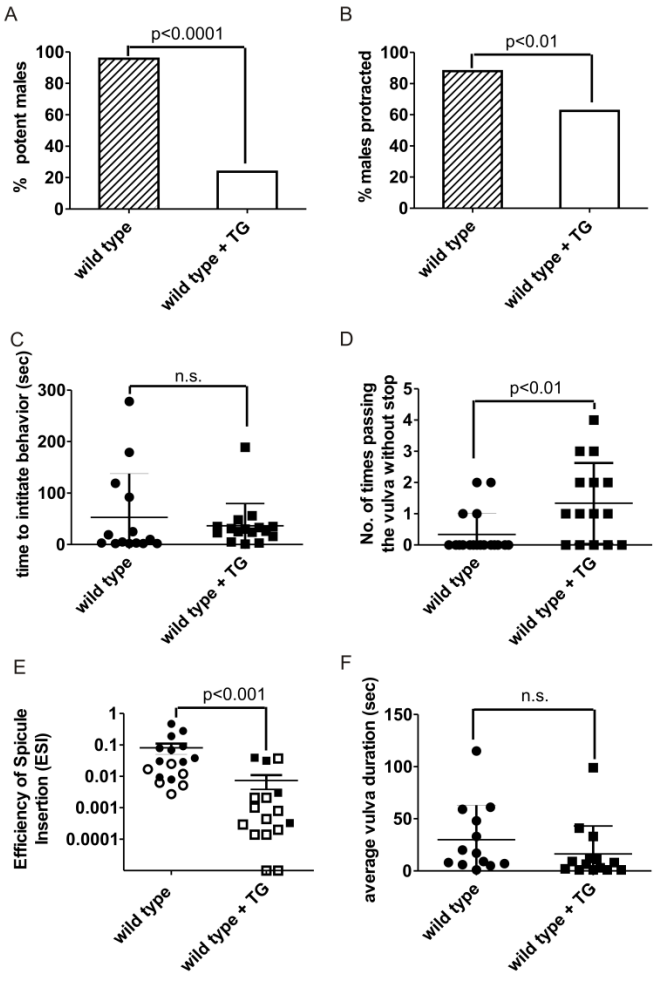

Figure 7. Feminization of the anal depressor causes multiple mating defects. (A) Mating potency of wild-type males (wild type, n=23) and wild-type males expressing the transgene *rg*Ex*698* [P*exp-1*:*tra-2* (IC)::SL2:::DsRed; P*unc-103*E:YFP::actin] (wild type + TG, n=21). The *p* value was calculated using Fisher's exact test. (B) Percentage of males that protracted their spicules in 1mM arecoline solution for wild-type males (wild type, n=50) and wild-type males expressing the transgene *rg*Ex*698* [P*exp-1*:*tra-2* (IC)::SL2:::DsRed; P*unc-103*E:YFP::actin] (wild type + TG, n=40). The *p* value was calculated using Fisher's exact test. (C) The time required for the wild-type males (wild type) and wild-type males expressing the transgene *rg*Ex*698* [P*exp-1*:*tra-2* (IC)::SL2:::DsRed; P*unc-103*E:YFP::actin] (wild type + TG) to initiate mating behavior. Each dot represents the metric of a single male observed. Mean $\pm$ SD is indicated. The *p* value was calculated using Mann-Whitney nonparametric test (n.s. = not significant). (D) Number of times for the wild-type males (wild type) or the wild-type males expressing the transgene *rg*Ex*698* [P*exp-1*:*tra-2* (IC)::SL2:::DsRed; P*unc-103*E:YFP::actin] (wild type + TG) to scan through the vulva region, but did not stop. Mean $\pm$ SD is indicated. The *p* value was calculated using Mann-Whitney nonparametric test. (E) Spicule insertion efficiency during 2 minutes of observation. Closed symbols indicate that the male successfully inserted its spicules. Open symbols indicate that the male did not insert his spicules. Mean $\pm$ SD is indicated. The *p* value was calculated using Mann-Whitney nonparametric test. (F) Average length of time that wild-type males (wild type) or the wild-type males expressing the transgene *rg*Ex*698* [P*exp-1*:*tra-2* (IC)::SL2:::DsRed; P*unc-103*E:YFP::actin] (wild type + TG) prodded against the vulva during the 2 minutes observation time. Mean $\pm$ SD is indicated. The *p* value was calculated using Mann-Whitney nonparametric test.

I first performed the mating potency assay by pairing a 1-day-old male with a 1-day-old hermaphrodite (Correa et al., 2012; Guo et al., 2012; Liu et al., 2011). The hermaphrodites possess the *pha-1(e2123)* temperature-sensitive mutation, and therefore at 20 °C only cross-progeny can survive. By counting the number of males that can sire progeny, I found that *tra-2*-transgenic males were less potent than wild-type males (Figure 7A). I then asked if the mating defect was due to reduced performance in behaviors that lead to spicule insertion and ejaculation (Correa et al., 2012; Garcia et al., 2001; LeBoeuf et al., 2014; Liu and Sternberg, 1995; Liu et al., 2011).

I conducted the arecoline drug assay to investigate if the feminized anal depressor affected spicule protraction (Figure 7B). The acetylcholine agonist, arecoline, promotes spicule protraction by activating nAChRs and mAChRs in the protractors muscles, SPC and post-cloacal sensilla neurons (Correa et al., 2012). I observed that the transgenic males were less sensitive to arecoline, compared to the wild type (Figure 7B). Previous work established that ablation of the anal depressor did not abolish the arecoline-induced protraction (Garcia, 2001). Therefore, the feminized anal depressor either developmentally or physically reduced the spicule protractor muscles' ability to contract.

Next, I examined if feminization impaired other mating behavioral steps. I introduced single males with paralyzed hermaphrodites and recorded their behaviors. Wild-type males were able to initiate scanning behavior, locate the vulva and insert their spicules within 5 minutes. For the transgenic males, they took similar amounts of time to initiate backing and scanning behavior (Figure 7C). However, they could not stop at the

vulva as efficiently as the wild type (Figure 7D). They hesitated around the vulva region, but continued backing without initiating the prodding behavior. Some of the males eventually positioned themselves over the vulva, but this was after several rounds of circling around the hermaphrodite. Therefore, they had very low spicule insertion efficiencies (Figure 7E). I speculate that the transformed anal depressor might interfere with the proper functions of other male muscles, such as the oblique and gubernaculum muscles. In the wild-type male, these posterior cloacal muscles are electrically connected to the anal depressor, which in turn is electrically coupled to the spicule muscles. The oblique and gubernaculum muscles function to press the male tail against the vulva and initiate spicule insertion attempts (Jarrell et al., 2012; Liu et al., 2011).

When the *tra-2*-transgenic males eventually position themselves over the vulva, they initiated spicule prodding behavior. The average prodding duration was similar between wild type animals and *tra-2*-transgenic animals (Figure 7F); but many of the males failed to insert their spicules (Figure 7E). In wild-type males, the SPC proprioceptive neurons make chemical synapses to both the anal depressor and spicule protractor muscles (Jarrell et al., 2012). These neurons are essential for copulation, and tonic contractions of the anal depressor and protractor muscles occur during full spicule insertion (Garcia et al., 2001). In the transgenic males, the low insertion ability might arise from reduced or absent signaling between the SPC and the transformed anal depressor; in addition, the transformed anal depressor might physically obstruct the protractor muscles' contractile efficiency. Therefore, I conclude that feminization of the anal depressor leads to defects in copulation behaviors.

Overexpressing FEM-3 in the larval hermaphrodite anal depressor induces male-like growth dynamics.

The results from the feminization of the male anal depressor experiment suggest that the muscle's L1 to early L4 development is regulated cell-autonomously. To confirm the observation, I performed the converse experiment and cell-autonomously masculinized the hermaphrodite anal depressor. I then asked if the potentially transformed muscle displayed male growth traits.

To convert the hermaphrodite sex determination pathway into a male one, I overexpressed the FEM-3 proteins in the hermaphrodite anal depressor using the *exp-1* promoter. Excess FEM-3 has been shown to overcome the inhibitory effect of TRA-2, thus suppressing TRA-1 activity and promoting male development (Lee and Portman, 2007; Mehra et al., 1999; Mowrey et al., 2014; White et al., 2007).

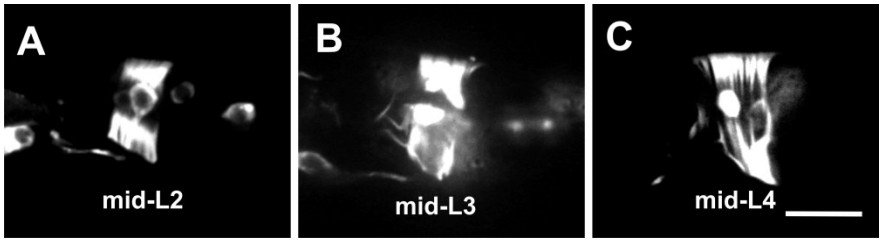

Figure 8. Masculinizing the hermaphrodite anal depressor. (A-C) Lateral views of the anal depressor of: mid-L2 (A) and mid-L3 (B), mid-L4 (C) stage males, which carry the transgene *rg*Ex*721* [P*exp-1*:*fem-3* cDNA::SL2:::DsRed; P*unc-103*E:YFP::actin]. The pictures were taken in the YFP emission channel. All the pictures are positioned as the anterior to the left and ventral to the bottom. In all of the images, the scale bar represents 10μm.

As I predicted, *fem-3*-expressing hermaphrodite anal depressor's larval growth kinetics were altered (Figure 8A-8C and 9A-9B). During the L2 and L3 stages, the masculinized anal depressor's anterior-posterior expansion was reduced compared to the wild-type hermaphrodite (Figure 9A and 9B). The dorsal expansion was not significantly different from the wild-type male anal depressor or the P*exp-1*: *fem-3* expressing control males. However, unlike a wild-type male anal depressor (Figure 4B), the masculinized anal depressor's dorsal growth continued during the L3-L4 stages (Figure 9D). Additionally, during the L4 stage, the masculinized hermaphrodite anal depressor did not extend an anterior branch or initiate anterior movement. However in 18% (n=17) of the animals, the actin filaments in the anterior sarcomere region were variably detectable (Figure 8C), hinting that the masculinized hermaphrodite anal depressor might be capable of reorganization. Although the results of this experiment are consistent with the idea that the early anal depressor's growth kinetics are cell autonomous in both sexes, I hypothesize that further gross masculine developmental changes require communication with neighboring masculinized cells.

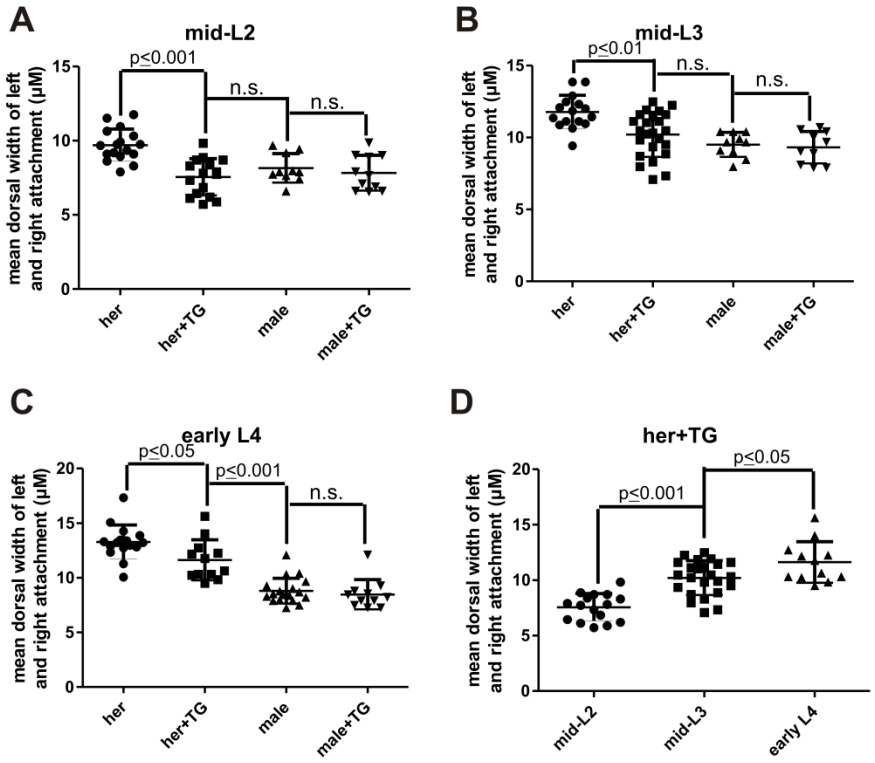

Figure 9. Masculinization repressed the dorsal expansion of the hermaphrodite anal depressor. (A-C) Mean comparisons of the anal depressor's dorsal width between the hermaphrodite wild-type anal depressor (her), wild-type hermaphrodite anal depressor expressing the transgene *rg*Ex*721* [P*exp-1*:*fem-3* cDNA::SL2:::DsRed; P*unc-103*E:YFP::actin] (her+TG), wild-type male anal depressor (male) and wild-type male anal depressor expressing the transgene *rg*Ex*721* [P*exp-1*:*fem-3* cDNA::SL2:::DsRed; P*unc-103*E:YFP::actin] (male+TG) at mid-L2 (A), mid-L3 (B) and early L4 (C) stages. Mean $\pm$ SD is indicated. The *p* value was calculated using one-way ANOVA with the Bonferroni's Multiple Comparison Test (n.s. = not significant). (D) Mean comparisons of the left and right dorsal width for the wild-type hermaphrodite anal depressor expressing the transgene *rg*Ex*721* [P*exp-1*:*fem-3* cDNA::SL2:::DsRed; P*unc-103*E:YFP::actin] at mid-L2, mid-L3 and early L4 stages. Mean $\pm$ SD is indicated. The *p* value was calculated using one-way ANOVA with the Bonferroni's Multiple Comparison Test (n.s. = not significant).

The anterior movement of the male anal depressor requires the developing male sex muscle cells.

Since feminizing the male anal depressor did not block the initiation of cellular reorganization, I entertained the possibility that the reorganization process required the participation of additional cells in the male tail. The adult male possesses unique copulatory structures in the tail region, including the male sex muscles and the copulatory spicules. The blast cells that give rise to those copulatory structures are either located in the male tail at L1 stage (the B cell that gives rise to the spicules, the F and U cells that give rise to the mating neurons, and the V and T seam cells that give rise to the rays) (Hunter et al., 1999; Kenyon, 1986; Salser and Kenyon, 1996; Sulston et al., 1980a), or migrate to the tail region at L3 stage (the M cell that give rise to the male sex muscles) (Sulston et al., 1980a). Therefore, during the L4 reorganization period, the male tail encompasses many male-specific cells in close proximity to the anal depressor, which might initiate the anterior movement of the muscle.

To test the hypothesis that developing male copulatory cells might present instructive signaling to promote the anal depressor's anterior movement, I either eliminated the copulatory structure, or disrupted the lineage from which the copulatory structures are derived. I then observed if the anal depressor's anterior movement was compromised. To determine the contributions of the spicules, spicule-associated neurons and the proctodeum cells, I laser-ablated the B.a and B.p progenitor cells. I also laser-ablated the F and U progenitor cells to determine if the male-specific interneurons contributed to the anal depressor reorganization. However, when I laser-ablated these

cells, I found that the L4 animals showed no anterior movement defects in the anal depressor (Figure 10A and 10B), suggesting that they do not initially participate in the anal depressor reorganization.

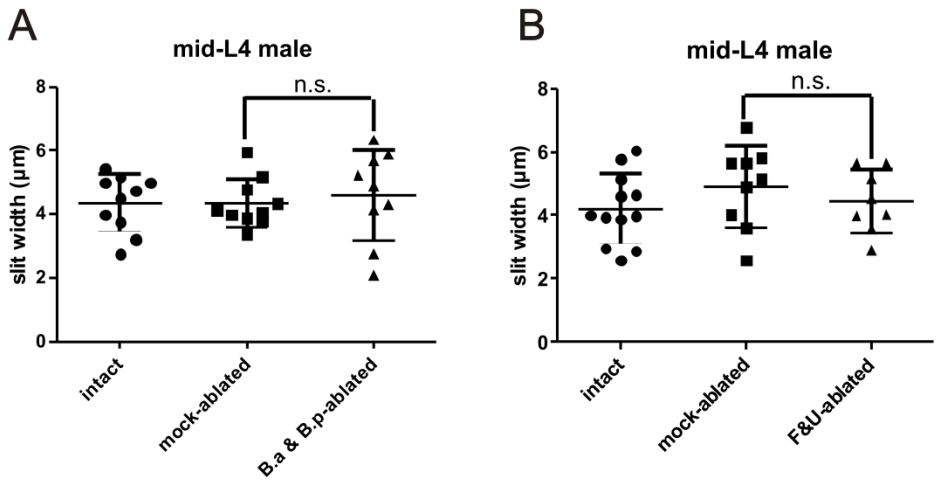

Figure 10. The spicule cells and proctodeum cells do not regulate the anterior movement of the anal depressor. (A and B) Comparisons of the slit width between the anal depressor's anterior and posterior domains in B.a and B.p-ablated (A) or F and U cell-ablated males (B) with mock-ablated males. Mean $\pm$ SD is indicated. The *p* value was calculated using the unpaired t test (n.s. = not significant).

To assess the importance of the male sex muscles and rays, I used the *mab-5(lf)* mutation to compromise the cell lineages that give rise to those structures. *mab-5* is a Hox gene that regulates the expression of genes that control cell fate specification in the M cell-sex muscle- and V5, V6-ray-lineages. The male M cell lineage generates nonessential body wall muscles and all of the male copulatory muscles, whereas V5 produces the cells contained in ray 1, and V6 produces the cells contained in rays 2 through 6 (Sulston et al., 1980a). In *mab-5(lf)* males, some M-derived sex myoblasts are missing, whereas other sub-lineages are miss-specified to produce additional sex myoblast-like cells (Harfe et al., 1998; Kenyon, 1986). Additionally, the lack of functional MAB-5 causes V5 and V6 to produce only seam cells or hypodermal-like cells (Kenyon, 1986). Therefore I examined *mab-5(lf)* males, to identify if the absence of signaling from the sex muscles and rays affects anal depressor development.

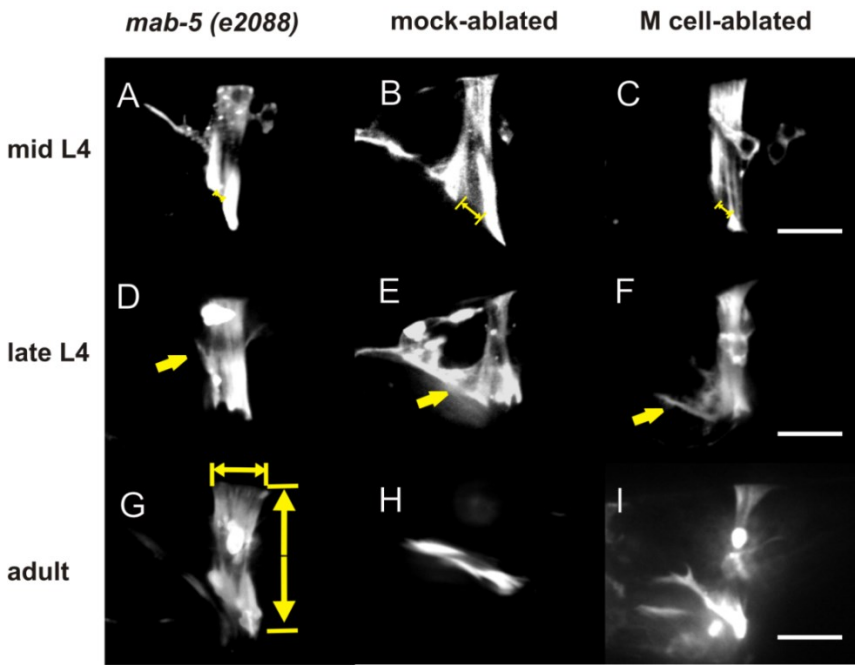

Figure 11. Compromising the male sex muscle activity affects the L4 development of the anal depressor. (A-I) Lateral views of the anal depressor of *mab-5 (e2088)* males at: mid-L4 (C), late L4 (F) and adult (I) stage; lateral views of the anal depressor of either mock-ablated males (B, E and H) or M cell-ablated males at: mid-L4 (C), late L4 (F) and adult (I) stage. The arrows in D, E and F indicate the anteriorly-migrating filopodia extending from the anterior domain of the anal depressor. The double arrows in (A-C) indicate the width of the slit measured. All the pictures are positioned as the anterior to the left and ventral to the bottom. For all of the images, the scale bar represents 10μm.

The anal depressor morphology of *mab-5(lf)* males was recorded at different time points during L4 development and adulthood (Figure 11A, 11D and 11G). I observed that during *mab-5(lf)* mid-L4 to adult development, the anal depressor had delayed specification and reduced movement of the anterior domain (Figure 3E, 11A and 12A). I also observed sarcomere disassembly defects in the posterior domain (Figure 11G, 12C and 12D).

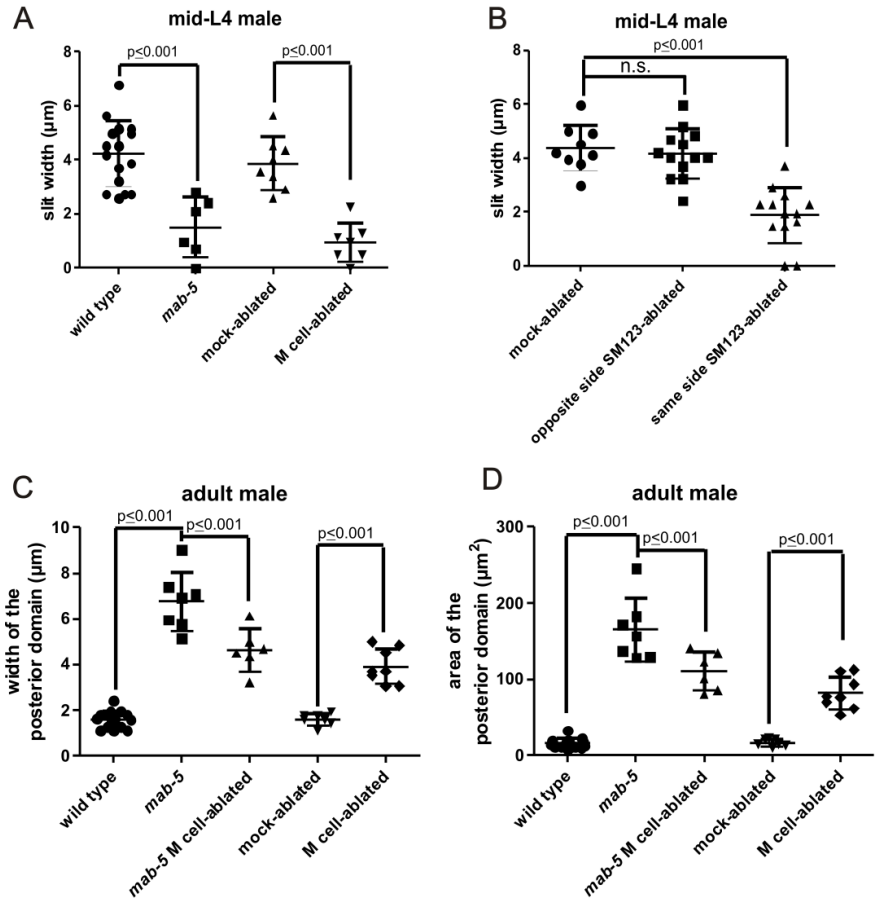

Figure 12. The anal depressor has anterior migration defects and sarcomere disassembly defects when the sex muscle morphogenesis is compromised. (A) Comparisons of the slit width between the anterior and posterior domains (the slit width is indicated in 11A, 11B and 11C by the arrows) among wild-type, *mab-5*, mock-ablated and M cell-ablated males at mid-L4 stage. Mean ± SD is indicated. The *p* value was calculated using one-way ANOVA with the Bonferroni's Multiple Comparison Test. (B) Comparisons of the slit width between the anterior and posterior domains among mock-ablated, opposite-side SM 1, 2 and 3-ablated (opposite SMs-ablated: SM1, 2 and 3, which are on the opposite side of the anal depressor attachment examined), and same-side SM 1, 2 and 3-ablated (same SMs-ablated: SM1, 2, and 3 which are on the same side of the anal depressor attachment examined) males at mid-L4 stage. Mean ± SD is indicated. The *p* value was calculated using the unpaired t test (n.s. = not significant). (C and D) Comparisons of the width (C) and the area (D) of the anal depressor's posterior domain among the wild-type, *mab-5*, *mab-5* M cell-ablated, mock-ablated and M cell-ablated males at adult stage. The width is indicated in 11G by the horizontal arrow, and the area is calculated as the result of the width multiplied by the length (vertical arrow) as indicated in 11G. Mean ± SD is indicated. The *p* value was calculated using one-way ANOVA with the Bonferroni's Multiple Comparison Test.

Since MAB-5 regulates two essential male specific behaviors during L4 anal depressor development, the transcription factor might also be involved in the male-specific regulation of the anterior-posterior expansion during L1 to L3 larva. Thus I examined *mab-5(lf)* male anal depressor development during the L1 to L3 stages. The *mab-5(lf)* males displayed wild-type dorsal growth at all larval stages (Figure 13A-13C). I concluded that MAB-5 expressed from the M lineage or rays only contributes to the male-specific regulation of the anal depressor development at L4.

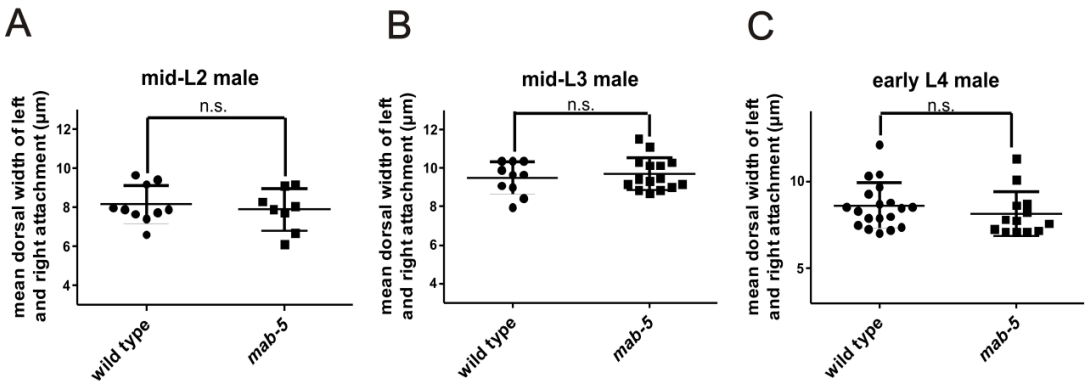

Figure 13. *mab-5* does not confer defects to the dorsal growth of the male anal depressor during early larval development. (A-C) Mean comparisons of the anal depressor's dorsal width between wild-type and *mab-5* mutants at: mid-L2 (A), mid-L3 (B) and early L4 (C) stages. Mean $\pm$ SD is indicated. The *p* value was calculated using the unpaired t test (n.s. = not significant).

The male-specific regulation of the anal depressor's anterior movement and posterior disassembly could be controlled by signaling from the M or V5, V6 lineage cells. I favored the M-lineage-derived male sex muscles to be the more likely signaling

source for these reorganization processes. The anal depressor physically contacts the spicule protractor muscles when the posterior sarcomere disassembly occurs and ultimately makes electrical connections to these muscles. Similar mechanisms can be found in the morphogenesis of neuromuscular junctions. The target neurons have been shown to secrete the guidance cues to initiate muscle arm extensions from the muscle cells (Seetharaman et al., 2011).

The M cell goes through several rounds of divisions, beginning at mid-L1 and ending at late-L3 stage to generate a few body wall muscles and all of the male sex muscle cells (Sulston et al., 1980a; Sulston and Horvitz, 1977). I laser-ablated the M cell at the early L1 stage, to ask if L1-operated males have similar anal depressor anterior and posterior defects, as in the *mab-5(lf)* males (Figure 11B, 11C, 11E, 11F, 11H and 11I). When I quantified the data, I found that the M cell-ablated animals displayed anterior movement defects similar to *mab-5(lf)* males (Figure 12A). Therefore the anterior movement defects seen in *mab-5(lf)* males were likely attributed to the cells of the M lineage. The adult males from those M cell-ablated animals had a larger posterior domain compared to the control (Figure 11H, 11I, 12C and 12D), indicating the M-lineage cells promote the disassembly of the posterior sarcomere. However, the *mab-5(lf)* adult anal depressor displayed more severe disassembly defects than the anal depressor of the M cell-ablated adults (Figure 11G and 11I, Figure 12C and 12D).

MAB-5 is also expressed in the male and hermaphrodite anal depressor embryonic progenitors (Cowing and Kenyon, 1992), but no obvious defects are seen in the hermaphrodite or larval male muscle. To test if cell-autonomous MAB-5 can rescue

the *mab-5(lf)*-induced L4 male anal depressor defects, I expressed the *mab-5* cDNA from the *exp-1* promoter. To confirm the functionality of the cloned *mab-5* cDNA, I also expressed the *mab-5* cDNA very early in the M lineage, using the *hlh-8* promoter. Gene expression from the *hlh-8* promoter is limited to the M lineage cells and coloemocytes (Harfe et al., 1998). The *hlh-8* promoter is active from embryonic stage till just before the sex myoblasts divide and differentiate into muscle cells during the L3 stage (Harfe et al., 1998). The P*hlh-8*:*mab-5* cDNA construct was sufficient to rescue the early *mab-5(lf)* division defects, and even specify some of the M-lineage progeny (Figure 14A-14B'). But the incomplete rescue was expected, since the M-lineage cells likely require continual *mab-5* expression from the endogenous promoter. In contrast to the partial rescue of the M-lineage cells, expressing the *mab-5* cDNA solely in the anal depressor, via the *exp-1* promoter did not alleviate the L4 stage posterior disassembly defects (Figure 14C and 14D). This result suggests that the transcription factor's function in this process is likely cell non-autonomous.

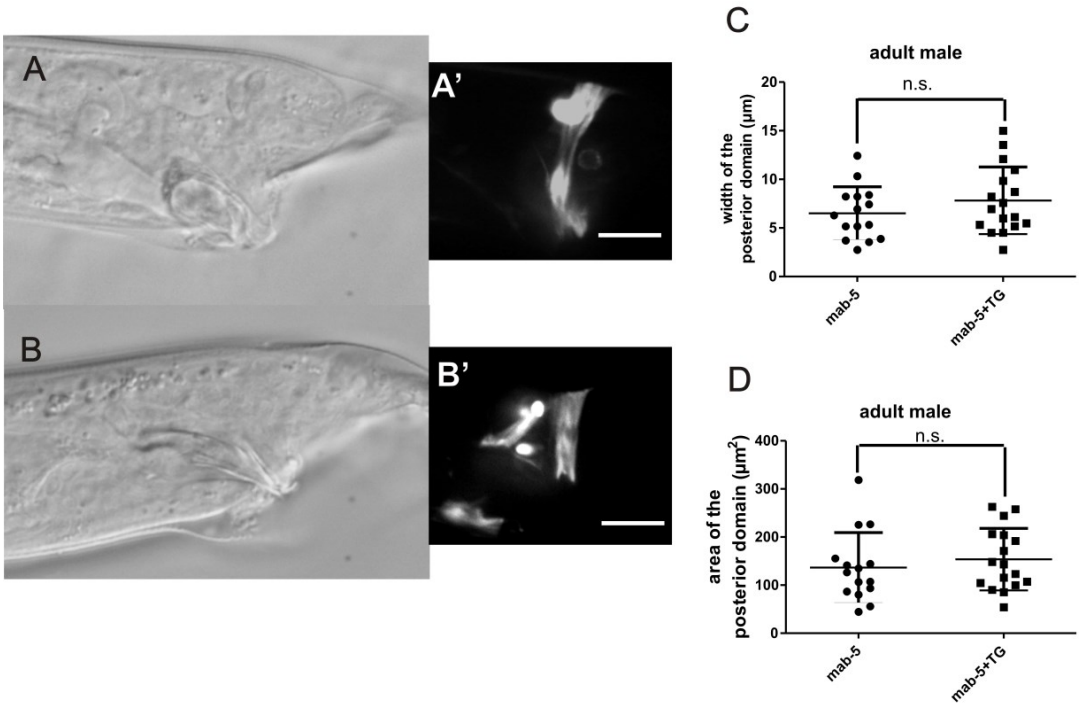

Figure 14. Cell-autonomous expression of *mab-5* did not rescue the anal depressor defects of *mab-5* mutants. (A and B) Lateral views of the adult male tail of *mab-5 (e2088)* males (A) and *mab-5 (e2088)* males, which carries the transgene *rg*Ex*722* [P*hlh-8*: *mab-5* cDNA::SL2:::DsRed; P*unc-103*E:YFP::actin] (B). The crumpled spicule defects were partially alleviated when *mab-5* was rescued in the M lineage, indicating that the cDNA was functional. (A' and B') Lateral views of the anal depressor of *mab-5 (e2088)* adult male (A') and *mab-5 (e2088)* adult male, which carries the transgene *rg*Ex*722* [P*hlh-8*: *mab-5* cDNA::SL2:::DsRed; P*unc-103*E:YFP::actin] (B'). The pictures were taken in the YFP emission channel. The sex muscle morphogenesis and orientation defects (A') were alleviated, but not enough to rescue the anal depressor defect (B'). (C and D) Comparisons of the width (C) and the area (D) of the anal depressor's posterior domain between the *mab-5 (e2088)* adult males (*mab-5*) and *mab-5 (e2088)* adult males, which carry the transgene *rg*Ex*723* [P*exp-1*: *mab-5* cDNA::SL2:::DsRed; P*unc-103*E:YFP::actin] (*mab-5*+TG). Mean $\pm$ SD is indicated. The *p* value was calculated using the unpaired t test (n.s. = not significant). All the pictures are positioned as the anterior to the left and ventral to the bottom. For all of the images, the scale bar represents 10µm.

Then I considered the possibility that the abnormal *mab-5(lf)* M-lineage cells had additional inhibitory effects on the disassembly of the posterior sarcomere. To test this possibility, I killed the M cell in L1 larval *mab-5(lf)* males. I found that in those operated

mab-5(lf) adult males, the size of the posterior domain was the same as the wild-type M cell-ablated adult males (Figure 12C and 12D). Therefore, I speculated that the posterior disassembly defects in *mab-5(lf)* males are due to the absence of normal signaling, in conjunction with neomorphic inhibitory effects from the abnormal M-lineage cells.

In wild-type males, the M-lineage produces a bilateral set of body wall muscle and sex muscle cells; thus I asked if the specification and movements of the anal depressor's bilateral anterior attachments are individually regulated by their cognate M-lineage neighbors. To address this possibility, I allowed the M cell to divide during the L1 larval stage to generate the bilateral body wall muscles and sex muscle mesoblasts, SM1, SM2 and SM3. The SM mesoblasts go through 3 additional rounds of divisions during the L3 stage to generate all of the sex muscles. During the L2 stage, I laser-ablated one set of SM 1, 2 and 3 (either the left or right); the M cell-derived body wall muscles were left intact. At L4 stage, I examined each side of the male tail to determine if the anal depressor's anterior domains were specified, and how much they moved. I found that the morphology of the anal depressor attachment was only affected when its cognate set of neighboring SM mesoblast cells was laser-ablated (Figure 12B). The severity of the anterior domain specification and movement defects were comparable to the M cell-ablated worms (Figure12A). This suggests that the sex muscle cells, which neighbors the anal depressor attachment and not the M-derived body wall muscles, likely contribute to the morphological changes of the anterior domain.

A masculinized M lineage is sufficient to induce anterior movement in the hermaphrodite anal depressor.

The M cell ablation experiments, in conjunction with the *mab-5(lf)* male phenotypes suggested that the anterior movement defects were attributed to the absence of signaling from the male sex muscles. However, those defects could still be due to unknown effects of the experimental design. To rule out this possibility, I masculinized the hermaphrodite early M lineage by using the *hlh-8* promoter to drive *fem-3* cDNA expression, and asked if a male-like M lineage can induce anterior movement of the hermaphrodite anal depressor.

In wild-type hermaphrodites, the M.dl/r cells divide during the L1 stage to form body wall muscles and coelomocytes, located in the worm's posterior region (Figure 15A, n=10). However, in L3 transgenic hermaphrodites, additional M.dl/r –derived cells, located at the posterior dorsal region confirmed that the P*hlh-8*: *fem-3* cDNA was functional (Figure 15B, n=7). Those additional cells are likely derived from an early masculinized M lineage, and resemble the SM1 and SM2 sex mesoblasts, which are born during the male L3 stage (Sulston et al., 1980a).

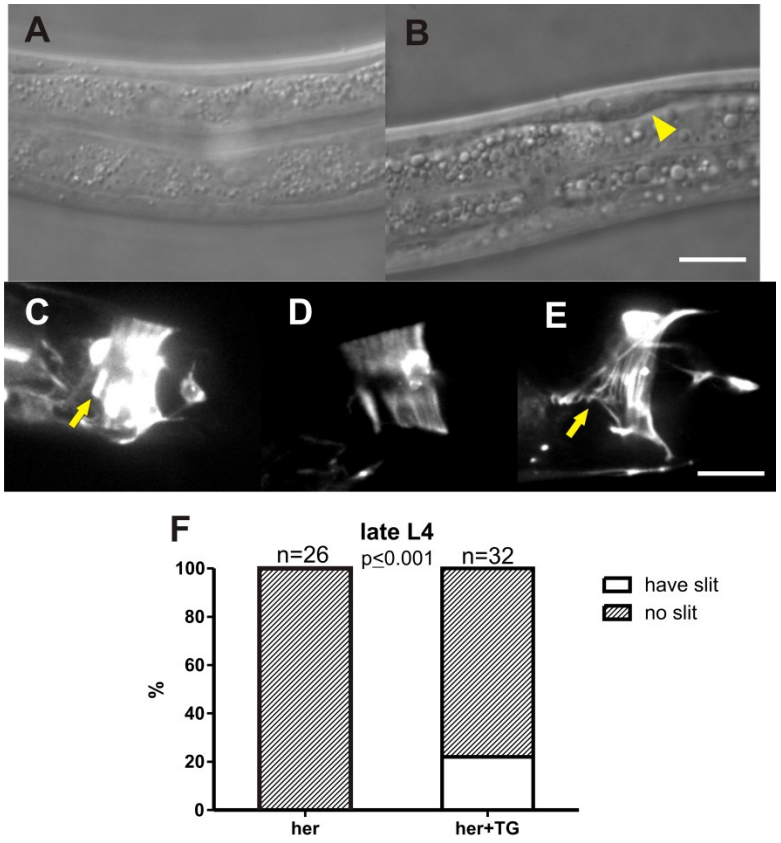

Figure 15. Masculinization of the hermaphrodite sex muscles is able to induce slit formation in the anal depressor. (A and B) Lateral views of the wild-type hermaphrodites' posterior half (A) and hermaphrodites that carry the transgene *rg*Ex*724* [P*hlh-8*: *fem-3* cDNA::SL2:::DsRed; P*unc-103*E:YFP::actin] (B) at early L3 stage. The arrowhead in B indicates the additional cells that were found adjacent to the body wall muscle cells. (C-E) Lateral views of the hermaphrodite anal depressor, which expressed the transgene *rg*Ex*724* [P*hlh-8*: *fem-3* cDNA::SL2:::DsRed; P*unc-103*E:YFP::actin] at late L3 (C), mid-L4 (D) and young adult (E) stages. The arrows in C and D indicate the ventral slits. The arrow in E indicates the reorganizing anterior domain. The pictures were taken in the YFP emission channel.(F) Percentage of animals that possess a ventral slit at late L4 stage in wild type hermaphrodites (her) and hermaphrodites, which expressed the transgene *rg*Ex*724* [P*hlh-8*: *fem-3* cDNA::SL2:::DsRed; P*unc-103*E:YFP::actin] (her+TG). The p value was calculated using Fisher's exact test. All the pictures are positioned as the anterior to the left and ventral to the bottom. For all of the images, the scale bar represents 10µm.

The masculinized early M lineage led to the formation of a ventral slit in the hermaphrodite anal depressor. At the late L3 stage, the ventral region of the muscle cell started to be demarcated into two domains (Figure 15C). During the L4 stage, the slit expanded (Figure 15D). I observed that some of the young adults even had a reorganized sarcomere (Figure 15E). The timing of those reorganization events fits with the wild-type male process (Figure 3D-3F). Therefore I concluded that the masculinization of the M lineage in the hermaphrodite was sufficient to induce anterior movement in the anal depressor muscle. However, only a small proportion of the transgenic hermaphrodites possessed this anal depressor phenotype (Figure 15F). One possible explanation is that the *hlh-8* promoter does not express enough *fem-3* to cause 100% conversion of the M lineage. Overall, the ventral slit in the transgenic hermaphrodite's anal depressor indicates that a male M lineage provides the signal to initiate the anal depressor's anterior movement.

The male endogenous pathway and exogenous signaling function additively to regulate the anterior movement process

The masculinization of the hermaphrodite M lineage confirms that the exogenous signals derived from the male sex muscles contributed to the anterior movement of the male anal depressor. I found that the P*exp-1*:*tra-2* IC transgenic males also possess anterior movement defects (Figure 16). To identify if the endogenous and exogenous signaling pathways are playing parallel or synergistic roles, I feminized the anal depressor in *mab-5* males. I found that the muscle cell had more severe anterior movement defects, compared to either *mab-5* mutants or *tra-2* transgenic worms (Figure

16). Thus I conclude that exogenous signaling and endogenous sex determination mechanisms function additively to regulate the anterior movement of the male anal depressor.

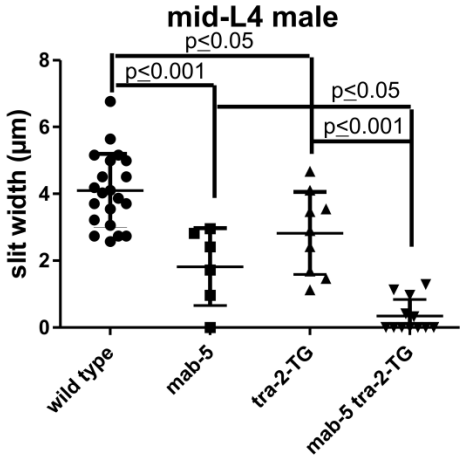

Figure 16. The male sex determination pathway and exogenous signals from the male sex muscles function additively to regulate the male anal depressor's anterior movement. Comparisons of the slit width between the anterior and posterior domains (the slit width is indicated in 5D and 11A by the arrows) among wild-type, *mab-5*, wild type expressing the transgene *rg*Ex*698* [P*exp-1*:*tra-2* (IC)::SL2:::DsRed; P*unc-103*E:YFP::actin] (tra-2-TG) and *mab-5* males expressing the transgene *rg*Ex*698* [P*exp-1*:*tra-2* (IC)::SL2:::DsRed; P*unc-103*E:YFP::actin] (tra-2-TG) at mid-L4 stage. Mean ± SD is indicated. The *p* value was calculated using one-way ANOVA with the Bonferroni's Multiple Comparison Test.

Defecation behavior does not require the male anal depressor during the L4 stage.

Finally, I addressed if the reorganizing anal depressor still participates in defecation behavior during the L4 stage. In larval males and hermaphrodites, the anal depressor projects a muscle arm to the pre-anal ganglion, which it uses to receive

stimulatory input from the defecation neuron DVB (McIntire et al., 1993b; Reiner and Thomas, 1995; Sulston et al., 1980a). I first asked if the larval male anal depressor alters its pre-anal ganglion muscle arm during development. To visualize the anal depressor cytoplasm, including the filopodia and muscle arm extension, I expressed the cytoplasmic DsRed protein from a pan-muscular *lev-11* tropomyosin promoter. This specific construct expresses in the body wall muscles and the anal depressor, but not in the pharyngeal or intestinal muscle.

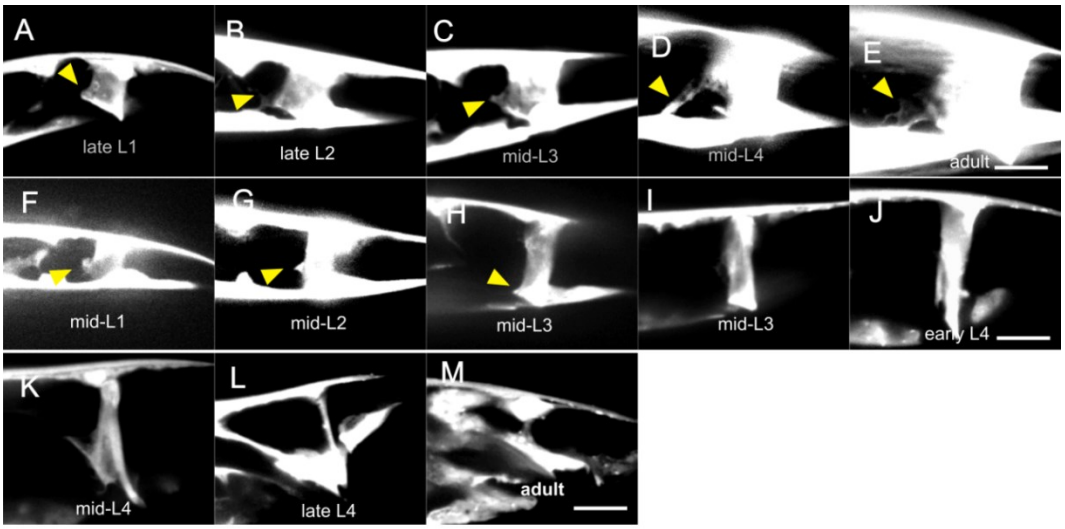

Figure 17. The male anal depressor retracts the muscle arm from the pre-anal ganglion at the L3 larval stage. (A-E) Lateral views of the anal depressor of: late L1 (A), late L2 (B), mid-L3 (C), mid-L4 (D) and an adult (E) stage hermaphrodite. All the animals imaged carried the integrated transgene *rg*Is*3* [P*lev-11*:Dsred; P*lev-11*:G-CaMP]. The P*lev-11*:G-CaMP happened to be part of the integrated transgene, and was not used for any analyses in this report. The arrowhead in each image indicates the muscle arm extended into the pre-anal ganglion region. (F-M) Lateral views of the male anal depressor at mid-L1(F), mid-L2(G), mid-L3(H and I), early L4(J), mid-L4(K), late L4(L) and adult(M) stage. All the animals imaged carried the integrated transgene *rg*Is*3* [P*lev-11*:Dsred; P*lev-11*:G-CaMP]. The arrowheads in (F-H) indicate the muscle arm extended into the pre-anal ganglion region. All the pictures are positioned as the anterior to the left and ventral to the bottom. For all of the images, the scale bar represents 10µm.

I found that the anal depressor muscle arm exhibited dynamic changes in the male. In the hermaphrodite, the anal depressor maintained an obvious muscle arm in the pre-anal ganglion region throughout adulthood (Figure 17A-17E and Table 1). However, in the male, the muscle arm began to retract during the L3 stage (Figure 17F-17H, and Table 1). Concurrent with the muscle arm retraction , I observed that the male anal depressor started to extend filopodia dorsal-anteriorly towards the sex muscle cells in 78% (n=18) of the males. By L4 stage, the male anal depressor muscle arm projection could not be easily identified in the pre-anal ganglion region (Figure 17I-17M, and Table 1). When I feminized the anal depressor with the *tra-2* IC construct, the muscle arm retraction also occurred, but was delayed to mid- to late L4 stage for the majority of the males (Figure 17G-17L, and Table 1). This indicates that aspects of this process might be regulated by the intrinsic sex of the anal depressor, in addition to the cell-cell interactions with neighboring male cells.

Table 1. Percentages of animals that have muscle arm extended into the pre-anal ganglion.

	Mid-L2	Mid-L3	Early L4	Mid-L4	Adult
Wild-type Her	100% (n=15)	100% (n=7)	100% (n=12)	100% (n=14)	100% (n=9)
Her+TG	100% (n=12)	100% (n=17)	100% (n=8)	100% (n=9)	100% (n=13)
Wild-type Male	100% (n=13)	44% (n=18)	0% (n=17)	0% (n=16)	0% (n=15)
Male+TG	100% (n=11)	82% (n=17) *	46% (n=26) **	19% (n=16)	0% (n=39)

* Fisher's exact test comparing mid-L3 wild-type males with mid-L3 males carrying the transgene (TG) [P*exp-1*: *tra-2* (IC)::SL2:::DsRed]; p=0.0354. ** Fisher's exact test comparing early L4 wild-type males with early L4 males carrying the transgene (TG) [P*exp-1*: *tra-2* (IC)::SL2:::DsRed]; p=0.0011.

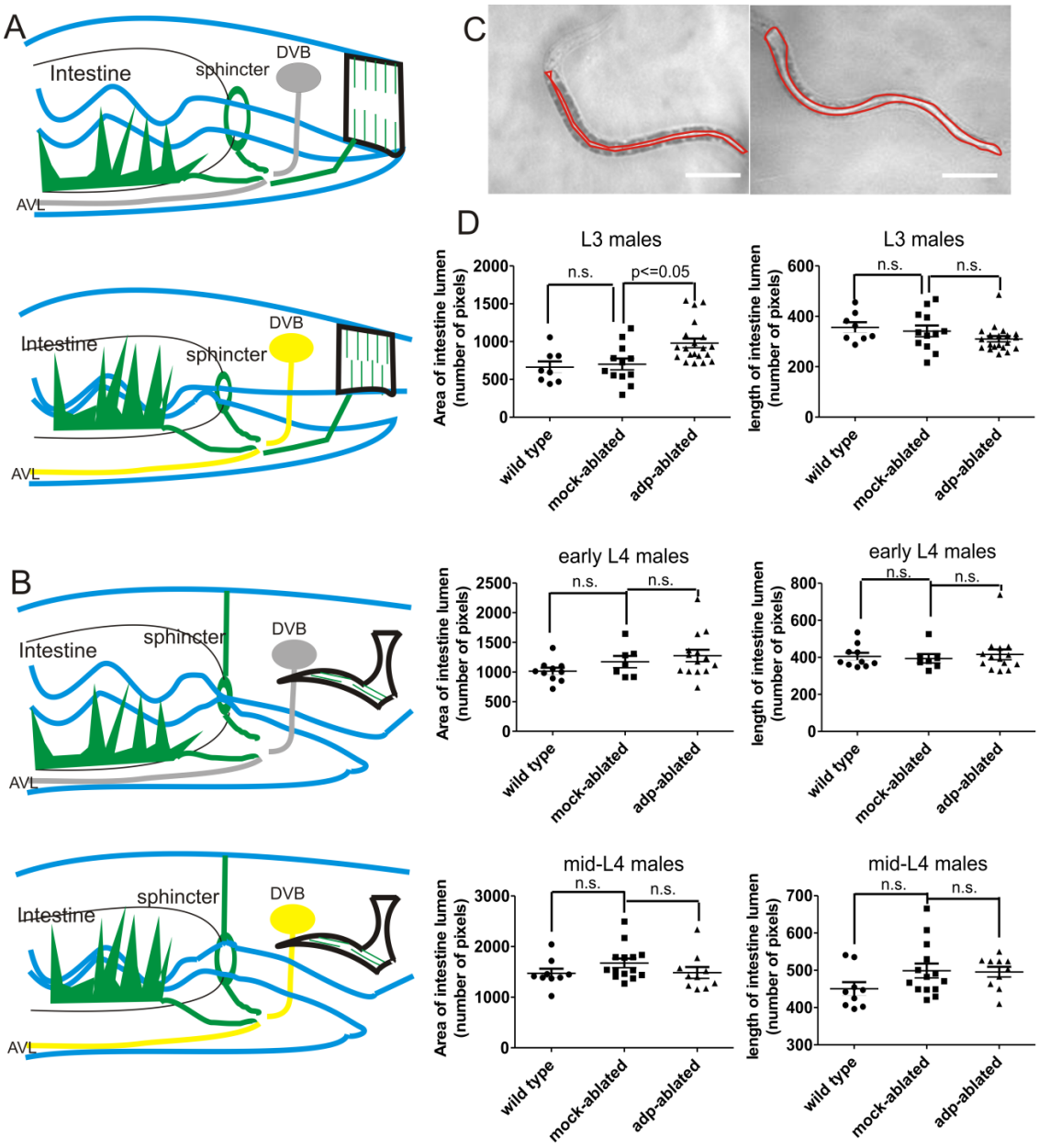
A
Intestine
sphincter
DVB
AVL
Intestine
sphincter
DVB
AVL
B
Intestine
sphincter
DVB
AVL
Intestine
sphincter
DVB
AVL
C
D
L3 males
n.s.
p<=0.05
Area of intestine lumen (number of pixels)
2000
1500
1000
500
0
wild type
mock-ablated
adp-ablated
L3 males
n.s.
n.s.
length of intestine lumen (number of pixels)
600
400
200
0
wild type
mock-ablated
adp-ablated
early L4 males
n.s.
n.s.
Area of intestine lumen (number of pixels)
2500
2000
1500
1000
500
0
wild type
mock-ablated
adp-ablated
early L4 males
n.s.
n.s.
length of intestine lumen (number of pixels)
800
600
400
200
0
wild type
mock-ablated
adp-ablated
mid-L4 males
n.s.
n.s.
Area of intestine lumen (number of pixels)
3000
2000
1000
0
wild type
mock-ablated
adp-ablated
mid-L4 males
n.s.
n.s.
length of intestine lumen (number of pixels)
700
600
500
400
300
wild type
mock-ablated
adp-ablated

Figure 18. Defecation does not rely on the reorganizing anal depressor during L4 development. (A) Expulsion in hermaphrodite and larval males. The top figure shows that when the expulsion step is not activated, the anus is closed and the sphincter is relaxed. The bottom figure shows that when expulsion occurs, the intestinal muscles and the sphincter contract to squeeze the intestinal contents posteriorly, and the contraction of the anal depressor helps to open the anus to allow expulsion to occur [adapted from (Thomas, 1990)]. (B) Expulsion in adult males. The top figure shows that when the expulsion step is not activated, the sphincter contracts to seal the intestine. When defecation occurs (bottom figure), the sphincter relaxes to allow the intestinal contents to pass through (McIntire et al., 1993a; McIntire et al., 1993b; Reiner and Thomas, 1995). The anal depressor does not participate in defecation in adult males [adapted from (Reiner and Thomas, 1995)]. (C) Worms that can defecate effectively have a long and thin intestine (left figure), whereas worms that have defecation defects have a bloated intestine (right figure). The intestinal area is measured as the number of pixels within the intestinal lumen (highlighted region). The scale bar is 100 μM. (D) Dot plots on the left compare the intestinal lumen area of mock-ablated animals with anal-depressor-ablated animals at L3, early L4 and mid-L4 stages. The dot plots on the right compare the length of the intestinal lumen to show that there was no difference regarding the worm size between the differentially operated worms. The *p* value was calculated using one-way ANOVA with the Bonferroni's Multiple Comparison Test (n.s. = not significant).

We know little of the mechanistic details of the adult male defecation program, other than the sphincter's requirement for molecules that promote inhibitory GABA signal transduction (Figure 18A, 18B) (Reiner and Thomas, 1995). During L4 stage, the sphincter alters the muscle fiber organization and becomes hypertrophied. In adult males, the inhibitory GABA signaling relaxes the sphincter and allows expulsion to occur (Reiner and Thomas, 1995; Sulston et al., 1980a). However, the correlation between the retraction of the anal depressor muscle arm and morphological reorganization suggests that the male adult defecation program might function as early as late L3 to L4 stage.

To determine when the adult male defecation system becomes functional, I laser-ablated the anal depressor nucleus in L1 animals. I noted that although the anal depressor corpse persisted throughout L1 to the end of the L3 larval stages, the operation led to ineffective expulsion, accumulation of intestine contents and a dilated (constipated) intestinal lumen (Figure 18C and 18D). When the anal depressor-ablated worms developed into L4 larva, the dilated intestine phenotype disappeared, suggesting that some level of defecation behavior was restored (Figure 18D). Therefore, I suggest that the reorganizing anal depressor does not participate in defecation behavior during L4 development, and likely, the defecation program used by the adult males is capable of functioning during the early L4 stage.

Chapter III summary

Both endogenous and exogenous sex determination mechanisms are required to achieve the sexually dimorphic development of the anal depressor. By illuminating the

sarcomere structure using YFP-tagged actin, I found that the male anal depressor alters the orientation of the sarcomere during L4 development. Feminized male anal depressor displays hermaphrodite-like anterior growth, whereas masculinized hermaphrodite anal depressor has restrained anterior growth. Therefore I concluded that early anterior growth of the anal depressor is controlled by the cell-autonomous sex determination pathway. The M cell-ablated male and the *mab-5* mutant male have defects to extend an anterior domain to disassemble the sarcomere. This suggests that the two processes are controlled by signaling derived from the male sex muscles. Additionally, laser ablation of the anal depressor does not affect defecation behavior after L4 development, indicating it does not function as a defection muscle after being reorganized. Therefore, the morphological change of the male anal depressor is accompanied by functional transition.

CHAPTER IV

WNT SIGNALING REGULATES DEVELOPMENT OF THE MALE ANAL DEPRESSOR

The sarcomere disassembly during L4 larval stage is controlled by the Wnt signaling pathway

Anal depressor development in male *C. elegans* is a sexually dimorphic process. The L4 developmental process is of particular interest because the sarcomere change is dramatic. During early L4 development, a ventral slit demarcates the muscle cell into anterior and posterior domains (Figure 19A and 19B). This process is accompanied by the anterior retraction of the tail tip cells (Figure 19A' and 19B'). By the time the tail tip cells are completely retracted from the cuticle (Figure 19C'), the anterior domain moves from the rectum to the top of the male developing sex muscles. Filopodia start to extend along the sex myoblasts and the sarcomere contained within the anterior domain disassembles (Figure 19C). The posterior domain remains intact until the hypodermal cells start to retract dorsally (Figure 19D'). The posterior sarcomere disassembles, and the length of the domain reduces as the dorsal retraction proceeds (Figure 19D and 19E). Morphogenesis of the rays also occurs during this time period (Figure 19E'). Just before L4 molt, the disassembled sarcomere filaments are depleted from the posterior domain. At L4 molt, a novel sarcomere is established on top of the sex muscles, running anterior-posteriorly (Figure 19F and 19F').

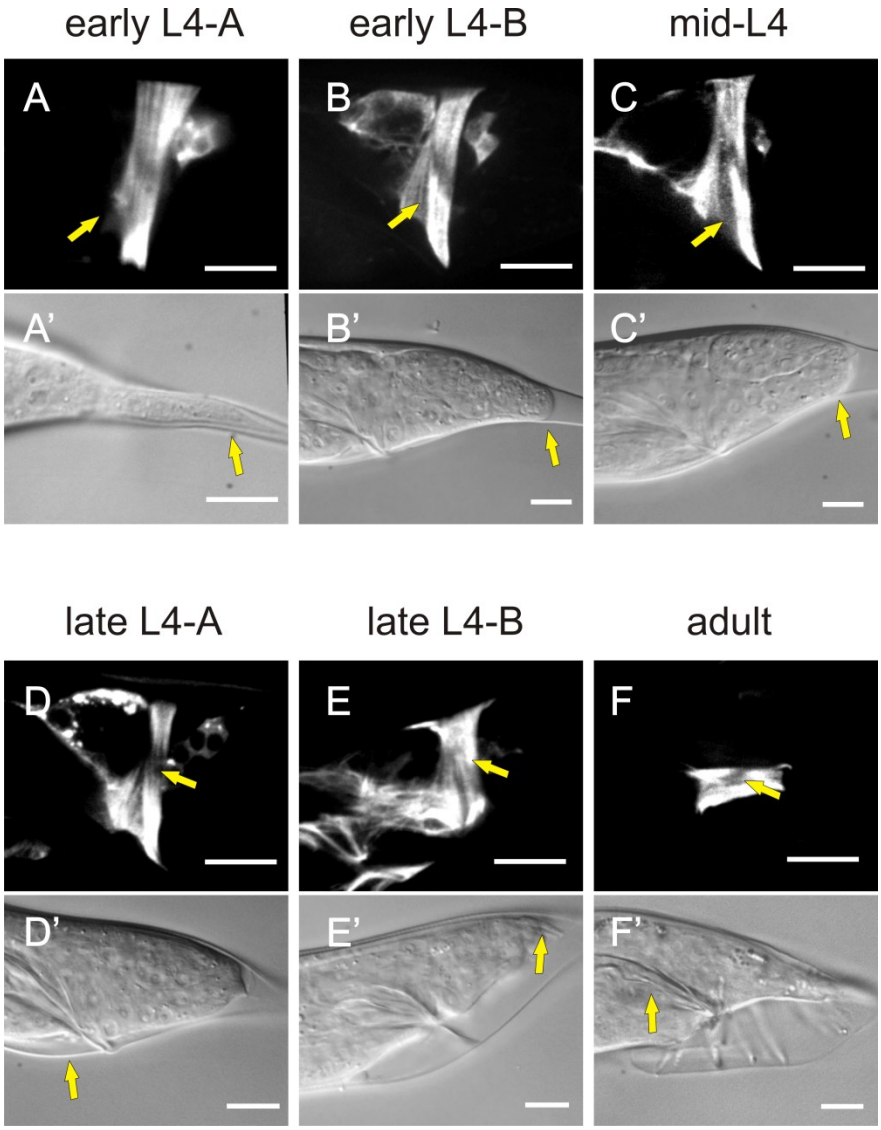

Figure 19. The male anal depressor reorganizes the sarcomere during L4 development. (A-F) Lateral view of the male anal depressor at: early L4 stage 1 (A), early L4 stage 2 (B), mid-L4 (C), late L4 stage 1 (D), late L4 stage 2 (E), and adult (F). All the animals imaged carry the transgene *rg*Ex*497* [P*unc-103*E:YFP::actin]. Arrows in (A-C) indicates the slit formed at the ventral region of the anal depressor. Arrow in (D) indicates the disassembled H zone in the posterior anal depressor. Arrow in (E) indicates the H zone disappears from the posterior domain of the anal depressor. Arrow in (F) indicates the H zone of the new sarcomere in the adult anal depressor. (A'-F') Corresponding Normaski images of the male tail for (A-F). (A' and B') The arrows indicate the retracting tail tip cells. (C') The arrow indicates that the tail tip cells complete anterior retraction. (D') The arrow indicates that the tail hypodermal cells start to retract dorsally. (E') The arrow indicates the rays. (F') The arrow indicates the spicules. All the pictures are positioned as the anterior to the left and ventral to the bottom. For all of the images, the scale bar represents 10μm.

Wnt signaling pathway has been shown to be involved in vertebrate cardiogenesis (Lin et al., 2007; Naito et al., 2006; Qyang et al., 2007; Ueno et al., 2007). It also has been shown to regulate cell polarity in *Drosophila* and cell migration in *C. elegans* (Chalfie et al., 1981; Kenyon, 1986). Therefore, it is a good candidate for regulating the anal depressor development during L4 stage. There are three Wnt ligands that are expressed from the hermaphrodite tail region during larval development: *egl-20*, *lin-44* and *cwn-1* (Figure 20A) (Herman et al., 1995; Inoue et al., 2004; Pan et al., 2006; Whangbo and Kenyon, 1999). Since the male tail may possess an expression pattern similar to the hermaphrodite, the Wnt ligands may be the morphogen to trigger the sarcomeric reorganization. I examined the *egl-20*, *lin-44* and *cwn-1* loss of function mutants to observe if they have anal depressor developmental defects (Figure 20B-20G).

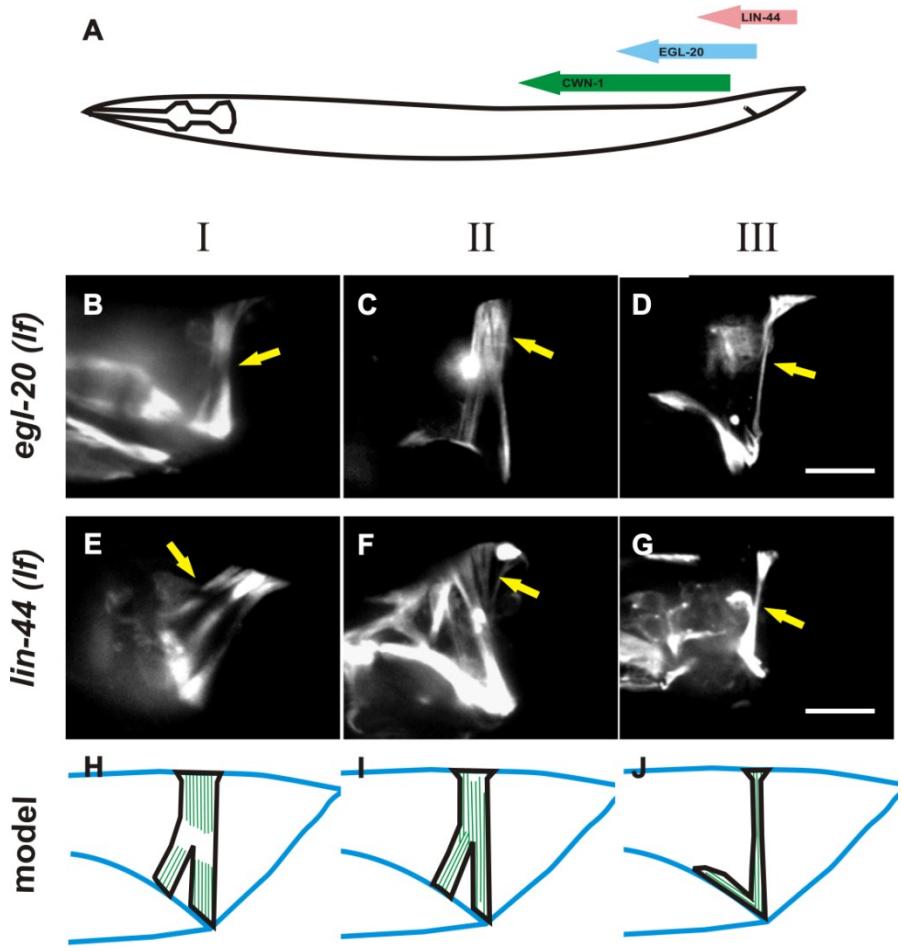

Figure 20. Wnt mutants possess anal depressor sarcomere disassembly defects. (A) Cartoon showing the expression domain of *lin-44*, *egl-20*, and *cwn-1* in the posterior half of the hermaphrodite. (B-D) Anal depressor of *egl-20 (n585)* adult males display defects in sarcomere disassembly. The posterior domain of the anal depressor either maintains the sarcomere (B) (type I), retains large amount of myofilaments (C) (type II), or retain residual myofilaments (D) (type III). (E-G) Anal depressor of *lin-44 (n1792)* adult males display defects in sarcomere disassembly. The posterior domain of the anal depressor either maintains the sarcomere (E) (type I), retains large amount of myofilaments (F) (type II), or retains residual myofilaments (G) (type III). All the animals assayed carry the transgene *rg*Ex*497* [P*unc-103*E:YFP::actin]. The arrows in (B) and (E) indicate the H zone of the sarcomere. The arrows in (C), (D), (F), and (G) indicate the myofilaments retained in the anal depressor. (H-J) Model images of the anal depressor for type I (H), type II (I) and type III (J) defectiveness. The actin filaments are represented by greenish blue lines. All the pictures are positioned as the anterior to the left and ventral to the bottom. For all of the images, the scale bar represents 10µm.

The *egl-20(n585)* adult males have variably defective anal depressor, which either fails to disassemble its sarcomere (Figure 20B) or fails to deplete the myofilaments (Figure 20C and 20D). Based on the severity of the phenotype, the defectiveness of the adult male depressor was classified into three types (Figure 20H-20J). Anal depressors that have the type I defects fail to initiate the disassembly process, and therefore maintain the posterior sarcomere (Figure 20H). The rest manage to start disassembling the sarcomere (indicated by the disappearance of the H zone), but fail to remove the myofilaments from the posterior domain. Based upon the amounts of filaments retained, the defects were classified as type II, if they contain large amounts of filaments (Figure 20I), and type III if they contain few filaments (Figure 20J). The type I defects are the most severe, in which the disassembly signaling is absent. The type III defects are the least severe in which the majority of the disassembly process is completed. The variability of the *egl-20(n585)* mutant phenotype indicates that there is compensating signaling derived from other Wnt ligands. As expected, *lin-44(n1792)* mutants also possess sarcomere disassembly defects similar to the *egl-20* mutants (Figure 20E-20G). I classified the defectiveness of *lin-44* mutant anal depressor using the same method as for *egl-20*; and I found that compared to *egl-20, lin-44* mutants have a higher mutant penetrance in regards to the anal depressor morphology (Figure 21B). I also measured the area of the anal depressor that is filled with retained myofilaments (Figure 21A). The broad range of the data shows that the disassembly defects are variable among individuals. The majority of the *cwn-1(ok546)* mutants display wild type anal depressor development (Figure 21A and 21B), indicating that CWN-1 plays a minor

role in regulating sarcomere disassembly. Therefore, I concluded that EGL-20 and LIN-44 play a major role in regulating sarcomere disassembly in the male anal depressor.

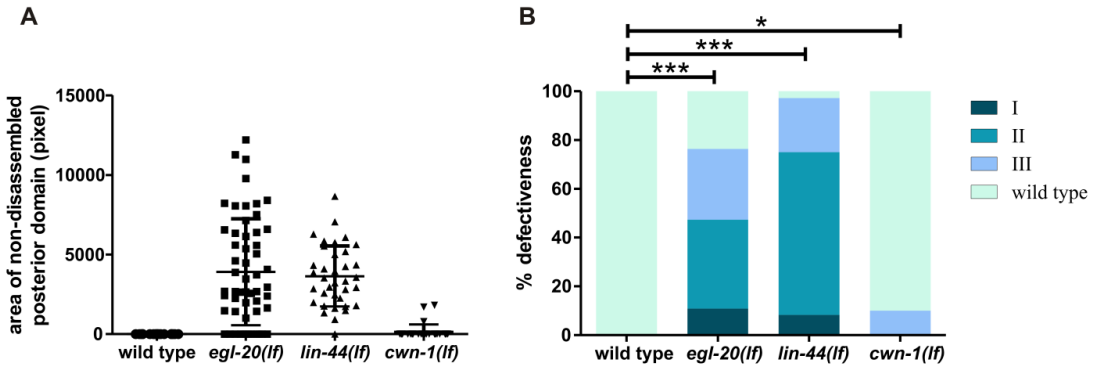

Figure 21. Quantification and classification of the anal depressor defects of Wnt mutants. (A) Area of the non-disassembled posterior domain of the anal depressor of wild type (n=52), *egl-20 (n585)* (n=55), *lin-44(n1792)* (n=36), and *cwn-1(ok546)* (n=30) adult males. All the animals assayed carry the transgene *rg*Ex*497* [P*unc-103*E:YFP::actin]. (B) Calculated percentage of anal depressor defects for wild type, *egl-20 (n585)*, *lin-44(n1792)*, and *cwn-1(ok546)* adult males based on data in (A): 100% of the wild type adult males have a wild type adult anal depressor; 10.9%, 36.4%, 29.1%, and 23.6% of the *egl-20 (n585)* adult males have type I, II, III and wild type anal depressors, respectively; 8.3%, 66.7%, 22.2%, and 2.8% of the *lin-44(n1792)* adult males have type I, II, III and wild type anal depressors, respectively; 0%, 0%, 10%, and 90% of the *cwn-1(ok546)* adult males have type I, II, III and wild type anal depressors, respectively. *** $p<0.0001$; * $p=0.0458$. The p values were calculated between the wild type and defective (I+II+III) groups using Fisher's exact test.

Wnt can activate different downstream components to trigger distinct cellular events (Komiya and Habas, 2008; Niehrs, 2012). The canonical Wnt pathway inhibits the APC-Axin-GSK3-CK1 complex and frees β-catenin to initiate cell fate gene expression. The Wnt-calcium pathway releases Ca^{2+} from the ER to activate downstream Ca^{2+} responsive proteins. The Wnt-PCP pathway activates ROCK and JNK, which then

regulate actin polymerization and cytoskeleton reorganization. To identify the signaling components that act downstream of EGL-20 and LIN-44, I first examined the canonical pathway mutants, including the Frizzled and β-catenin mutants. *C. elegans* has four homologs for Frizzled: *lin-17*, *mig-1*, *cfz-2* and *mom-5*. I have examined two of them: *lin-17* and *mig-1*. *lin-17(e620)* mutant males have anal depressor disassembly defects (Figure 22A and 22B). However, the anal depressor defects in 30% of the *lin-17(e620)* mutants (n=17) are more severe compared to the *egl-20(lf)* mutants (Figure 21B, 22A-22B). This might be that the *lin-17(e620)* mutation confers pleiotropic developmental defects to the male tail, which also compromise the anal depressor's morphology. To confirm the role of LIN-17 in regulating sarcomere disassembly, I knocked down *lin-17* expression using RNAi feeding method. The RNAi-treated males develop a more normal tail, indicating that the residue LIN-17 activity allows early larval development to occur normally. However, I still observed sarcomere disassembly defects in the anal depressor, and the defect level is comparable to the Wnts mutants (Figure 21A and 22C). This suggests that LIN-17 is involved in the regulation of sarcomere disassembly, and the disassembly process is sensitive to LIN-17 dosage. None of the *mig-1* mutants display any anal depressor defects, indicating the MIG-1 Wnt receptor is not involved in the reorganization process.

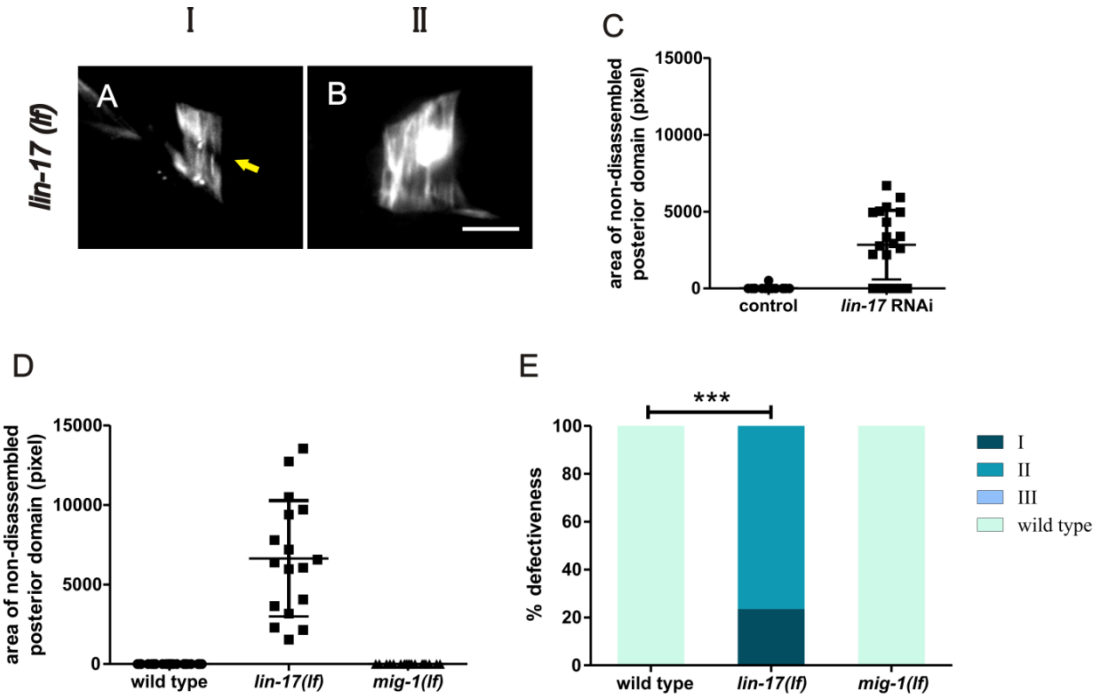

Figure 22. Frizzled mutants possess anal depressor disassembly defects. (A-B) Anal depressor of *lin-17(e620)* adult males display defects in sarcomere disassembly. The posterior domain of the anal depressor either maintains the sarcomere (A) (type I), or retains large amounts of myofilaments (B) (type II). The arrow in (A) indicates the H zone of the sarcomere. (C) Area of non-disassembled posterior domain of the anal depressor of RNAi control (n=25) and *lin-17* RNAi (n=20) adult males. (D) Area of non-disassembled posterior domain of the anal depressor of wild type (n=52), *lin-17(e620)* (n=17), and *mig-1(e1787)* (n=18) adult males. (E) Calculated percentages of anal depressor defectiveness for wild type, *lin-17(e620),* and *mig-1(e1787)* adult males based on data in (D): 100% of the wild type adult males have a normal anal depressor; 23.5%, 76.5%, 0% and 0% of the *lin-17(e620)* adult males have type I, II, III and wild type anal depressors, respectively; 100% of the *mig-1(e1787)* males have a wild type adult anal depressor. *** $p<0.0001$. The p value was calculated between the wild type and defective (I+II+III) groups using Fisher's exact test. (A-E) All the animals assayed carry the transgene *rg*Ex*497* [P*unc-103*E:YFP::actin]. All the pictures are positioned as the anterior to the left and ventral to the bottom. For all of the images, the scale bar represents 10μm.

Among the β-catenin homologs in *C. elegans*, *bar-1* and *hmp-2* are the possible downstream effectors to promote anal depressor sarcomere disassembly. The other β-catenin homolog, *wrm-1,* is involved in a non-canonical Wnt pathway which is essential

for embryonic development (Rocheleau et al., 1999). Therefore it is difficult to assess the role of *wrm-1* during post-embronyic development. *bar-1(ga80)* mutant males have the anal depressor sarcomere disassembly defects (Figure 23A-23C). In addition, the *bar-1* mutation confers a novel phenotype that was not observed in other Wnt mutant lines (Figure 23B). Besides anterior migration, the anterior domain exhibits anterior lateral growth on top of the sex muscles (Figure 23B). For the type I defects observed in *bar-1* mutants, the anal depressor maintains an intact sarcomere in both the anterior and posterior domain (Figure 23A). This indicates that in those animals, the sarcomere disassembly signaling is absent in both the anterior and posterior domain. The differences regarding the defectiveness between the *bar-1* and Wnt mutants (*egl-20* and *lin-44*) indicate that BAR-1 regulates a wider range of cellular events than EGL-20 and LIN-44. Or alternatively, BAR-1 is the common effector for both LIN-44 and EGL-20; if this possibility is correct, then *lin-44 egl-20* double mutants should display the same level of defects as the *bar-1* single mutants. HMP-2 is the β-catenin that is localized to the adheren junction complex and basically functions as a structural protein instead of a signaling protein (Korswagen et al., 2000). Therefore, only a small proportion of the *hmp-2* mutants exhibit minor disassembly defects (Figure 23D and 23E).

Based on the data for Wnt, Frizzled and β-catenin mutants, I concluded that the Wnt-canonical signaling pathway regulates the disassembly of anal depressor sarcomere.

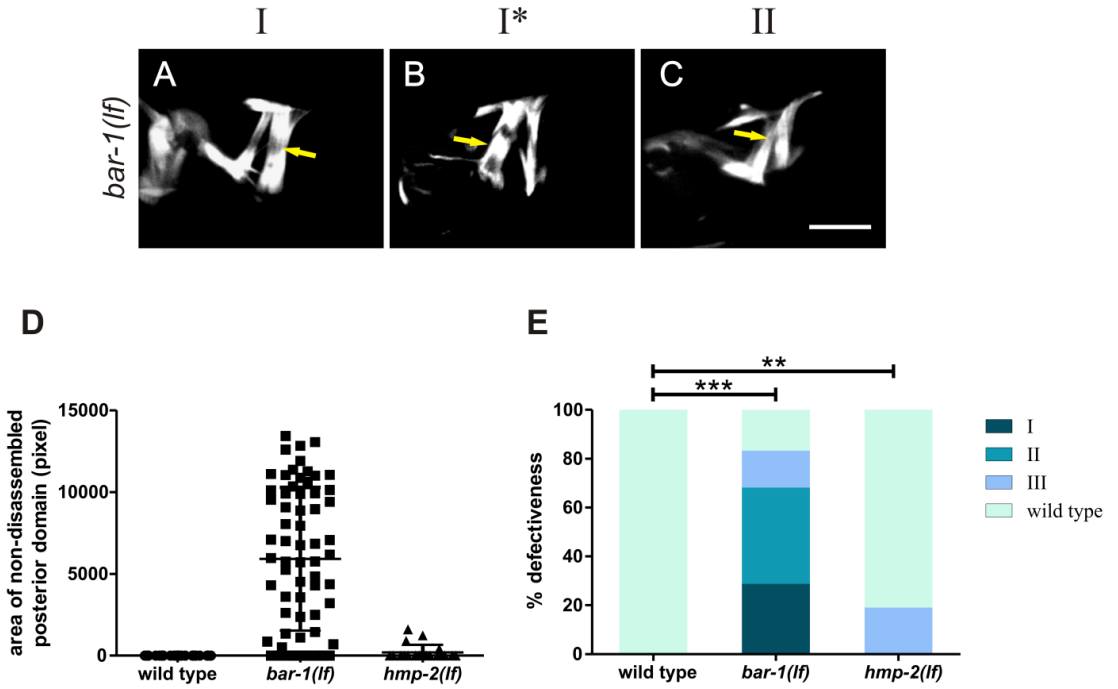

Figure 23. β-catenin mutants have anal depressor disassembly defects. (A-C) Anal depressor of *bar-1(ga-80)* adult males display sarcomere disassembly defects. The posterior domain of the anal depressor either maintains the sarcomere (A-B) (type I), or retains large amount of myofilaments (B) (type II). I* indicates the novel type of defects, in which the anterior domain grows anteriorly (arrow). The arrow in (A) indicates the H zone of the sarcomere; the arrow in D indicates the myofilaments retained in the anal depressor. (D) Area of non-disassembled posterior domain of the anal depressor of wild type (n=55), *bar-1(ga80)* (n=66), and *hmp-2(qm39)* (n=21) adult males. (E) Calculated percentages of anal depressor defectiveness for wild type, *bar-1(ga80),* and *hmp-2(qm39)* adult males based on data in (D): 100% of the wild type adult males have a wild type adult anal depressor; 28.8%, 39.4%, 15.2%, and 16.6% of *bar-1(ga80)* adult males have type I, II, III and wild type anal depressors, respectively; 19% and 81% of *hmp-2(qm39)* adult males have type III and wild type anal depressors, respectively. *** $p<0.0001$; ** $p=0.0047$. The p values were calculated between the wild type and defective (I+II+III) groups using Fisher's exact test. (A-E) All the animals assayed carry the transgene *rg*Ex*497* [P*unc-103*E:YFP::actin]. All the pictures are positioned as the anterior to the left and ventral to the bottom. For all of the images, the scale bar represents 10μm.

Determining the site of action of Wnt-canonical pathway

There are two possible mechanisms Wnt-canonical signaling uses to regulate the sarcomere disassembly of the anal depressor. The Wnt signaling could act on the anal depressor itself, by initiating expression of muscle remodeling genes or differentiation genes. Or it could be affecting the cell fate specification of the neighboring cells, which serve as the signaling center for anal depressor remodeling. To differentiate between these two possibilities, I first examined the expression pattern of the Wnts, receptors and β-catenin.

I used the fluorescent protein *Timer*, which shifts its fluorescence emission from green to red over time, to examine the timing and the expression domain of *egl-20* in the male tail (Figure 24A-24C). EGL-20 is expressed from the male sex myoblasts and the anal depressor as early as late L3, just before the anal depressor starts to form a ventral slit (Figure 24A and 24B). The expression persists throughout L4 development (Figure 24C). Therefore, EGL-20 is actively expressed from the developing sex muscles and the anal depressor itself over the time period of the male anal depressor reorganization.

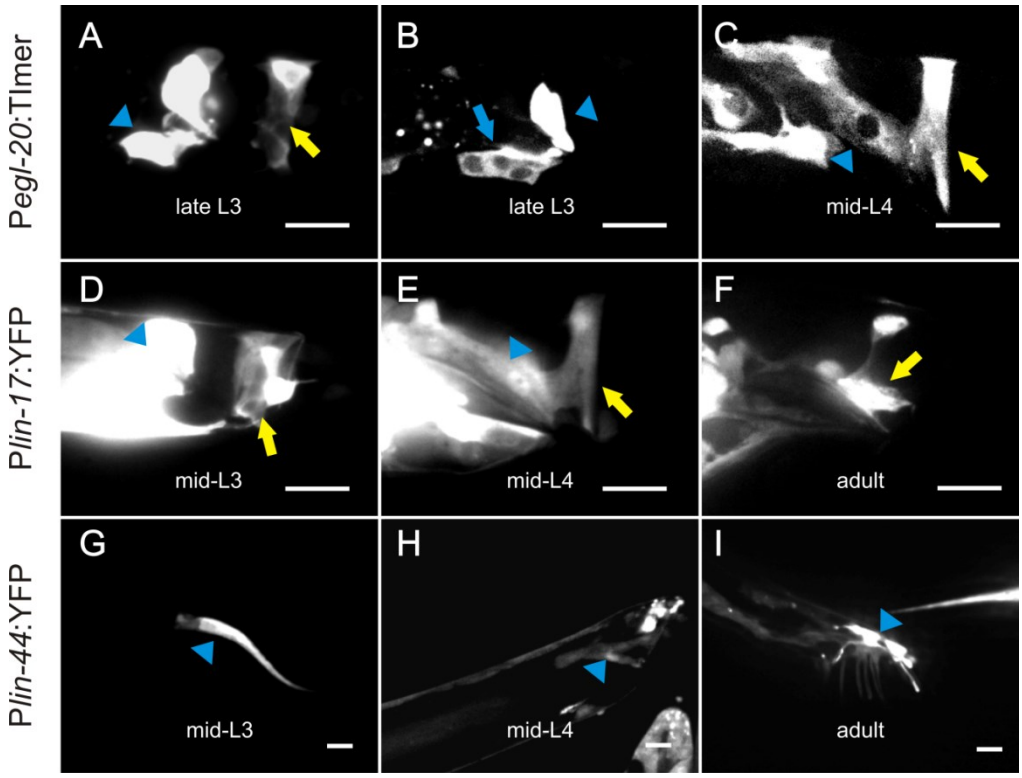

Figure 24. Expression profile of Wnt and Frizzled during different developmental stages. (A-C) *egl-20* is expressed from the anal depressor (yellow arrow in A and C), the sex myoblasts (blue arrow in B and blue arrowhead in C), and the B lineage cells that form the cloaca (blue arrowhead in A and B) at L3 (n=4) and L4 larvae (n=10). All the animals imaged carry the transgene *rg*Ex*726* [P*egl-20*:Timer]. All the images were taken with the wavelength of 540nm. (D-F) *lin-17* is expressed from the anal depressor (yellow arrow in D, E and F), the proctodeum (arrowhead in D), and the B lineage cells that form the spicules (arrowhead in E) during larval (n=25) and adult development (n=16). All the animals imaged carry the transgene *rg*Ex*804* [P*lin-17*:YFP]. (G-I) *lin-44* is expressed from the hyp 8-11 (arrowhead in G and H) throughout larval development (n=22). In the adults (n=5), some of the ray neurons also express LIN-44 (arrowhead in I). All the animals imaged carry the transgene *rg*Ex*802* [P*lin-44*:YFP]. All the pictures are positioned as the anterior to the left and ventral to the bottom. For all of the images, the scale bar represents 10μm.

The M cell-derived male sex muscles have been shown to promote sarcomere disassembly in the anal depressor (Figure 11I, 12C and 12D). Unless they produce additional cues for anal depressor reorganization, the male sex muscles are likely the

signaling source of EGL-20. However, the anal depressor defects seen in the M cell-ablated worms are less severe compared to the *egl-20* mutants (Figure 11I and 20B). This indicates that either there is still residue EGL-20 signaling from the M-cell-operated sex muscles, or that the anal depressor-derived EGL-20 signaling also contributes to the disassembly of the posterior sarcomere. Autocrine Wnt signaling has been seen mainly in stem cell or cancer cell self-renewal (Akiri et al., 2009; Bafico et al., 2004; Lim et al., 2013). However, self-promoting Wnt has not been shown to regulate sarcomere disassembly. I rescued *egl-20* expression in the anal depressor in *egl-20* mutants. The transgenic worms show complete rescue of the sarcomere disassembly defects (Figure 25A and 25B). This indicates that autocrine Wnt signaling is sufficient to induce anal depressor reorganization. However, the endogenous EGL-20 signaling from the anal depressor might be weaker compared to transgene expression, and therefore still requires the additional EGL-20 secreted from the sex muscles. To assess the role of self-derived EGL-20 signaling, anal depressor-specific knock-out of EGL-20 needs to be conducted to observe if there are any disassembly defects.

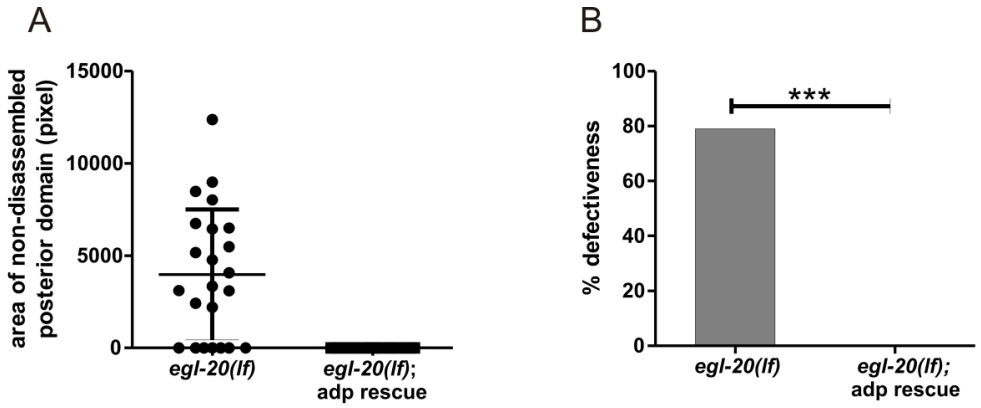

Figure 25. Cell-specific rescue of *egl-20* expression from the anal depressor rescued the sarcomere disassembly defects. (A) Area of the non-disassembled posterior domain of the anal depressor of *egl-20(n585)* adult males (*egl-20(lf)*; n=23), or *egl-20(n585)* adult males that carry the transgene *rg*Ex*803* [P*aex-2*:*egl-20*::SL2:::DsRed; P*unc-103E*:YFP::actin] (*egl-20(lf)*; adp rescue; n=26). (B) Percentage of anal depressor defects of *egl-20(n585)* adult males (*egl-20(lf)*), or *egl-20(n585)* adult males that carry the transgene *rg*Ex*803* [Paex-2: EGL-20::SL2:::DsRed; Punc-103E: YFP::actin] (*egl-20(lf)*; adp rescue) based on data in (A): 79% of the *egl-20(n585)* adult males have defective anal depressor; 100% of the *egl-20(n585)* adult males that carry the transgene have wild type anal depressor. *** $p < 0.0001$. The p value was calculated using Fisher's exact test.

I also examined the tissues that express LIN-44. I found that *lin-44* promoter activity was very strong in the male tail. During larval stage (L1 to L4), LIN-44 was expressed from the tail hypodermal cells: hyp 8, 9, 10 and 11 (Figure 24G). During mid L4, when they fused and completed retraction from the tail tip, those hypodermal cells were still expressing LIN-44 (Figure 24H). The expression persists until adulthood (Figure 24I). Starting from late L4, some of the ray precursor cells also express LIN-44 (Figure 24I). Thus in contrast to EGL-20, where the expression domain is anterior to the anal depressor, tissues that express LIN-44 are located posterior to the anal depressor.

LIN-17 is expressed in the anal depressor, the proctodeum, and the B lineage cells that form adult spicules during larval and adult development (Figure 24D-24F). The expression in the sex myoblasts initiates at around early L4 and persists until adulthood (Data not shown). However, the sex muscle expression is weaker and less consistent compared to the expression in the anal depressor. The expression from the sex muscles is seen in 52% of the L4-adult worms examined (n=29), whereas 93% of those worms express LIN-17 in the anal depressor. Therefore, LIN-17 is more likely to function in the anal depressor, rather than the sex muscles.

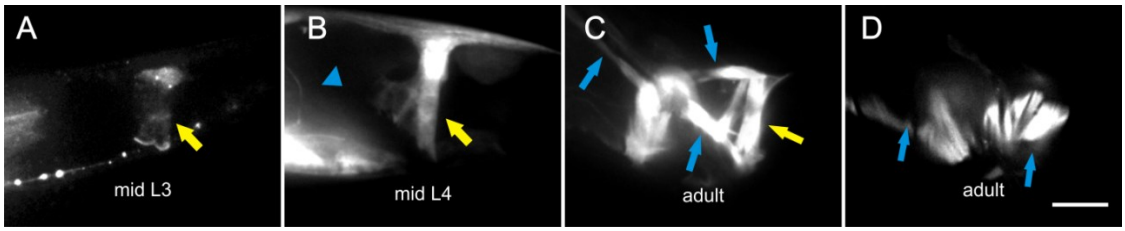

Figure 26. *bar-1* is expressed from the anal depressor during larval development. (A-B) *bar-1* is expressed in the anal depressor (yellow arrow) at mid-L3 (A) and mid-L4 (B). Note that there is no expression in the sex myoblasts during L4 development (blue arrowhead in B). The animals assayed all carry the transgene *rg*Ex*783* [P*bar-1*:*bar-1*::YFP; P*bar-1*:CFP]. (A) is taken at the wavelength of 525nm; (B) is taken at the wavelength of 480nm. (C-D) *bar-1(ga80)* mutant males have wild type morphogenesis of sex muscles. The blue arrows in C and D indicate the correctly localized sex muscles, the yellow arrow indicates the anal depressor. The animals assayed carry the transgene *rg*Ex*497* [P*unc-103*E:YFP::actin]. All the pictures are positioned as the anterior to the left and ventral to the bottom. For all of the images, the scale bar represents 10μm.

To monitor the expression pattern of β-catenin, I used the promoter of *bar-1* to drive the expression of CFP, or *bar-1* promoter driving expression of BAR-1 protein

tagged with YFP (Eisenmann et al., 1998). The second construct allows me to monitor active β-catenin signaling in the anal depressor. I found that BAR-1 is actively expressed and functionally active in the male anal depressor during larval and adult development (Figure 26A and 26B, n=36). None of those constructs displayed any expression in the sex muscles during L4 development (Figure 26B), indicating there is no active form of BAR-1 in the sex muscles. I did not examine the BAR-1 activity in earlier M lineage. But the *bar-1* mutants did not display any obvious defects in sex muscle morphogenesis (Figure 26C and 26D, n=66). Therefore, *bar-1* mutation seems to confer defects at the site of the anal depressor. To confirm the site of action of BAR-1, I need to tissue specifically rescue BAR-1 in the anal depressor in the *bar-1* mutant.

Mutagenesis to identify parallel pathways that co-regulate anal depressor development

The Wnt-canonical pathway has been shown to regulate sarcomere disassembly in the anal depressor. However, the anal depressor phenotype of *bar-1* mutants is not fully penetrant (Figure 23E). This led us to think that there is compensatory mechanism to co-regulate the disassembly process. To identify other signaling components involved in the anal depressor reorganization, I conducted an EMS mutagenesis to search for mutants that have similar phenotype as the Wnt mutants (*egl-20* and *lin-44*).

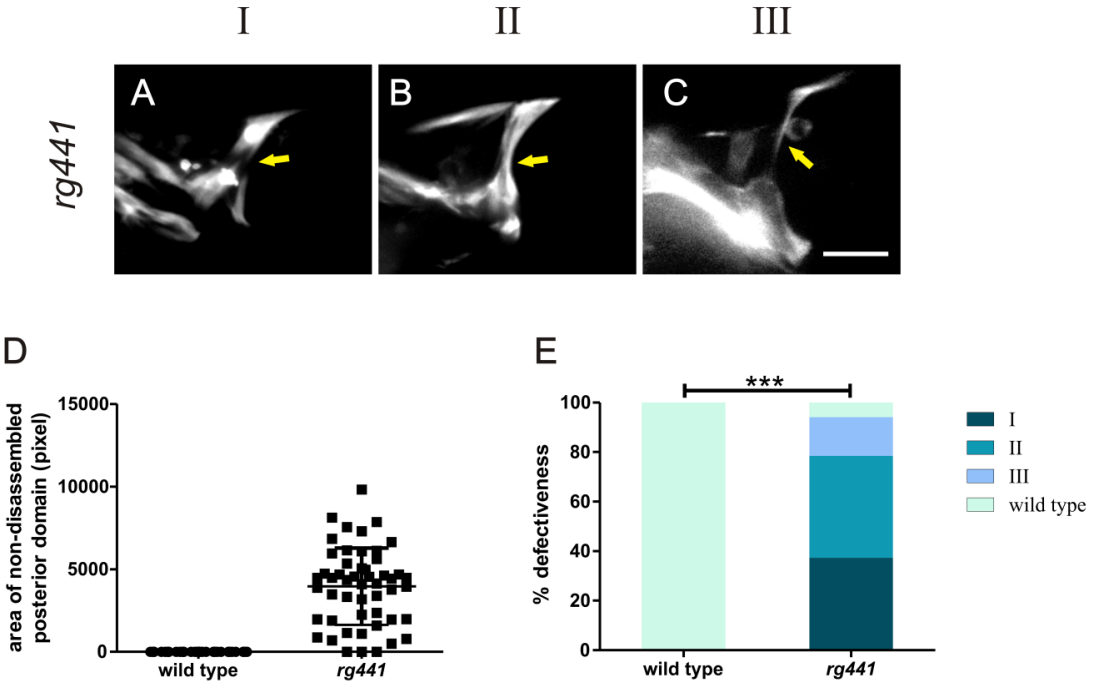

Figure 27. *rg441* mutant males possess anal depressor sarcomere disassembly defects. (A-C) Anal depressor of *rg441* adult males display defects in sarcomere disassembly. The posterior domain of the anal depressor either maintains the sarcomere (A), retains large amount of myofilaments (B), or retain residual myofilaments (C). The arrow in (A) indicates the H zone of the anal depressor sarcomere, and the arrows in (B) and (C) indicates the retained myofilaments in the anal depressor. (D) Area of non-disassembled posterior domain of the anal depressor of wild type (n=55) or *rg441* (n=51) adult males. All the animals assayed carry the transgene *rg*Ex*497* [P*unc-103*E:YFP::actin]. (E) Calculated percentages of anal depressor defects for wild type and *rg441* adult males based on data in (D): 100% of the wild type adult males have a wild type adult anal depressor; 37.3%, 41.2%, 15.7%, and 5.8% of *rg441* adult males have type I, II, III and wild type anal depressors, respectively. *** $p < 0.0001$. The p value was calculated between the wild type and defective (I+II+III) groups using Fisher's exact test. (A-C) are positioned as anterior to the left, and ventral to the bottom. For all of the images, the scale bar represents 10μm.

I identified one mutant line, *rg441*, which possesses the same phenotype as *egl-20* mutants (Figure 27A-27C). Using SNP mapping strategy, I mapped the mutation to the left end of chromosome V (Supplementary Table 1). Then I did whole genome

sequencing, and found several mutations located within that small chromosomal interval. I found that there is a nonsense mutation located within the coding sequence of *egl-8* (Figure 28). *egl-8* encodes the *C. elegans* homolog of phospholipase C-β (PLC-β). PLC-β functions to cleave PIP2 to generate DAG and IP_3. Both products activate some key mediators of signaling pathways, such as PKC and JNK, which then trigger different cellular responses. I set up several experiments to identify if the mutation is responsible for the *rg441* anal depressor phenotype. First I verified that *rg441* mutation is recessive (Table 2). Therefore complementation test can be set up between *rg441* and other known mutant lines to verify which gene is responsible for the phenotype. The heterozygous *rg441/n488* (a classical allele of *egl-8*) males have the *rg441* phenotype (Table 2). This indicates that the mutation located within *egl-8* confers the *rg441* phenotype. Additionally, the *egl-8(n488)* males also possess the posterior sarcomere disassembly defects (Table 2). The *rg441* phenotype was rescued using *egl-8* genomic sequence (Figure 29). This confirms that PLC-β is required for sarcomere disassembly process in the male anal depressor.

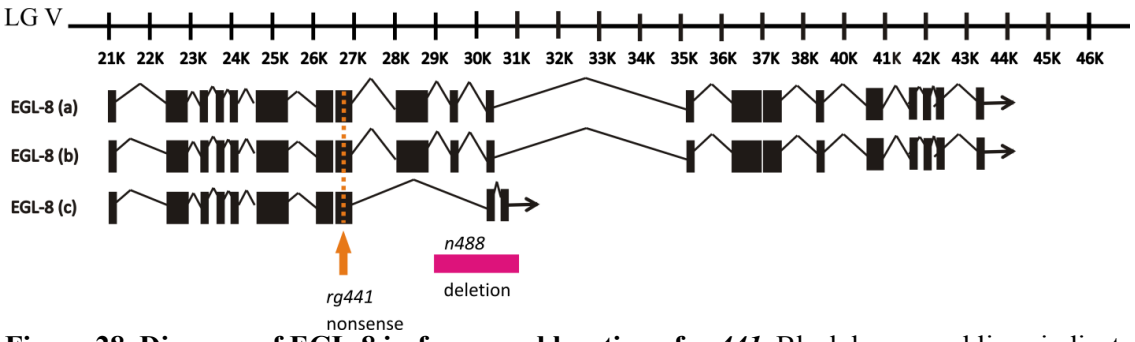

Figure 28. Diagram of EGL-8 isoforms and location of *rg441*. Black boxes and lines indicate exons and introns in *egl-8*. Three major isoforms of EGL-8 are shown here: a, b and c. Orange arrow and dotted lines indicate the location of *rg441* mutation. Magenta box indicates the classic deletion allele, *n488*.

Table 2. Mutation in *egl-8* contributes to the anal depressor defects.

Genotype	**wild type adp**	**defective adp**	**N**	**% defectiveness**
rg441	3	48	51	90.6
rg441/+	18	0	18	0
rg441/*n488* or *rg441*/+ *	18	15	33	45.5
egl-8 (n488)	8	21	29	72.4

*F1 males derived from *rg441* hermaphrodite crossed with *egl-8 n488*/+ males.

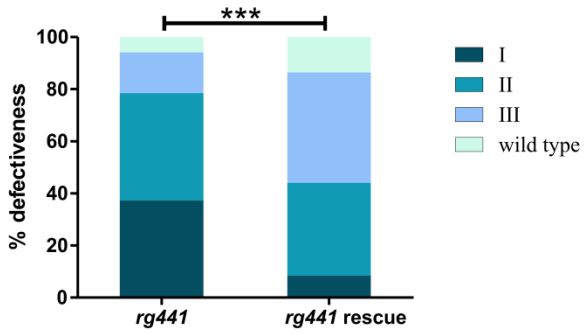

Figure 29. The anal depressor defects in *rg441* males were rescued using *egl-8* genomic DNA. Percentages of anal depressor defects for *rg441* adult males (n=51) and *rg441* adult males which carry transgene *rg*Ex*778* [P*egl-8*:*egl-8*; P*lev-11*: DsRed] (*rg441* rescue) (n=59): 37.3%, 41.2%, 15.7% and 5.9% of the *rg441* males have type I, II, III and wild type anal depressors, respectively; 8.5%, 35.6%, 42.4%, and 13.6% of *rg441* rescue males have type I, II, III and wild type anal depressors, respectively. *** p= 0.0004. The p value was calculated using Fisher's exact test between type I group and none type I group (II+III+wild type).

PLC-β has been indicated to trigger Ca^{2+} signaling by inducing Ca^{2+} efflux from the endoplasmic reticulum. The signaling components upstream of PLC-β have been shown to be some behavior-related G-protein-coupled receptors (Wu et al., 1993). Muscarinic acetylcholine receptors activate Gq, which then activates PLC-β to activate muscle contraction. To verify if acetylcholine activation is upstream of PLC-β to induce sarcomere disassembly, I examined Gq loss of function mutants *egl-30*. The *egl-30(ad805)* mutants have wild type anal depressor development (data not shown). Unless Gαs in *C. elegans* can compensate for the role of EGL-30, it is less likely that Gq-mediated PLC-β activation is required for sarcomere disassembly in the male anal depressor.

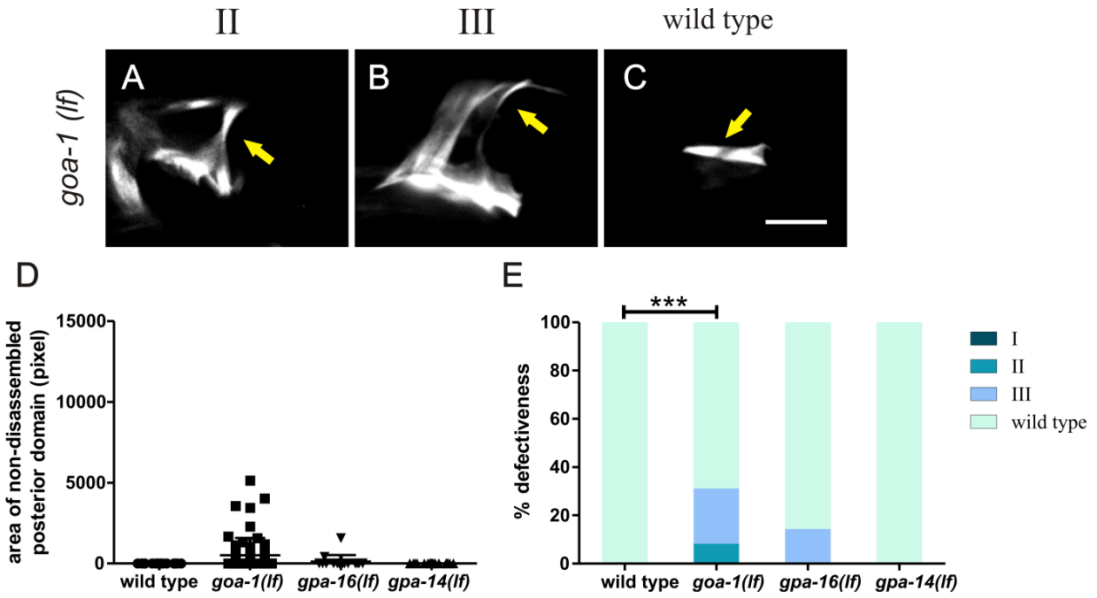

Figure 30. *goa-1* mutants possess anal depressor sarcomere disassembly defects. (A-C) Anal depressor of *goa-1* adult males display defects in sarcomere disassembly. The posterior domain of the anal depressor either retains large amount of myofilaments (A), retain residual myofilaments (B), or have a wild type anal depressor (C). The arrows in (A) and (B) indicates the retained myofilaments in the anal depressor, and the arrow in (C) indicates the H zone of the newly-established anal depressor sarcomere. (D) Area of non-disassembled posterior domain of the anal depressor of wild type (n=50), *goa-1(n1134)* (n=61), *gpa-16(it143)* (n=16) or *gpa-14(pk347)* (n=18) adult males. All the animals assayed carry the transgene *rg*Ex*497* [P*unc-103*E:YFP::actin]. (E) Calculated percentages of anal depressor defects for wild type, *goa-1(n1134), gpa-16(it143)* , or *gpa-14(pk347)* adult males based on data in (D): 100% of the wild type adult males have wild type adult anal depressor; 0%, 8.2%, 23%, and 68.9% of *goa-1(n1134)* adult males have type I, II, III and wild type anal depressors, respectively; 14.3% and 85.7% of *gpa-16(it143)* males have type III and wild type anal depressors, respectively; 100% of the *gpa-14(pk347)* males have a wild type anal depressor. *** $p < 0.0001$. The p value was calculated using Fisher's exact test between wild type group and defective group (I+II+III). (A-C) are positioned as anterior to the left, and ventral to the bottom. For all of the images, the scale bar represents 10µm.

The Wnt signaling pathway has also been shown to activate Ca^{2+} signaling through PLC-β, known as the Wnt- Ca^{2+} pathway. In this pathway, the Wnt receptor Frizzled functions as a G-protein coupled receptor (Sheldahl et al., 1999). However,

instead of using Gq as a mediator, the Wnt-calcium pathway uses Go/i to activate downstream effectors (Katanaev et al., 2005). *C. elegans* have 16 Gα proteins (Jansen et al., 1999), among which GOA-1 is the identified ortholog for Go. To verify if Go is involved in the disassembly process, I examined the *goa-1* loss of function mutant. *goa-1* mutants only have partial defects (Figure 30A-30E). There might be redundancy between GOA-1 and other *C. elegans* Gα units in regulating the sarcomere disassembly process. GPA-14 and GPA-16 are two other Gαs that display the highest sequence similarity with GOA-1 (Correa et al., 2015). Therefore, I also examined *gpa-14* and *gpa-16* mutants. However, none of these mutants exhibit substantial defects for anal depressor developmental (Figure 30D-30E). Therefore, more Gα mutants, or even double or triple Gα mutants, need to be examined.

Wnt-calcium pathways activate Ca^{2+} signaling, through PLC-β and IP_3R. On the sarcoplasmic reticulum, there is also the Ca^{2+}-gated Ca^{2+} channel, UNC-68, which functions to amplify the Ca^{2+} signaling. Both the *itr-1* RNAi mutant and *unc-68* loss of function mutants have the anal depressor disassembly defects (Figure 31). The *unc-68* mutation confers a 95%-penetrant phenotype (Figure 31D). However, the *itr-1* RNAi assay only gives a 50% penetrance (Figure 31B). This might be due to that RNAi only creates knock-down rather than knock-out effect. But it also raises the possibility that there might be other Ca^{2+} triggers for UNC-68.

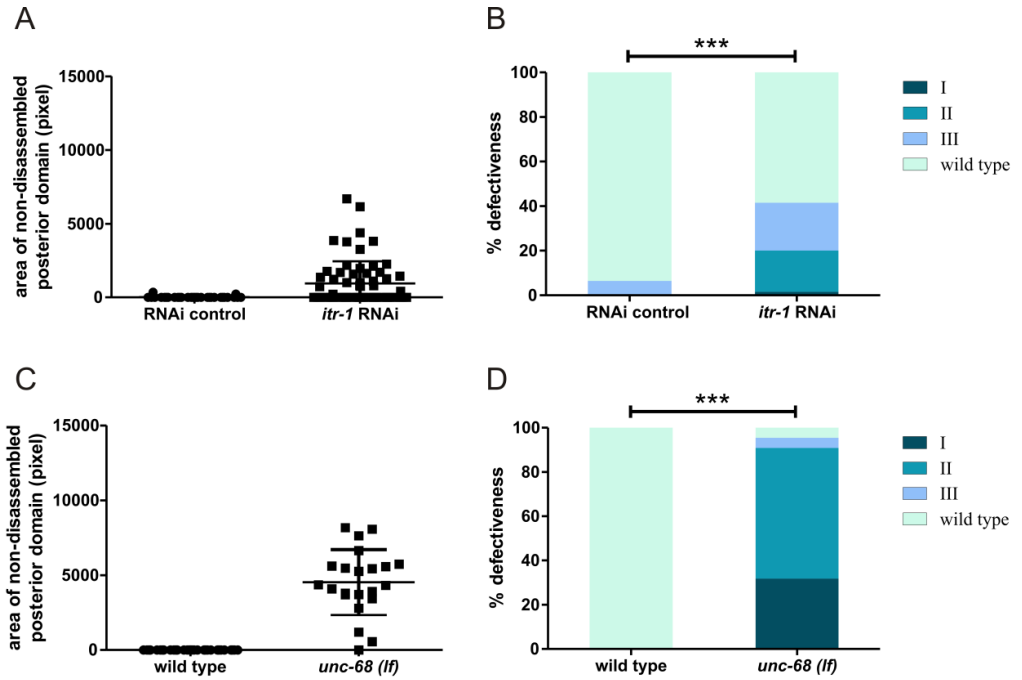

Figure 31. Quantification and classification of the anal depressor defects of *itr-1* and *unc-68* mutants. (A) Area of non-disassembled posterior domain of the anal depressor of RNAi control (n=31) and *itr-1* RNAi (n=65) adult males. All the animals assayed carry the transgene *rg*Ex*497* [P*unc-103*E:YFP::actin]. (B) Calculated percentage of anal depressor defects for RNAi control and *itr-1* RNAi adult males based on data in (A): 93.5% and 6.5% of the RNAi control adult males have wild type and type III anal depressor, respectively; 1.5%, 18.5%, 21.5%, and 58.5% of the *itr-1* RNAi adult males have type I, II, III and wild type anal depressor, respectively. (C) Area of non-disassembled posterior domain of the anal depressor of wild type (n=50) and *unc-68(r1158)* (n=22) adult males. All the animals assayed carry the transgene *rg*Ex*497* [P*unc-103*E:YFP::actin]. (D) Calculated percentage of anal depressor defects for wild type and *unc-68(r1158)* adult males based on data in (C): 100% of the wild type adult males have a wild type anal depressor; 31.8%, 59.2%, 4.5%, and 4.5% of the *unc-68(r1158)* adult males have type I, II, III and wild type anal depressors, respectively. *** $p<0.0001$. The p values were calculated between the wild type and defective (I+II+III) groups using Fisher's exact test.

The Wnt-calcium pathway mutants also possess the anal depressor disassembly defects. Therefore, I concluded that besides Wnt-β-catenin pathway, Wnt-calcium pathway also functions to regulate sarcomere disassembly of the anal depressor.

Determine the site of action of Wnt-calcium pathway

The final output of the Wnt-calcium pathway is to regulate cell movement rather than cell fate determination (Kohn and Moon, 2005; Moon et al., 2004). To first verify if EGL-8 functions in the sex muscles or the tail hypodermal cells (signaling cells for EGL-20 or LIN-44) to modulate their migration, I examined the expression pattern of *egl-8* in the male tail (Figure 32). I found that *egl-8* is expressed from both the sex muscles and the male anal depressor. But the sex muscle expression starts only from L4 molt, whereas the expression from the anal depressor persists throughout L4 development (Figure 32). This indicates that EGL-8 does not influence the migration of the male sex muscles. Therefore EGL-8 most likely regulates the anal depressor development in the muscle cell itself.

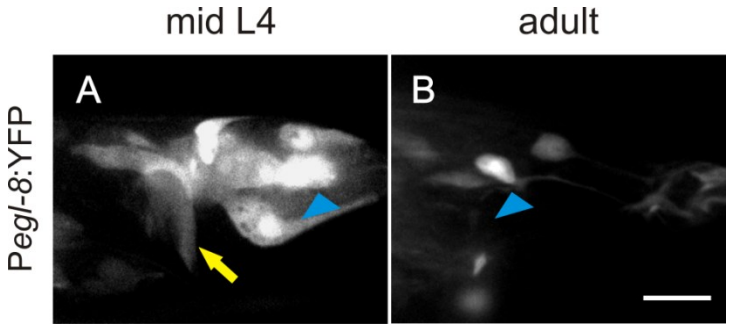

Figure 32. *egl-8* expression pattern in the male tail. (A) In mid-L4 males, *egl-8* is expressed in the anal depressor (yellow arrow) and the ray precursor cells (blue arrowhead), but not in the sex myoblasts (n=11). (B) In the adults, *egl-8* is expressed in the ray neurons (blue arrowhead) and the anal depressor (n=4). All the males carry the transgene *rg*Ex*589* [P*egl-8:*YFP]. All the images are positioned as anterior to the left, and ventral to the bottom. For all of the images, the scale bar represents 10µm.

If the hypothesis that Wnt-calcium signaling pathway functions in the anal depressor to modulate sarcomere disassembly is correct, elevated cytoplasmic calcium levels should be observed in the anal depressor. Calcium signaling tends to trigger cellular responses instantaneously. Therefore it is less likely that the calcium events occur much earlier than the time of anal depressor reorganization. I observed the calcium dynamics in the anal depressor during L4 development, when the remodeling events occur. G-CaMP is a Ca^{2+} sensor that increases the level of fluorescence as the amount of Ca^{2+} binding increases. By expressing G-CaMP in the anal depressor, I was able to monitor the Ca^{2+} changes that occur from the time when the anterior sarcomere starts to disassemble, till the time when disassembly completes in the posterior domain. I found that there is a continuous increase of Ca^{2+} levels in the anal depressor during this time period (Figure 33). The result indicates that there is active Ca^{2+} signaling in the anal depressor during the time of reorganization.

Therefore, I concluded that Wnt-calcium signaling acts in the anal depressor during L4 development, possibly directly regulating the sarcomere disassembly process.

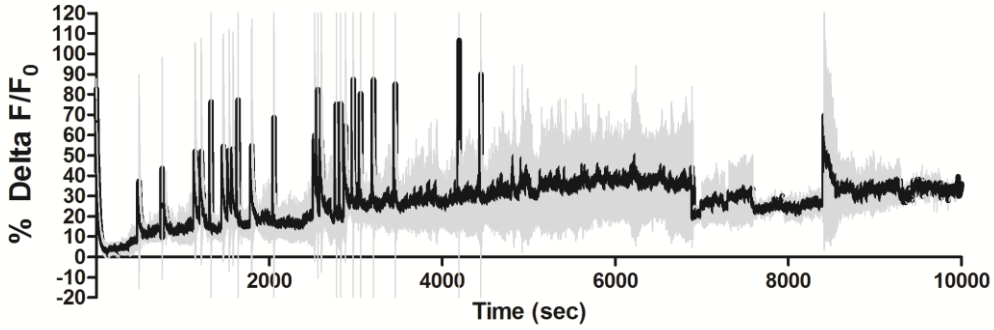

Figure 33. Calcium dynamics in the anal depressor during midL4-L4 molt transition time. For each male recorded, the starting point is mid L4 and the ending point is L4 molt. The average % Delta F/F_0 is determined for all the males tested (n=3). The light gray lines indicate the SD. All the animals assayed carry the transgene *rg*Ex*794* [P*aex-2*:G-CaMP::SL2:::DsRed].

Ca^{2+} responsive proteins promote sarcomere disassembly

How does the Ca^{2+} signaling contribute to sarcomere disassembly? There are a group of kinases and proteins that respond to the Ca^{2+} signaling and activate downstream effectors (Hogan et al., 2003; Khorchid and Ikura, 2002; Luo and Weinstein, 1993). Those proteins might phosphorylate or dephosphorylate the sarcomeric proteins, compromise the integrity of the sarcomere and therefore trigger disassembly. The well-known downstream effectors of the Wnt-calcium pathway include PKC and CaMKII. PKC-2 is the protein kinase that has homology to the classical PKC family of calcium/DAG activated kinases. However, the *pkc-2* mutant has a wild type anal depressor (Figure 34D and 34E). The UNC-43/CaMKII mutant males have constitutively protracted spicules (LeBoeuf et al., 2007), indicating that they also have a wild type anal depressor. Therefore, the canonical Ca^{2+} activated proteins might not play essential roles in regulating sarcomere disassembly in the anal depressor.

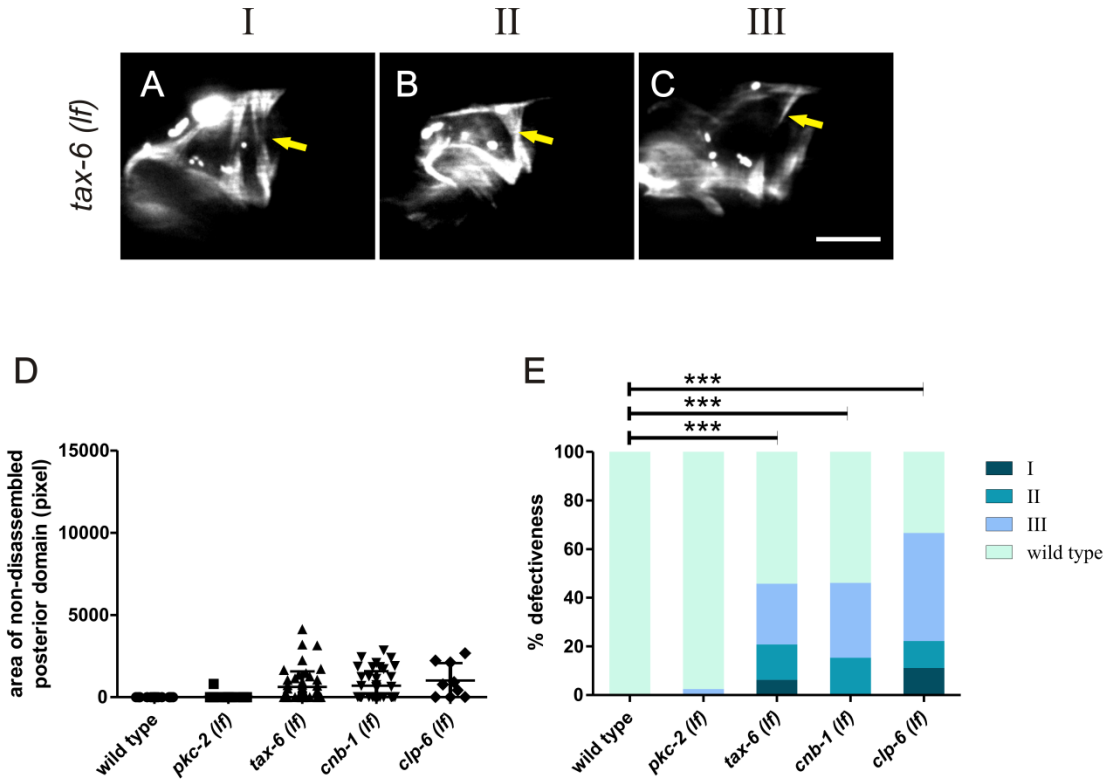

Figure 34. Ca^{2+} responsive proteins regulate sarcomere disassembly in the anal depressor. (A-C) Anal depressor of *tax-6(ok2065)* adult males display defects in sarcomere disassembly. The posterior domain of the anal depressor either maintains the sarcomere (A), retains large amount of myofilaments (B), or retain residual myofilaments (C). The arrow in (A) indicates the H zone of the anal depressor sarcomere, and the arrows in (B) and (C) indicates the retained myofilaments in the anal depressor. (D) Area of non-disassembled posterior domain of the anal depressor of wild type (n=33), *pkc-2(ok328)* (n=41), *tax-6(ok2065)* (n=48), *cnb-1(jh103)* (n=39) and *clp-6(ok1779)* (n=9) adult males. All the animals assayed carry the transgene *rg*Ex*497* [P*unc-103*E:YFP::actin]. (E) Calculated percentages of anal depressor defects for wild type, *pkc-2(ok328), tax-6(ok2065)*, *cnb-1(jh103)* and *clp-6(ok1779)* adult males based on data in (D): 100% of the wild type adult males have wild type adult anal depressor; 0%, 0%, 2.4%, and 97.6% of *pkc-2(ok328)* adult males have type I, II, III and wild type anal depressor, respectively; 6.3%, 14.6%, 25%, and 54.2% of *tax-6(ok2065)* males have type I, II, III and wild type anal depressors, respectively; 0%, 15.4%, 30.8%, and 53.8% of *cnb-1(jh103)* adult males have type I, II, III and wild type anal depressors, respectively; 11%, 11%, 44.5%, 33.3% of *clp-6(ok1779)* adult males have type I, II, III and wild type anal depressors, respectively. *** $p<0.0001$. The p values were calculated between the wild type and defective (I+II+III) groups using Fisher's exact test. (A-C) are positioned as anterior to the left, and ventral to the bottom. For all of the images, the scale bar represents 10µm.

In mammals, there is a group of Ca^{2+} responsive phosphatases called calcineurins, which participate in muscle remodeling. The calcineurins can dephosphorylate and activate nuclear factor of activated T cell (NFAT), which then initiate muscle remodeling gene expression (Hogan et al., 2003). *C. elegans* also has the Calcineurin homologs, TAX-6 and CNB-1. *tax-6* encodes the subunit that has the phosphatase activity whereas *cnb-1* encodes the regulatory domain. Both *tax-6* and *cnb-1* loss of function mutants have anal depressor sarcomere disassembly defects (Figure 34A-34E). However, the level of penetrance and the phenotype severity of either mutant line are not comparable to the *unc-68* or *egl-8* mutants (Figure 27D-27E, 31C-31D). This indicates there might still be other effectors that act in parallel to calcineurin to regulate sarcomere disassembly. Calpains are Ca^{2+}-activated cysteine proteases which have been shown to facilitate myofibrillar protein degradation during muscle fiber turnover (Huang and Forsberg, 1998). *C. elegans* have a group of Calpain homologs. Among those homologs, *clp-6* and *clp-3* are the two that have the male-specific elevation of expression level at L4 stage (http://www.wormbase.com). Therefore I wondered if there is any correlation between Calpain activity and anal depressor sarcomere disassembly. I examined the Calpain mutant *clp-6* and found that *clp-6* loss of function mutants possess the anal depressor sarcomere disassembly defects (Figure 34D-34E). But still, the level of penetrance and the severity of individual defects are not comparable to *unc-68* mutants. This may be due to the redundancy between *clp-6* and *clp-3*. However, Calpains can only digest part of the myofibrillar proteins (Huang and Forsberg, 1998). Therefore additional proteases or protein kinases must be activated to promote

degradation of other sarcomeric proteins. Since *unc-68* or *egl-8* mutants display more severe defects, the activity of those proteases or protein kinases must also be compromised because of the lack of calcium signaling.

Behavior calcium regulates sarcomere disassembly

unc-68 mutants (UNC-68 is the calcium-gated calcium channel) have 95%-penetrant phenotype, which is higher compared to *egl-8* mutants. However, if *egl-8* signaling is the sole source of calcium for UNC-68 activation, one would expect that they have the same level of penetrance. The difference in penetrance level may be due to the fact that none of the *egl-8* alleles that I used are null. However, the *rg441* mutation truncates 65% of the protein, thus should function as a null. Therefore, there must be other signaling pathways that contribute to the calcium change and activate UNC-68. Cation or calcium channels are able to induce calcium influx upon neurotransmitter activation. The known calcium channels that are expressed from the anal depressor are EXP-1 and EGL-19. EXP-1 is the excitatory GABA receptor, which induce cation influx upon GABA binding. EGL-19 is the voltage-gated Ca^{2+} channel, which opens under activated membrane potential. Both channels are activated during the expulsion step of the defecation cycle, to induce contraction of the anal depressor. Although the male anal depressor no longer functions as a defecation muscle in the adults, the *exp-1* promoter remains active during adulthood (data not shown). Therefore, even during L4 stage when the males reorganize their defecation wiring (Chen and Rene Garcia, 2015), there might still be GABA signaling which activates the calcium channels and induces Ca^{2+} influx in the anal depressor. To identify the role of those calcium channels, I examined *exp-1* and

egl-19 mutants to observe if they have anal depressor defects. Around 24% of the *exp-1* mutants and around 64% of the *egl-19* mutants have the sarcomere disassembly defects (Figure 35). This indicates that the calcium channels located on the cell membrane also induces Ca^{2+} influx to promote sarcomere disassembly. The assay highlights the importance of behavior-induced calcium in modulating muscle development.

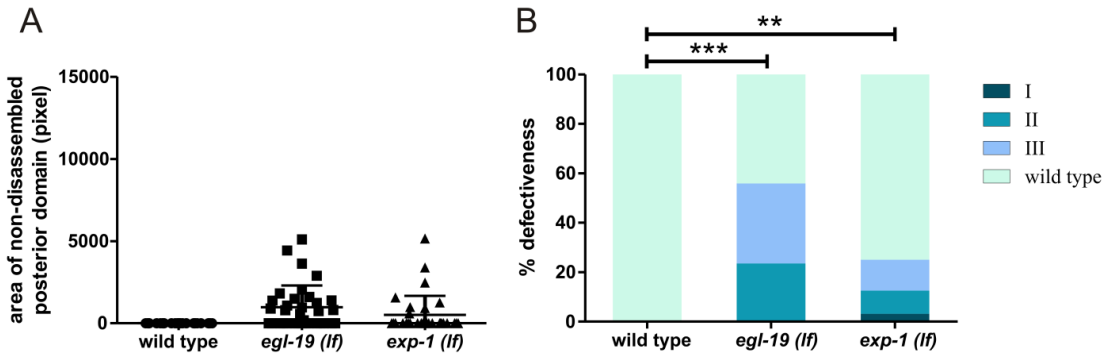

Figure 35. Quantification and classification of the anal depressor defects of *egl-19* and *exp-1* mutants. (A) Area of non-disassembled posterior domain of the anal depressor of wild type (n=33), *egl-19(n582)* (n=34), and *exp-1(ox276)* (n=32) adult males. All the animals assayed carry the transgene *rg*Ex*497* [P*unc-103*E:YFP::actin]. (B) Calculated percentage of anal depressor defects for wild type, *egl-19(n582)*, and *exp-1(ox276)* adult males based on data in (A): 100% of the wild type adult males have a wild type anal depressor; 0%, 23.5%, 32.4%, and 44.1% of *egl-19(n582)* adult males have type I, II, III and wild type anal depressors, respectively; 3.1%, 9.4%, 12.5%, and 75% of *exp-1(ox276)* adult males have type I, II, III and wild type anal depressors, respectively. *** $p<0.0001$; ** $p=0.0021$. The p values were calculated between the wild type and defective (I+II+III) groups using Fisher's exact test.

Determine the relationship between the Wnt-β-catenin pathway and Wnt-calcium pathway

Muscle defects in the calcium mutants confirm that calcium signaling plays an essential role in regulating sarcomere disassembly in the male anal depressor. However, previous experiments show that the Wnt-β-catenin pathway also functions in the anal depressor to regulate sarcomere disassembly (Figure 21-Figure 23). The severity of *unc-68* mutants indicates that calcium signaling is mainly responsible for the sarcomere disassembly process. Additionally, the capability of the Ca^{2+} responsive proteins to interact with sarcomeric proteins suggests that calcium signaling directly regulates sarcomere disassembly. This puts β-catenin signaling to be upstream of the calcium signaling to control anal depressor reorganization. The question then becomes: how does the β-catenin pathway interact with the calcium pathway in the male anal depressor?

Studies in mammalian systems show that there is antagonism between the Wnt-canonical pathway and the Wnt-calcium pathway (Ishitani et al., 2003; Ishitani et al., 1999). Since the Wnt-calcium pathway is required for the disassembly of the anal depressor, the Wnt-canonical pathway needs to be downregulated in order for the calcium signaling to be active. However, the β-catenin mutants do show defects in disassembling the anal depressor sarcomere. There are two possibilities that explain this scenario. First, the Wnt- β-catenin-pathway is interacting with the calcium pathway in a novel, synergistic manner. Second, the β-catenin signaling is required during earlier developmental stage to lay foundation for subsequent reorganization events.

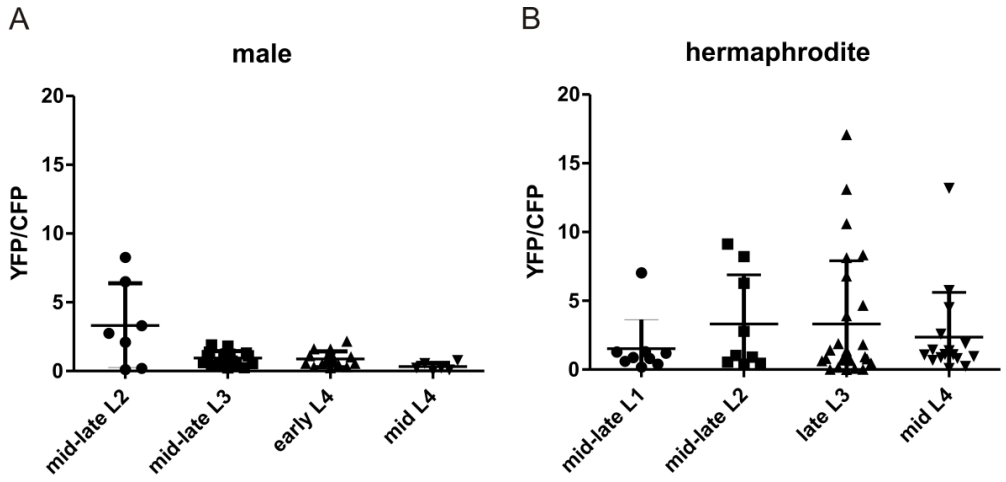

Figure 36. BAR-1 signaling in the anal depressor at different larval stages. (A) The accumulation of BAR-1 was calculated using CFP as control in the wild type male anal depressor at mid-late L2 (n=7), mid-late L3 (n=17), early L4 (n=16), and mid L4 (n=6) larval stages. (B) The accumulation of BAR-1 was calculated using CFP as control in the wild type hermaphrodite anal depressor at mid-late L1 (n=9), mid-late L2 (n=9), late L3 (n=26), and mid L4 (n=16) larval stages. The animals assayed carried the transgene *rg*Ex*783*[*Pbar-1*:BAR-1::YFP; P*bar-1*:CFP].

To distinguish between these two possibilities, I first examined timing of Wnt-β-catenin signaling. When Wnt signaling is active, β-catenin is free from degradation from the APC complex and enters the nucleus to promote target gene transcription. When Wnt signaling is off, β-catenin is degraded and the cytosolic and nucleus localized β-catenin levels will be low (MacDonald et al., 2009). Therefore, by determining the levels of the cytosolic and nucleus-localized β-catenin at different development stages, I would be able to determine when Wnt-β-catenin signaling is active. I tagged the C-terminus of BAR-1 with YFP, and the total fluorescence levels of YFP within the anal depressor should represent the BAR-1 protein levels. The construct has been tested to rescue the

bar-1 vulva phenotype (Eisenmann et al., 1998), therefore should produce functional protein. I injected the construct into wild type animals to observe the β-catenin levels in the anal depressor. Using the *bar-1* promoter driving CFP as an internal control, I calculated the YFP/CFP fluorescence ratio in the anal depressor (Figure 36A and 36B). A high YFP/CFP ratio (>1.5) indicates an elevated level of β-catenin signaling, whereas a low ratio (>0.5 and <1.5) indicates reduced levels of Wnt signaling. Extremely low YFP/CFP ratio (<0.5) indicates the absence of Wnt signaling. I found that BAR-1 is active from L1 till early L4 larval, but is deactivated at mid-L4 stage (Figure 36A). This is different from the hermaphrodite anal depressor, in which β-catenin remains active throughout lifespan (Figure 36B). Therefore there is a male-specific downregulation of β-catenin signaling during L4 development. This agrees with my observation that Wnt-calcium signaling is active at L4 larvae, and the antagonistic effects of the β-catenin signaling needs to be eliminated.

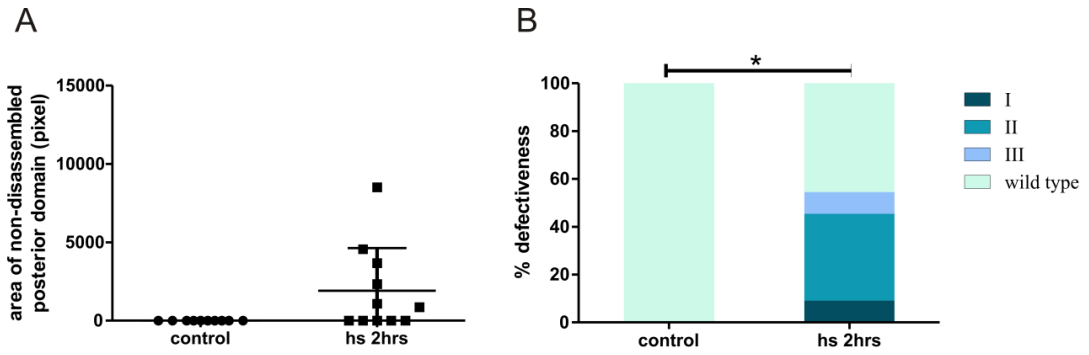

Figure 37. Heat-shock induced BAR-1 signaling disrupt the remodeling of the male anal depressor. (A) Area of non-disassembled posterior domain of the anal depressor of control adult males (n=10) which carry the transgene *rg*Ex*497* [P*unc-103*E:YFP::actin] (control), or adult males that carry the transgene *rg*Ex*782* [*hsp-16*: ΔNT *bar-1*::SL2:::DsRed; P*unc-103*E:YFP::actin] (hs 2hrs). Both the control males and heat-shock males were heat-shocked for 2hrs at Late L3 stage. (B) Calculated percentage of anal depressor defectiveness for control adult males and hs-2hrs adult males based on data in (A): 100% of the control adult males have wild type anal depressor; 9.1%, 36.4%, 9.1% and 45.5% of the hs-2hrs males have type I, II, III and wild type anal depressor, respectively. * p= 0.0141. The p value was calculated between the wild type and defective (I+II+III) groups using Fisher's exact test.

To test the hypothesis that active β-catenin signaling during L4 development would antagonize calcium signaling in the anal depressor, I introduced a constitutively active form of BAR-1 into the anal depressor during L4 development (Figure 37). I found that the ectopic BAR-1 activity during L4 development compromised anal depressor remodeling (Figure 37A and 37B). Myofilaments were retained in the anal depressor posterior domain. Therefore, the downregulation of BAR-1 activity during L4 development is necessary for reorganization to occur.

Then the question becomes how is β-catenin signaling turned off? The presence of Ca^{2+} signaling during L4 larval indicates that there is still active binding of Wnt ligands. I hypothesize that β-catenin signaling is off, possibly because Ca^{2+} pathway

utilizes a different Wnt ligand, which outcompetes the Wnt of β-catenin signaling for receptor binding. Previous studies show that the Wnt-canonical pathway and Wnt-calcium pathway utilize different Wnts for activation (Mikels and Nusse, 2006). It is also possible that both canonical and calcium pathways can be activated by upstream Wnt binding. But the Wnt-calcium pathway can inhibit β-catenin pathway. Wnt-calcium pathway has been shown to inhibit β-catenin signaling through the CaMKII-TAK-NLK cascade (Ishitani et al., 2003). Therefore I asked if knocking down *lit-1*/NLK expression would induce ectopic β-catenin signaling and block anal depressor development. Indeed, I found that *lit-1* RNAi-treated males have anal depressor disassembly defects (Figure 38A and 38B). But more evidence needs to be collected; for example asking whether β-catenin activity is up-regulated during L4 development in the *lit-1* knock-down mutants. Additionally, the inhibitory effect of the Wnt-calcium pathway on the Wnt-canonical pathway has also been shown to be mediated by the calcineurin-NFAT cascade (Huang et al., 2011). Therefore, the anal depressor defects that I see in calcineurin mutants may be due to the upregulation of β-catenin activity.

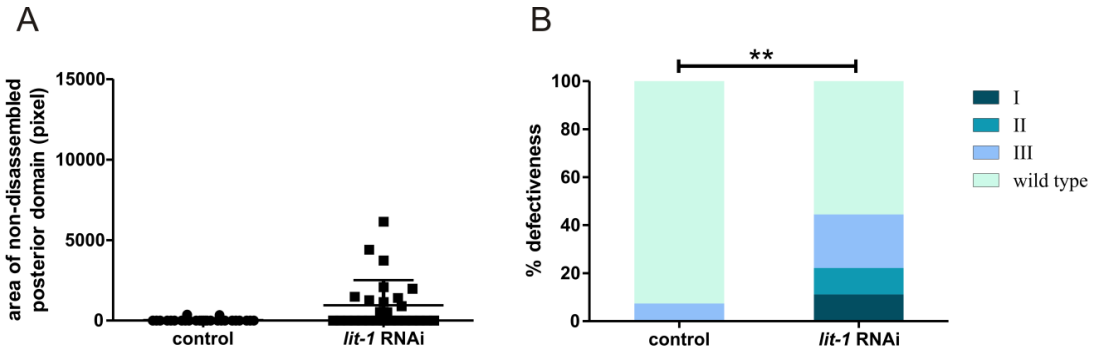

Figure 38. Quantification and classification of the anal depressor defects of *lit-1* RNAi mutants. (A) Area of non-disassembled posterior domain of the anal depressor of RNAi control (n=27) and *lit-1* RNAi (n=27) adult males. All the animals assayed carry the transgene *rg*Ex*497* [P*unc-103*E:YFP::actin]. (B) Calculated percentages of anal depressor defects for RNAi control and *lit-1* RNAi adult males based on data in (A): 92.6% and 7.4% of the RNAi control adult males have wild type and type III anal depressors, respectively; 11.1%, 11.1%, 22.2%, and 55.6% of the *lit-1* RNAi adult males have type I, II, III and wild type anal depressors, respectively. ** p=0.0041. The p value was calculated between wild type and defective (I+II+III) groups using Fisher's exact test.

The data tells us that during L4 larval development, BAR-1 plays negative roles in regulating anal depressor development. However, the *bar-1* mutant phenotype indicates that the activation of BAR-1 during L1 to L3 larvae is essential for anal depressor development. Additionally, the level of BAR-1 in the male anal depressor is lower compared to the hermaphrodite of the same age (Figure 36A and 36B). The sex-differential BAR-1 levels indicate that BAR-1 may regulate different cellular events between the two genders. The male anal depressor exhibits a different pattern of lateral growth compared to hermaphrodite. Therefore, it is possible that the low level of BAR-1 promotes a restricted lateral growth, whereas higher levels promote expanded lateral growth.

Determine what Wnts are involved in regulating β-catenin and calcium pathway

The BAR-1 activity during earlier developmental stages indicates that Wnt ligands binding occurs earlier than L4 development. Different Wnt ligands may be utilized to activate different Wnt pathways at respective developmental stage. I tried to determine which Wnt ligands activate the β-catenin signaling during L1 to L3 larval, and which ligands activate the calcium signaling during L4 development.

I monitored the β-catenin levels in the anal depressor during L2 to L4 larvae in the *egl-20* mutants. I found that *egl-20* loss of function mutants have lower β-catenin levels in the anal depressor compared to the wild type males (Figure 39A-39C). Therefore, *egl-20* is at least partially responsible for the β-catenin activity during L2 to L4 larvae in the male anal depressor.

I also monitored the calcium dynamics in the anal depressor in the *egl-20* mutants. I found that from mid L4 until L4 molt, the increase of calcium levels is less significant compared to wild type (Figure 33 and 40). Therefore, EGL-20 is also the ligand to activate Wnt-calcium signaling.

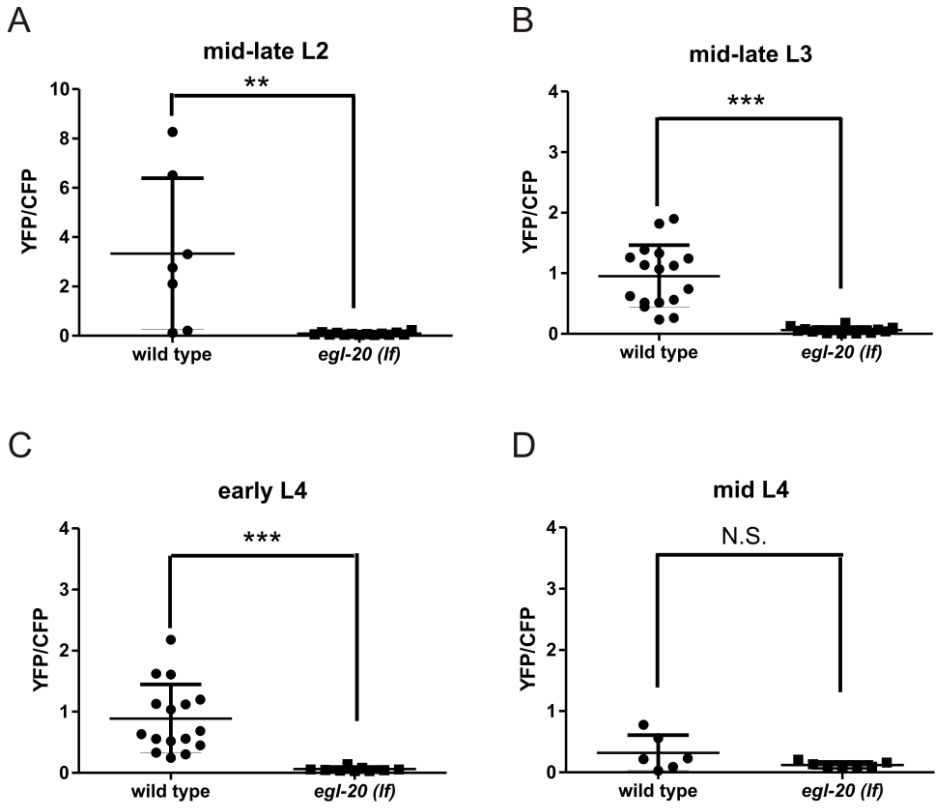

Figure 39. *egl-20(lf)* mutant males have decreased level of BAR-1 signaling in the anal depressor. (A) The accumulation of BAR-1 in the anal depressor in wild type (n=7) and *egl-20 (n585)* mutants (n=14) are compared at mid-late L2. (B) The accumulation of BAR-1 in the anal depressor in wild type (n=17) and *egl-20 (n585)* mutants (n=16) are compared at mid-late L3. (C) The accumulation of BAR-1 in the anal depressor in wild type (n=16) and *egl-20 (n585)* mutants (n=9) are compared at early L4. (D) The accumulation of BAR-1 in the anal depressor in wild type (n=6) and *egl-20 (n585)* mutants (n=7) are compared at mid-L4 stage. The males assayed carried the transgene *rg*Ex*811* [P*bar-1*:*bar-1*::YFP; P*bar-1*:CFP]. (A) ** p=0.0012. (B) *** p< 0.0001. (C) *** p< 0.0001. (D) N.S.=not significant, p=0.1807. All the p values were calculated using Mann-Whitney nonparametric test.

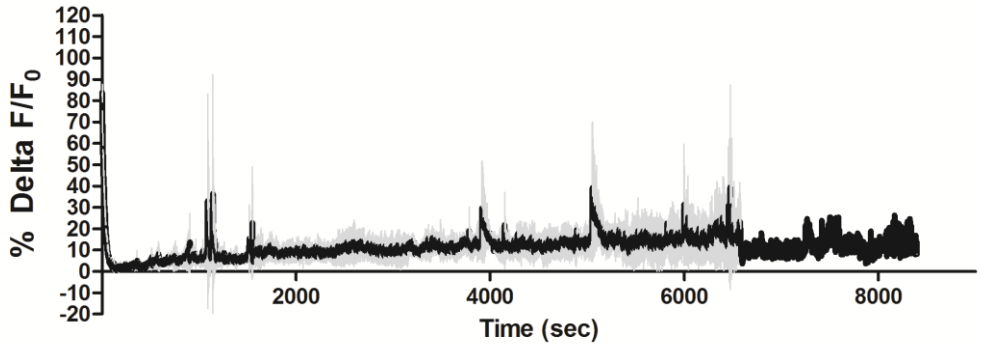

Figure 40. Calcium dynamics in the anal depressor during midL4-L4 molt transition time in *egl-20(n585)* mutant males. For each male recorded, the starting point is mid L4 and the ending point is L4 molt. The average % Delta F/F_0 is determined for all the males tested (n=3). The light gray lines indicate the SD. All the animals assayed carry the transgene *rg*Ex*803* [P*aex-2*:G-CaMP::SL2:::DsRed].

These data suggest that EGL-20 may be functioning throughout larval development to regulate different developmental events in the anal depressor. Since β-catenin signaling and calcium signaling may function in a linear pathway, rescuing only one pathway will not be able to rescue all of the anal depressor defects. I tested this idea by rescuing *egl-20* expression at different larval stages, and observed if it rescues the anal depressor defects. Using a heat shock promoter to drive the expression of *egl-20*, I found that rescuing *egl-20* at L2, L3 or L4 larvae was unable to rescue the anal depressor defects in the *egl-20* mutants (Figure 41A). I also tested double heat shock at L2 and L3 stage, and found that the defects were also not rescued (Figure 41B). The length of heat shock time should be long enough to induce a continuous wave of EGL-20 signaling. Therefore, rescuing the *egl-20* defects requires EGL-20 activity throughout larval development (L1-L4) to rescue both the Wnt-canonical and calcium pathway. A better

heat shock method needs to be developed so that EGL-20 signaling can be sustained at a moderate level throughout larval development.

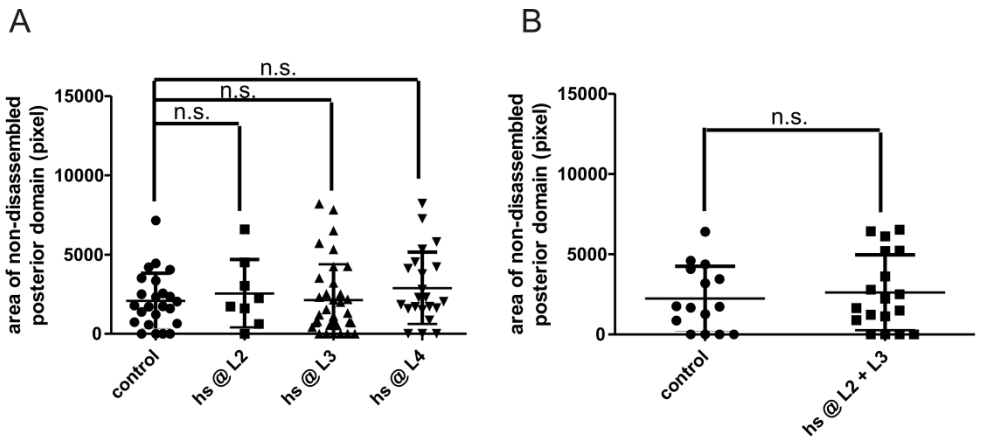

Figure 41. Attempts of using heat-shock-induced *egl-20* expression to rescue the anal depressor defects in *egl-20(lf)* mutant males. (A) Area of non-disassembled posterior domain of the anal depressor in control *egl-20 (n585)* adult males (n=24), or *egl-20 (n585)* adult males that have been heat-shocked at L2 larva (n=8), L3 larva (n=35), or L4 larva (n=22). (B) Area of non-disassembled posterior domain of the anal depressor in control *egl-20 (n585)* adult males (n=15), or *egl-20 (n585)* adult males that have been heat-shocked twice at L2 and L3 larval stages (n=18). All the males assayed carried the transgene *rg*Ex*807* [*hsp-16*:*egl-20*::SL2:::DsRed; P*exp-1*:YFP::actin]. (n.s.= not significant.) All the p values were calculated using Mann-Whitney nonparametric test.

The role of Wnt-PCP pathway in regulating anal depressor development

The Wnt-PCP (planer cell polarity) pathway regulates cell polarity and cell movement through RHOA and JNK. Since the final output of Wnt-PCP pathway is the regulation of actin polymerization and cell migration, I tested its role in anal depressor development. *rho-1* is the *C. elegans* homolog for RHOA. And *lin-18* is the homolog for

Ryk, which is a co-receptor for Wnt PCP signaling. When I knocked down the expression of the *rho-1* and *lin-18* using RNAi, around 90% and 70% of the males displayed anal depressor disassembly defects, respectively (Figure 42). This indicates that the Wnt-PCP signaling pathway also regulates sarcomere disassembly in the male anal depressor. The context of LIN-18 signaling, as well as the signaling components upstream of *rho-1* need to be identified.

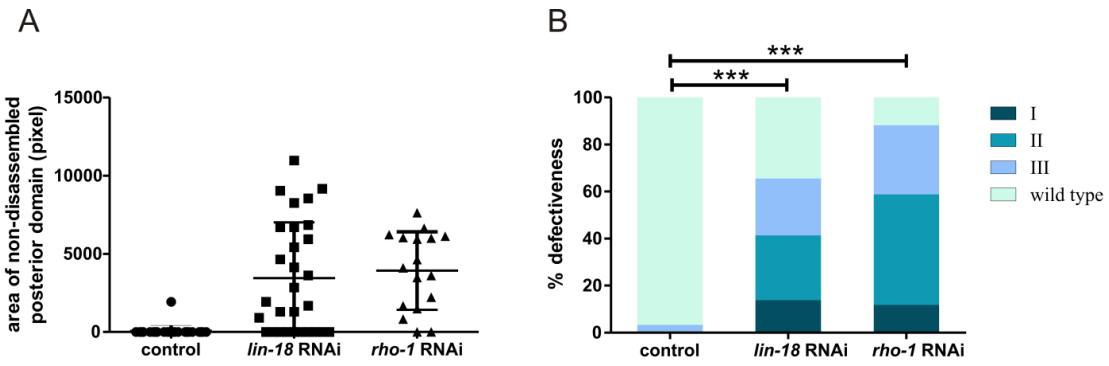

Figure 42. Quantification and classification of the anal depressor defects of *lin-18* and *rho-1* RNAi mutants. (A) Area of the non-disassembled posterior domain of the anal depressor of RNAi control (n=30), *lin-18* RNAi (n=29) and *rho-1* RNAi (n=17) adult males. All the animals assayed carry the transgene *rg*Ex*497* [P*unc-103*E:YFP::actin]. (B) Calculated percentage of anal depressor defectiveness for RNAi control, *lin-18* RNAi and *rho-1* RNAi adult males based on data in (A): 96.7% and 3.3% of the RNAi control adult males have wild type and type III anal depressor, respectively; 13.7%, 27.6%, 24.1%, and 34.5% of the *lin-18* RNAi adult males have type I, II, III and wild type anal depressors, respectively; 11.8%, 47.1%, 29.4%, and 11.8% of the *rho-1* RNAi adult males have type I, II, III and wild type anal depressors, respectively. *** $p < 0.0001$. The p values were calculated between wild type and defective (I+II+III) groups using Fisher's exact test.

Chapter IV summary

The Wnt-canonical pathway and the Wnt-calcium pathway are activated during different developmental stages to regulate sarcomere disassembly in the anal depressor. Mutant analyses of *egl-20*, *lin-44*, *lin-17* and *bar-1* suggest that the Wnt-canonical signaling functions in the anal depressor to regulate sarcomere disassembly. A forward genetic screen identified the *egl-8(rg441)* mutation, which also confers the mutant phenotype. Mutant analyses of potential *egl-8* interactors, *goa-1*, *itr-1*, *unc-68* suggest that Wnt-calcium pathway also promote the disassembly of the sarcomere. Calcium imaging in the anal depressor reveals increased calcium levels during L4 development. This indicates that the Wnt-calcium signaling is activated during L4 development. Monitoring BAR-1 levels in the anal depressor suggest that β-catenin signaling is active during earlier larval stage. The disruption of the remodeling process by ectopic BAR-1 activity suggests that β-catenin signaling antagonizes calcium signaling. Therefore, the two Wnt pathways are sequentially activated to avoid mutual inhibition.

CHAPTER V

THE SYMMETRICAL DEVELOPMENT OF THE ANAL DEPRESSOR REQUIRES WNT SIGNALING IN BOTH THE MALE AND THE HERMAPHRODITE

The symmetrical development of anal depressor is maintained through Wnt signaling

In wild type animals, the anal depressor maintains symmetry between the left and right attachments (Figure 2). In a screen searching for abnormal anal depressor development, I found that *lin-17*, which is one of the *C. elegans* homologs of the Frizzled receptors, controls the symmetrical development of the anal depressor in both hermaphrodite and males. In *lin-17* loss of function mutants, the development of the left and right attachment becomes asymmetrical, with the majority of the animals have an expanded left attachment and a reduced right attachment (Figure 43).

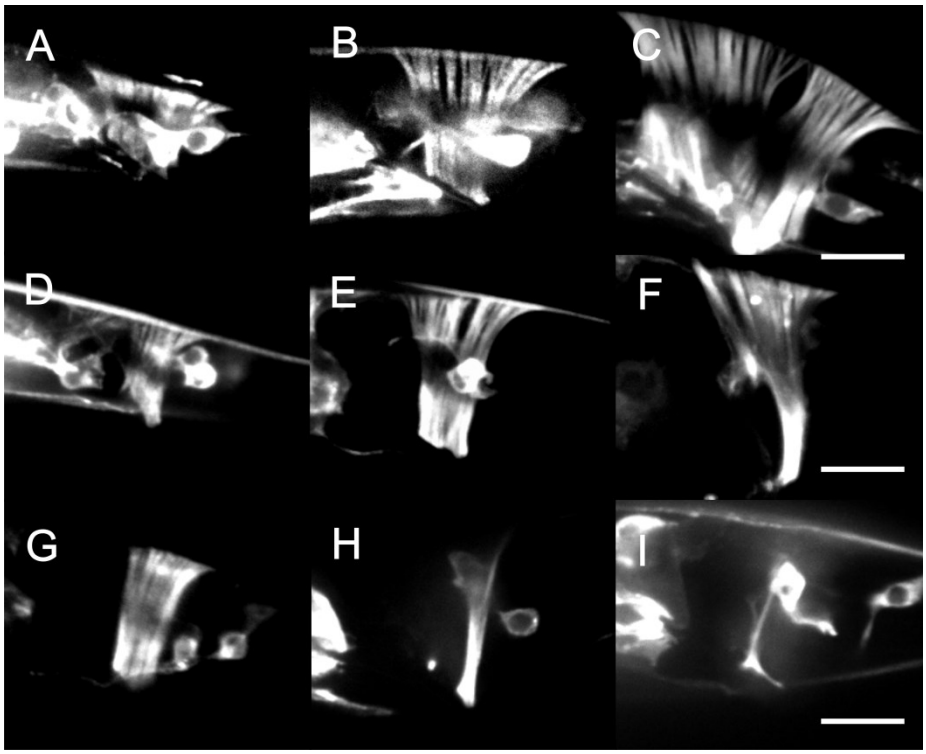

Figure 43. The *lin-17(lf)* mutants have asymmetrical anal depressor development. (A-C) The left attachments of the hermaphrodite anal depressor of *lin-17(e620)* mutants at L1 (A), mid-L3 (B), and mid-L4 (C) larval stages. (D-F) The left attachments of the male anal depressor of *lin-17(e620)* mutants at L1 (B), mid-L3 (E), and mid-L4 (F) larval stage. (G-I) Three representative types of right attachments of the male anal depressor of *lin-17(e620)* mutants: wild type (G), less-reduced (H), and severely reduced (I). All the animals assayed carry the transgene *rg*Ex*497* [P*unc-103*E:YFP::actin].

The *lin-17* mutants, which have an expanded left attachment were studied in more detail to identify how the myofilaments in the right attachment are trans-located to the left attachment. Based on the severity of the phenotype, the right attachment can be categorized into three groups: the right attachment is either wild type (Figure 43G), or mildly-reduced (Figure 43H), or completely lost (Figure 43I) to the left side. For the phenotype seen in Figure 43H, a ventral attachment is maintained in the right side, but

the dorsal attachment is shifted from the right side to the left side, and is positioned posteriorly to the dorsal part of left attachment. This dorsal attachment is fused to the original dorsal attachment of the left attachment.

At the expense of right attachment, the dorsal side of the left attachment becomes enormously expanded compared to wild type left attachment (Figure 43A-43F). Additionally, in wild type animals the dorsal attachment is parallel to the mid line of the body. But in *lin-17* mutants, the dorsal side of the left attachment occupies the entire dorsal body wall of the left side, with posterior end standing close to the midline, and the anterior end standing close to the left lateral hypodermis (Figure 45A). The majority of the expanded left attachments maintain sarcomere structure (Figure 43A-43E), whereas a small proportion does not (Figure 43F).

Since the wild type hermaphrodite anal depressor expands in dorsal width throughout its lifespan, I studied if expanded left attachment in the *lin-17(lf)* hermaphrodite also maintains the capability to grow. In *lin-17* mutant hermaphrodite, once the asymmetry is established in L1 larval animals, the left attachment does not expand dorsally until mid L3 (Figure 44A-44C and 45B). But from mid-L3 until mid-L4, a large proportion of the animals substantially expand the dorsal width of the left attachment (Figure 45B). To identify the origin for expansion, I compared the ratio of animals that have reduced dorsal right attachment (Figure 43H-43I) and found that the ratio increases from mid-L3 to mid-L4. It is possible that some of the mid-L3 animals, which originally have a complete right attachment (Figure 43G) lost more symmetry to the left during the L3-L4 development. Therefore, in *lin-17(lf)* hermaphrodites, the

expanded left attachment lost the growth capability and the expansion of the left dorsal width at mid-L4 stage is due to increased level of right attachment atrophy.

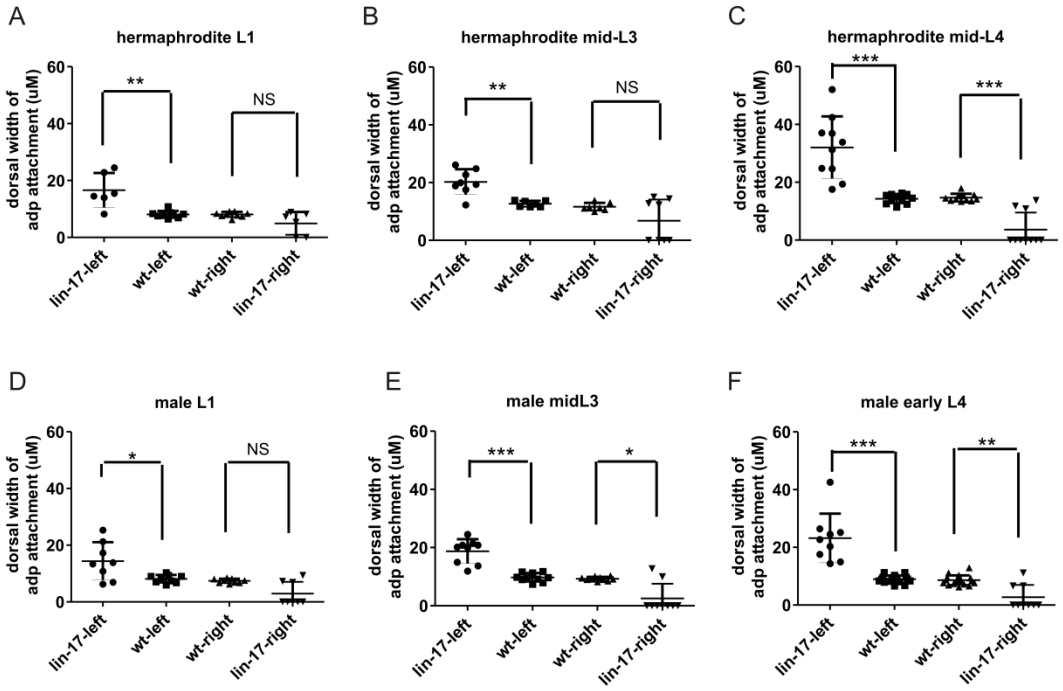

Figure 44. Quantification of asymmetrical developmental defects of *lin-17(lf)* mutants. (A-C) Mean comparisons of the anal depressor's dorsal width of the either left or right attachments between wild type (wt) and *lin-17(e620)* mutants hermaphrodites at L1 (A), mid-L3 (B), and mid-L4 (C) larval stages. (D-F) Mean comparisons of the anal depressor's dorsal width of the either left or right attachments between wild type (wt) and *lin-17(e620)* mutants males at L1 (A), mid-L3 (B), and mid-L4 (C) larval stages. The *p* values were calculated using the unpaired t test (n.s. = not significant). All the animals assayed carry the transgene *rg*Ex*497* [P*unc-103*E:YFP::actin].

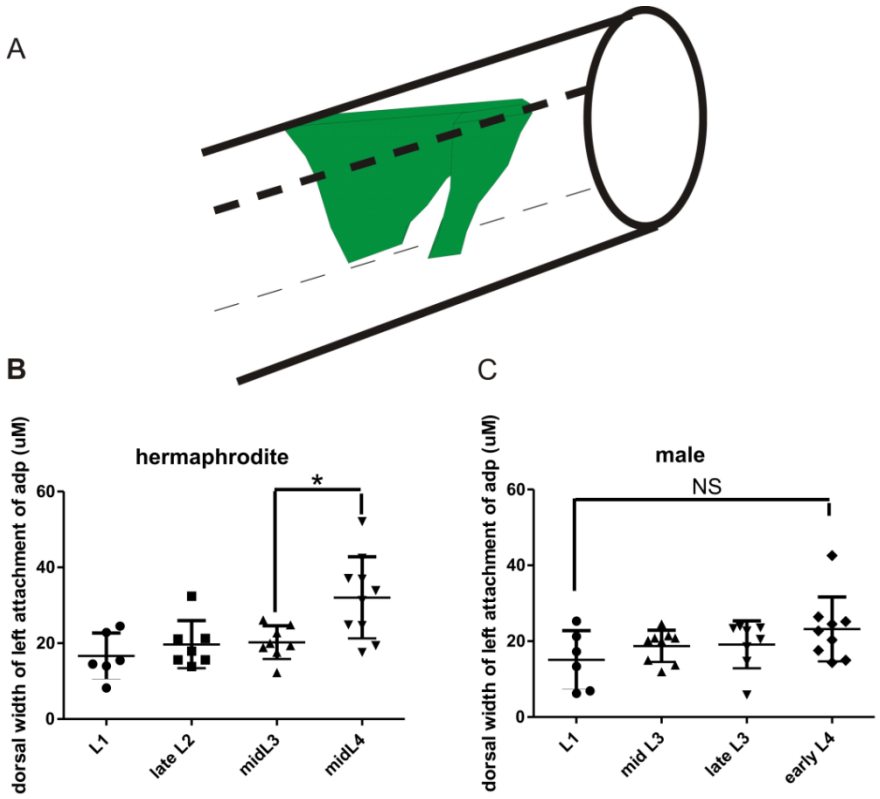

Figure 45. Growth dynamics of expanded left attachment in *lin-17(lf)* hermaphrodites and males. (A) Model of the anal depressor of *lin-17(lf)* mutants. Anterior is to the left and ventral to the bottom. The anal depressor attachments are colored as green. (B-C) dorsal growth dynamics of the expanded left attachments of the anal depressor in *lin-17(e620)* hermaphrodites (B) and males (C). The *p* values were calculated using the unpaired t test (n.s. = not significant). All the animals assayed carry the transgene *rg*Ex*497* [P*unc-103*E:YFP::actin].

For the wild type males, the dorsal growth for the attachment is restrained, but expansion tendency are obvious (Figure 4B). For the *lin-17* mutant males, the left dorsal width remains unchanged throughout these stages (Figure 45C). Thus in *lin-17(lf)* males, the expanded left attachment also loses the capability to grow.

LIN-44 is the Wnt ligand to maintain the symmetry of the anal depressor

To determine which Wnt ligand signals through LIN-17 to maintain the symmetrical development of the anal depressor, I examined *lin-44*, *egl-20* and *cwn-1* loss of function mutants. *lin-44(lf)* animals display similar asymmetrical anal depressor defects as the *lin-17(lf)* mutants, whereas *egl-20* and *cwn-1* loss of function mutants maintain symmetrical development for the anal depressor (data not shown). Therefore, LIN-44 and LIN-17 regulate the symmetrical development of the anal depressor in the male and the hermaphrodite.

Chapter V summary

lin-44 and *lin-17* mutants have an anal depressor asymmetry phenotype. This suggests that Wnt signaling is required for symmetrical development of the anal depressor in both the hermaphrodite and the male. But the downstream signaling components need to be identified.

CHAPTER VI

SUMMARY OF EXPERIMENTS AND DISCUSSION

Summary of experimental results

Both endogenous and exogenous sex determination mechanisms are required to achieve the sexually dimorphic development of the anal depressor. By illuminating the sarcomere structure using YFP-tagged actin, I found that the male anal depressor alters the orientation of the sarcomere during L4 development. A feminized male anal depressor displays hermaphrodite-like anterior growth, whereas a masculinized hermaphrodite anal depressor has restrained anterior growth. Therefore I concluded that early anterior growth of the anal depressor is controlled by the cell-autonomous sex determination pathway. The M cell-ablated male and the *mab-5* mutant male have defects in extending an anterior domain to disassemble the sarcomere. This suggests that the two processes are controlled by signaling derived from the male sex muscles. Additionally, laser ablation of the anal depressor does not affect defecation behavior after L4 development, indicating it does not function as a defecation muscle after being reorganized. Therefore, the morphological change of the male anal depressor is accompanied by functional transition.

The Wnt-canonical pathway and the Wnt-calcium pathway are activated during different developmental stages to regulate sarcomere disassembly in the anal depressor. Mutant analysis of *egl-20*, *lin-44*, *lin-17* and *bar-1* suggest that the Wnt-canonical signaling functions in the anal depressor to regulate sarcomere disassembly. A Forward

genetic screen identified the *egl-8(rg441)* mutation, which also confers the phenotype. Mutant analysis of potential *egl-8* interactors, *goa-1*, *itr-1*, *unc-68* suggest that Wnt-calcium pathway also promote the disassembly of the sarcomere. Calcium imaging in the anal depressor reveals increased calcium levels during L4 development. This indicates that the Wnt-calcium signaling is activated during L4 development. Monitoring BAR-1 levels in the anal depressor suggest that β-catenin signaling is active during earlier larval stage. The disruption of the remodeling process by ectopic BAR-1 activity suggests that β-catenin signaling antagonizes calcium signaling. Therefore, the two Wnt pathways are sequentially activated to avoid mutual inhibition.

Discussion

Heart formation requires the function of different Wnt pathways at different developmental stages

My study shows that both the Wnt-canonical signaling and the Wnt-calcium signaling are involved in anal depressor development (Figure 46). The activation of β-catenin during early larval development may be necessary to maintain the identity of the muscle cell, and the activation of calcium signaling during L4 development promotes the reorganization of the muscle sarcomere. The model of male anal depressor development provides the scenario which is partially represented in mammalian heart muscle development.

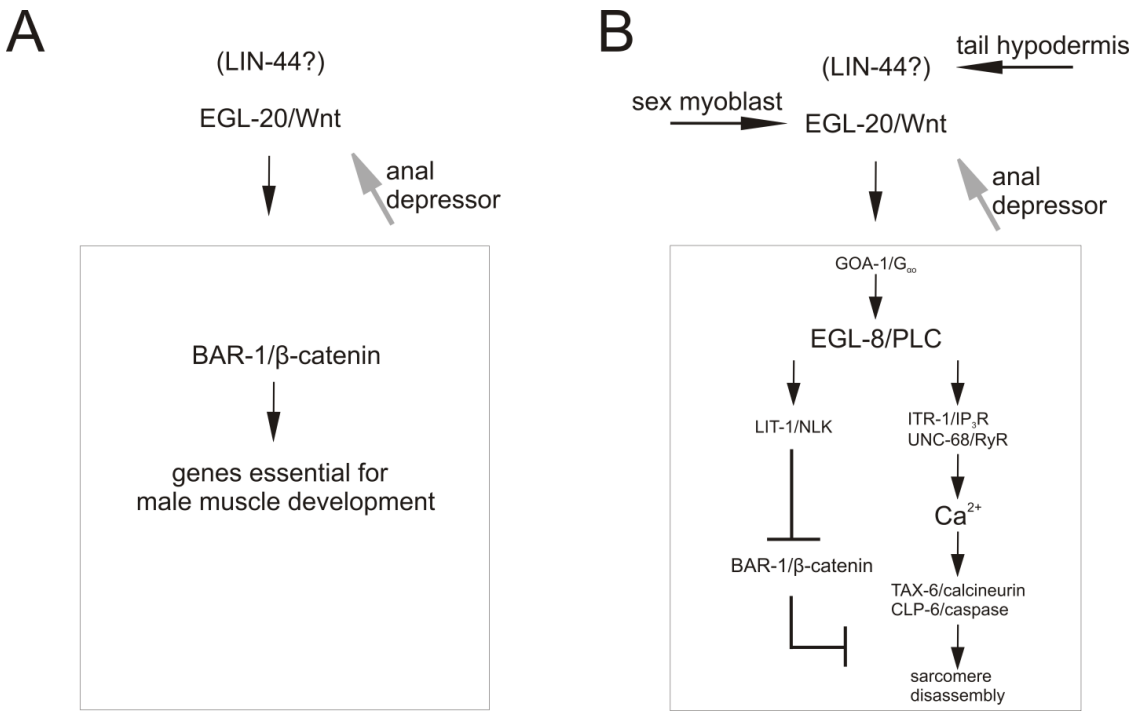

Figure 46. Model of Wnt signaling pathways regulating different remodeling events in the male anal depressor. (A) During early larval development (L1-L3), EGL-20 derived from the anal depressor activates Wnt-β-catenin signaling, which is essential for activation of male developmental genes. The role of LIN-44 in this process is not identified. (B) During L4 development, EGL-20 from both the sex myoblasts and the anal depressor activates Wnt-calcium signaling. The Wnt-calcium pathway, on one hand, activates proteases and phosphatase to promote sarcomere disassembly. On the other hand, calcium signaling antagonizes β-catenin signaling, possibly through the TAK/NLK cascade, to eliminate the repressive effect it has on muscle reorganization. The role of hypodermis-derived LIN-44 needs to be examined.

Wnt-canonical signaling displays biphasic roles on cardiogenesis when induced at different developmental stages (Naito et al., 2006; Ueno et al., 2007). While early induction promotes heart tissue formation, late induction represses the process. In this case, the repressive effects of the Wnt-β-catenin signaling may be due to the altered signaling context. Heart development at later stage may require a different group of cardiac marker gene expression compared to earlier development. In case of anal

depressor development, the inhibitory effects of β-catenin signaling on muscle remodeling are possibly due to the antagonism against the Wnt-calcium signaling. In mammalian models, inhibition of Wnt-canonical signaling is also necessary to facilitate heart development.

Wnt inhibition by antagonist Dkk-1 or Crescent is sufficient to induce cardiogenesis in noncardiogenic tissues (Marvin et al., 2001; Schneider and Mercola, 2001). However, injection of other Wnt antagonists was unable to induce cardiogenesis the same way as *dkk-1* or crescent. The dominant negative XWnt8 was able to inhibit the Wnt target gene *Siamois* expression. But it only induced very weak level of expression of Nkx2.5, and no induction of later muscle markers was found. The similar expression level was observed when injected with WIF-1, FrzA or Szl (Schneider and Mercola, 2001). The difference in heart induction activity may be due to the different antagonizing property of Wnt antagonists.

Wnt antagonists can be classified into two functional classes, the sFRP class and the Dickkopf class (Kawano and Kypta, 2003). The sFRPs inhibits Wnt signaling by directly binding to Wnt ligands. The Dickkopf class specifically binds to LRP5/LRP6 of the receptor complex (Jones and Jomary, 2002). Therefore members of the Dickkopf class may only inhibit the Wnt-canonical signaling; Whereas the sFRPs inhibits all Wnts.

Dkk-1 and Crescent belongs to the Dickkopf family. WIF-1, FrzA and Szl belong to the sFRP class. Therefore, the heart inducing capability of Dkk-1 and Crescent might

because that they only inhibits the Wnt-canonical signaling, but leaves other Wnt signaling pathways (PCP and calcium pathway) intact.

This hypothesis is supported by study that shows that Wnt11 is required for heart formation in *Xenopus* embryos (Pandur et al., 2002). Wnt11 has been established to activate the PCP or calcium pathway (Heisenberg et al., 2000; Kuhl et al., 2000). Therefore, both the inhibition of the Wnt-canonical pathway and the activation of Wnt-calcium pathway needs to be fulfilled in order for cardiogenesis to occur.

Relating anal depressor remodeling to heart regeneration therapy

Muscle hypertrophy is the physiological response to heart infarction to compensate for the loss of muscle fibers (Bassel-Duby and Olson, 2006). Muscle remodeling genes are turned on to make new sarcomeric proteins, which then make new muscle fibers to meet the physiological demands. However, muscle hypertrophy usually leads to heart chamber enlargement and consequently heart muscle atrophy. Therefore maintaining the hypertrophy program under control is essential to prevent heart failure.

The lateral growth of the anal depressor resembles the hypotrophy process (Figure 1C-1G). The anal depressor continues to expand the size of the sarcomere laterally by adding new myofilaments. The process is modulated so that the expansion of the sarcomere never exceeds the length of the rectum. However, I did observe over-expansion phenotype in the *lin-44* and *lin-17* mutants (Figure 43). In those mutant animals, one attachment of the anal depressor expands dorsally with no control. The abnormal morphology of the sarcomere possibly disrupts its contractility. Therefore, Wnt signaling modulates the muscle expansion process so that coordinated sarcomere

establishment occur. Studying the signaling mechanisms that govern the growth of the anal depressor will shed light on heart repair study utilizing the endogenous hypertrophy program.

Heart regeneration studies in rats and zebrafish uncovered other possible mechanisms to repair heart injury. The differentiated cardiomyocytes serve as the source of new compensating muscle cells (Bersell et al., 2009; Jopling et al., 2010; Raya et al., 2003). Cell proliferation either occurs without dedifferentiation, or proceeds with the activation of a novel dedifferentiation program. The cardiomyocytes detach from each other, disassemble their sarcomere during mitosis, and then reassemble the sarcomere in the daughter cells. This process shares some similarity with the reorganization process occurred in the male anal depressor (Figure 19A-19F). The slit formed at the ventral region of the anal depressor might be equivalent to the cleavage furrow that separates the two daughter cells. As the size of the slit enlarges, the sarcomere disassembles to allow morphological changes to occur. Whether the anal depressor undergoes dedifferentiation process is not known. However, the reorganization of the muscle sarcomere might utilize the common mechanisms. Therefore, studying the signaling network to activate sarcomere reorganization in the male anal depressor shed light on the heart regeneration therapy using pre-existing cardiomyocytes.

Disassembled sarcomere: type I, type II, type III defects; what do they mean?

Calcium-activated proteins phosphorylate or dephosphorylate sarcomeric proteins so that the sarcomere structure disassembles. When calcium signaling is strong, all responsive proteins are activated, so that all sarcomere filaments can be disassembled. But if

calcium signaling is weak, then only the proteins that have high affinity to calcium can be activated. Therefore, only part of the sarcomere proteins can be disassembled, whereas sarcomeric structures are retained. Therefore, type I anal depressor defects may display the outcome of the lowest level of calcium signaling. Type II defects indicates that a low level of calcium signaling can activate some calcium responsive proteins, which can remove part of the myofilaments of the old sarcomere structure. Type III defects indicates that there is a high level of calcium signaling that is sufficient to activate most of the responsive proteins, which can remove the majority of the myofilament, albeit not all of the myofilaments of the larval sarcomere.

Cell-autonomous sarcomere disassembly signaling is promoted by male sex determination mechanism.

The feminized male anal depressor is able to extend an anterior domain towards the sex myoblasts during mid L4 stage (Figure 5D). However, subsequent sarcomere disassembly processes are blocked (Figure 5E and 5F). Feminization of the male anal depressor should not affect the cells neighboring the anal depressor from providing signals for remodeling. The hermaphrodite anal depressor also expresses EGL-20 (Whangbo and Kenyon, 1999). Therefore feminizing the male anal depressor does not affect the EGL-20 secretion from itself. Additionally, in my experimental design, the artificial feminization is limited to the anal depressor, and should not directly influence the male sex muscles or other male-specific structures. The ability of the feminized anal depressor to extend an anterior arm (Figure 5D) indicates that the signaling capability of the male sex muscle is not affected. Therefore, the inability to disassemble the sarcomere

in the intact signaling environment can only be due to that the cell-autonomous inability to respond to male sex muscle developmental signals. Since TRA-1 functions as a transcription factor, it may repress the transcription of receptors (like Frizzled) or other effectors in the anal depressor (Figure 5E and 5F), thus disrupting the downstream signaling. This hypothesis is supported by the fact that when TRA-1 activity is suppressed by overexpression of FEM-3, around 18% of the hermaphrodite anal depressor start to disassemble the sarcomere (Figure 8C). However, suppression of TRA-1 activity is not sufficient to induce sarcomere disassembly. The sarcomere disassembly phenotype is not observed until L4 development (Figure 8A-8C), indicating that additional factors initiated at L4 larvae is required to disassemble the sarcomere.

TRA-1 has been shown to repress the transcription of hox genes that promote male-specific development (Conradt and Horvitz, 1999; Yi et al., 2000). Therefore, TRA-1 may indirectly block the signaling transmission, by repressing the expression of hox genes that are essential for the direct effectors (such as the calcium responsive Calpain and Calcineurin proteins) that disassemble the male sarcomere.

Mechanisms to restrain signaling response within a subcellular domain

The L4 development of the male anal depressor shows how cellular compartments move sequentially to achieve cell attachment alterations. Cell migration usually involves coordinated movements of the whole cell (Mattila and Lappalainen, 2008). During migration, the cell's leading edges first extend protrusions toward the guidance cues, and then the cellular components move toward the leading edges. The

rear of the cell is pulled forward by the contractions of stress fibers that are attached to the posteriorly located adhesion molecules.

However during male L4 development, the anterior domain of the anal depressor moves independently of the posterior domain. This independence could be established by polarized distribution of migration molecules. It is possible that the receptors and stress fibers that mediate the response to the cue might be restricted to the anterior domain.

Cell polarity might also be established when the anterior domain disassembles its sarcomere structure. The signaling pathway that mediates muscle atrophy may not regulate this polarized disassembly process, since it should trigger the disassembly of the sarcomere within the whole cell. The muscle atrophy pathway activates MuRF1 and MAFbx ubiquitin ligases, which promote protein degradation (Bodine et al., 2001). If the muscle atrophy pathway is activated uniformly in the anal depressor, the sarcomere proteins will be rapidly degraded. Thus if the atrophy pathway is to be used, it must be coupled to some type of hypothetical compartmentalization mechanism.

During the mid- to late L4 stage, the sarcomere disassembly occurs in the anterior domain before the posterior domain. This might be because the transmission of the disassembly signals from an anterior source(s) (possibly, from the developing spicule protractor muscle cells) might be graded and slow. The EGL-20 secreting sex myoblasts migrate into the tail region at around early-mid L4 development (Figure 24A-24C). What migrates with the sex myoblasts is the EGL-20 morphogen gradient, which first reaches the anterior domain of the anal depressor, and this might be why the anterior

sarcomere first disassembles at around early-mid L4. Meanwhile, the LIN-44 secreting tail hypodermal cells retract from the tail tip at mid-late L4 and moves into proximity to the anal depressor prior to the time that the sarcomere in the posterior domain disassembles (Figure 24G-24I). As the tail hypodermal cells contacts the anal depress, the disassembly signal becomes strengthened in the posterior domain and eventually triggers sarcomere disassembly.

Another possibility for the sequential sarcomere disassembly is that the posterior sarcomere is required to provide structural support for the dynamic changes occurring in the cell's anterior, relative to the other gross alterations occurring in the male tail. After the anterior domain establishes its new contacts with the protractor muscles, the posterior domain of the anal depressor might then receive the signal to atrophy.

Future Experiments

My study of the anal depressor development shows that the anal depressor development is controlled by both internal and external sex determination mechanisms. The sarcomere disassembly of the male anal depressor is regulated by the Wnt-canonical and Wnt-calcium pathway. However, some aspects of the study still remain unanswered.

Specifying the role of EGL-20 in regulating sarcomere disassembly of the anal depressor.

EGL-20 is required during both early and late larval development to activate the canonical and calcium pathways (Figure 39 and 40). However, the developmental events that occur at a particular time point might be triggered by signals from a specific tissue. During early larval development (L1-L3), the source of EGL-20 for the activation of the

β-catenin signaling cannot be the sex myoblasts, since they have not migrated into the tail region (Sulston et al., 1980b). This leaves the B lineage cells and the anal depressor itself as the candidates (Figure 24A-24B). In the hermaphrodites, the B lineage cells that will form the future cloaca display the same EGL-20 expression pattern as in the males (Whangbo and Kenyon, 1999). Therefore, it is less likely that EGL-20 derived from these cells would trigger any male-specific events, unless the male anal depressor displays a sex-differential response to the signal. To identify the role of self-derived Wnts on activation of Wnt-canonical pathway, I will tissue-specifically knock out EGL-20 expression in the anal depressor and observe the BAR-1 levels in the L1-L3 male anal depressor. Rescuing EGL-20 expression using the anal depressor-specific promoter may not be a good choice, since providing a local source of signaling will rescue the phenotype, but it cannot help to distinguish between the endogenous expression domains. Autocrine Wnt signaling has been discovered in stem cells and cancer cells to promote self-renewal (Akiri et al., 2009; Bafico et al., 2004; Lim et al., 2013). β-catenin is activated and required for the proliferation to occur. Therefore, self-derived EGL-20 might be the signal to promote male-identity maintenance in the male anal depressor via the β-catenin-dependent pathway.

Specifying the role of LIN-44 in regulating sarcomere disassembly of the anal depressor.

LIN-44 has been identified as one of the Wnt ligands to regulate the sarcomere disassembly process (Figure 20E-20G). However, the specific signaling pathway that LIN-44 regulates was not well studied. *lin-44* is expressed from the tail hypodermal cells

during larval development (Figure 24G-24H). Previous studies show that LIN-44 controls the symmetrical cell division in the B lineage (Wu and Herman, 2006). Therefore, the LIN-44 morphogen gradient is high enough to reach the site of anal depressor and activate downstream signaling.

To identify if LIN-44 activates the Wnt-β-catenin pathway in the anal depressor, I will monitor the BAR-1 levels in the anal depressor in *lin-44(lf)* mutant males. To perform this assay, I will first introduce the transgene [P*bar-1*:*bar-1*::YFP; P*bar-1*:CFP] into *lin-44(lf)* mutants by microinjection. During L4 development, the tail hypodermal cells have migrated to the anal canal region, and therefore are immediately on top of the anal depressor. Therefore, it is highly possible that LIN-44 consolidates the effects of EGL-20, by upregulating the calcium levels in the anal depressor. To identify if LIN-44 activates the Wnt-calcium pathway in the anal depressor, I will introduce the transgene [P*aex-2*:GCaMP::SL2:::DsRed] into *lin-44(lf)* mutants, and monitor the calcium activity in the anal depressor of *lin-44(lf)* mutant males. If *lin-44* is tested to activate either the Wnt-canonical pathway, or the Wnt-calcium pathway, or both, I will introduce the transgene [*hsp-16*:*lin-44*::SL2:::DsRed] into *lin-44(lf)* mutants. The transgenic mutant males will undergoes heat shock treatment under different larval stages, to determine the timing of LIN-44 action.

Determine if the function of the Wnt-canonical pathway during early larvae serves as a prerequisite for the Wnt-calcium pathway activity during later stage

Although the relationship between the Wnt-canonical and Wnt-calcium pathway is antagonistic (Ishitani et al., 2003; Ishitani et al., 1999), the development of the male

anal depressor sequentially requires both pathways. The high defective anal depressor penetrance level in the calcium mutants (Figure 31C-31D) indicates that the Wnt-canonical and the Wnt-calcium pathway function in the same pathway. Therefore, it is possible that β-catenin activity in early larvae initiates gene transcription that is essential for the activation of the Wnt-calcium pathway during later development stage.

The Wnt-canonical and non-canonical pathways differ a lot regarding the downstream signaling proteins. However, the upstream ligands and receptors do share a common mechanism in their interactions (Grumolato et al., 2010). In mammals, certain Wnt ligands tend to activate a particular Wnt pathways: Wnt3A and Wnt8 activate the canonical pathway, whereas Wnt5A and Wnt11 activate the non-canonical pathway (Kawano and Kypta, 2003). But the specificity of the pathway being activated is determined by the co-receptors (Grumolato et al., 2010). It is possible that BAR-1 activates the transcription of the co-receptor that is essential for the subsequent Wnt-calcium pathway.

It is also possible that BAR-1 activates the transcription of the calcium-responsive proteases or phosphatase, which serve as the downstream effectors for Wnt-calcium pathway. *clp-6*/Calpain and *clp-3*/Calpain are activated specifically during L4 development. Therefore, I will clone the promoter of those genes, and compare their activity between wild type and *bar-1* mutant. I will observe the calcium dynamics in the L4 anal depressor of *bar-1* mutant to tell if BAR-1 activity is required to activate the calcium signaling.

Identify the signaling components downstream of LIN-44 and LIN-17 to regulate the symmetrical development of the anal depressor.

LIN-44 and LIN-17 are identified as the regulator of the symmetrical development of the anal depressor in both the males and the hermaphrodites. However, the downstream signaling effectors remain elusive. None of the Wnt-canonical or Wnt-calcium mutants that have been examined in my study display the same asymmetrical phenotype as *lin-44* or *lin-17*. *lin-44* and *lin-17* have been indicated to control the asymmetrical cell division within the B lineage via the Wnt PCP pathway (Wu and Herman, 2006). Therefore, I will examine mutants of the PCP pathway to determine if they have the same phenotype as *lin-44* and *lin-17*.

REFERENCES

Ai, D., Fu, X., Wang, J., Lu, M. F., Chen, L., Baldini, A., Klein, W. H., and Martin, J. F. (2007). Canonical Wnt signaling functions in second heart field to promote right ventricular growth. Proceedings of the National Academy of Sciences of the United States of America *104*, 9319-9324.

Akiri, G., Cherian, M. M., Vijayakumar, S., Liu, G., Bafico, A., and Aaronson, S. A. (2009). Wnt pathway aberrations including autocrine Wnt activation occur at high frequency in human non-small-cell lung carcinoma. Oncogene *28*, 2163-2172.

Allen, D. G., Lamb, G. D., and Westerblad, H. (2008). Skeletal muscle fatigue: Cellular mechanisms. Physiology Reviews *88*, 287-332.

Antebi, A., Norris, C.R., Hedgecock, E., Garriga, G. (1997). Cell and Growth Cone Migrations. In *C. elegans* II, D.L. Riddle, Blumenthal, T., Meyer, B.J., Priess, J.R., ed. (NY: Cold Spring Harbor).

Ault, K. T., Durmowicz, G., Galione, A., Harger, P. L., and Busa, W. B. (1996). Modulation of *Xenopus* embryo mesoderm-specific gene expression and dorsoanterior patterning by receptors that activate the phosphatidylinositol cycle signal transduction pathway. Development *122*, 2033-2041.

Bafico, A., Liu, G., Goldin, L., Harris, V., and Aaronson, S. A. (2004). An autocrine mechanism for constitutive Wnt pathway activation in human cancer cells. Cancer Cell *6*, 497-506.

Bargmann, C. I., and Avery, L. (1995). Laser killing of cells in *Caenorhabditis elegans*. Methods in Cell Biology *48*, 225-250.

Bassel-Duby, R., and Olson, E. N. (2006). Signaling pathways in skeletal muscle remodeling. Annual Review of Biochemistry *75*, 19-37.

Beg, A. A., and Jorgensen, E. M. (2003). EXP-1 is an excitatory GABA-gated cation channel. Nature Neuroscience *6*, 1145-1152.

Bersell, K., Arab, S., Haring, B., and Kuhn, B. (2009). Neuregulin1/ErbB4 signaling induces cardiomyocyte proliferation and repair of heart injury. Cell *138*, 257-270.

Bodine, S. C., Latres, E., Baumhueter, S., Lai, V. K., Nunez, L., Clarke, B. A., Poueymirou, W. T., Panaro, F. J., Na, E., Dharmarajan, K., *et al.* (2001). Identification of ubiquitin ligases required for skeletal muscle atrophy. Science *294*, 1704-1708.

Brand, T. (2003). Heart development: Molecular insights into cardiac specification and early morphogenesis. Developmental Biology *258*, 1-19.

Brenner, S. (1974). The genetics of *Caenorhabditis elegans*. Genetics *77*, 71-94.

Busa, W. B., and Gimlich, R. L. (1989). Lithium-induced teratogenesis in frog embryos prevented by a polyphosphoinositide cycle intermediate or a diacylglycerol analog. Developmental Biology *132*, 315-324.

Cai, C. L., Liang, X., Shi, Y., Chu, P. H., Pfaff, S. L., Chen, J., and Evans, S. (2003). Isl1 identifies a cardiac progenitor population that proliferates prior to differentiation and contributes a majority of cells to the heart. Developmental Cell *5*, 877-889.

Can, S., Zhu, Y. S., Cai, L. Q., Ling, Q., Katz, M. D., Akgun, S., Shackleton, C. H., and Imperato-McGinley, J. (1998). The identification of 5 alpha-reductase-2 and 17 beta-hydroxysteroid dehydrogenase-3 gene defects in male pseudohermaphrodites from a Turkish kindred. The Journal of Clinical Endocrinology and Metabolism *83*, 560-569.

Chalfie, M., Horvitz, H. R., and Sulston, J. E. (1981). Mutations that lead to reiterations in the cell lineages of *C. elegans*. Cell *24*, 59-69.

Chan, S. D., Karpf, D. B., Fowlkes, M. E., Hooks, M., Bradley, M. S., Vuong, V., Bambino, T., Liu, M. Y., Arnaud, C. D., Strewler, G. J., and et al. (1992). Two homologs of the Drosophila polarity gene frizzled (fz) are widely expressed in mammalian tissues. The Journal of Biological Chemistry *267*, 25202-25207.

Chen, X., and Rene Garcia, L. (2015). Developmental alterations of the *C. elegans* male anal depressor morphology and function require sex-specific cell autonomous and cell non-autonomous interactions. Developmental Biology *398*, 24-43.

Christian, J. L., Olson, D. J., and Moon, R. T. (1992). Xwnt-8 modifies the character of mesoderm induced by bFGF in isolated Xenopus ectoderm. The EMBO Journal *11*, 33-41.

Conradt, B., and Horvitz, H. R. (1999). The TRA-1A sex determination protein of *C. elegans* regulates sexually dimorphic cell deaths by repressing the egl-1 cell death activator gene. Cell *98*, 317-327.

Cook, D., Fry, M. J., Hughes, K., Sumathipala, R., Woodgett, J. R., and Dale, T. C. (1996). Wingless inactivates glycogen synthase kinase-3 via an intracellular signalling pathway which involves a protein kinase C. The EMBO Journal *15*, 4526-4536.

Cooke, J., Symes, K., and Smith, E. J. (1989). Potentiation by the lithium ion of morphogenetic responses to a *Xenopus* inducing factor. Development *105*, 549-558.

Correa, P., LeBoeuf, B., and Garcia, L. R. (2012). *C. elegans* dopaminergic D2-like receptors delimit recurrent cholinergic-mediated motor programs during a goal-oriented behavior. PLoS Genetics *8*, e1003015.

Correa, P. A., Gruninger, T., and Garcia, L. R. (2015). DOP-2 D2-Like Receptor Regulates UNC-7 Innexins to Attenuate Recurrent Sensory Motor Neurons during *C. elegans* Copulation. Journal of Neuroscience *35*, 9990-10004.

Cowing, D. W., and Kenyon, C. (1992). Expression of the homeotic gene *mab-5* during *Caenorhabditis elegans* embryogenesis. Development *116*, 481-490.

de Bono, M., Zarkower, D., and Hodgkin, J. (1995). Dominant feminizing mutations implicate protein-protein interactions as the main mode of regulation of the nematode sex-determining gene *tra-1*. Genes & Development *9*, 155-167.

Dirksen, R. T. (2009). Sarcoplasmic reticulum-mitochondrial through-space coupling in skeletal muscle. Applied Physiology and Nutrition Metabolism *34*, 389-395.

Duchen, M. R. (1999). Contributions of mitochondria to animal physiology: From homeostatic sensor to calcium signalling and cell death. The Journal of Physiology *516 (Pt 1)*, 1-17.

Eddy, E. M., Washburn, T. F., Bunch, D. O., Goulding, E. H., Gladen, B. C., Lubahn, D. B., and Korach, K. S. (1996). Targeted disruption of the estrogen receptor gene in male mice causes alteration of spermatogenesis and infertility. Endocrinology *137*, 4796-4805.

Edwards, S. L., Charlie, N. K., Milfort, M. C., Brown, B. S., Gravlin, C. N., Knecht, J. E., and Miller, K. G. (2008). A novel molecular solution for ultraviolet light detection in Caenorhabditis elegans. PLoS Biology *6*, e198.

Eisenmann, D. M., Maloof, J. N., Simske, J. S., Kenyon, C., and Kim, S. K. (1998). The beta-catenin homolog BAR-1 and LET-60 Ras coordinately regulate the Hox gene *lin-39* during *Caenorhabditis elegans* vulval development. Development *125*, 3667-3680.

Frasch, M. (1995). Induction of visceral and cardiac mesoderm by ectodermal Dpp in the early Drosophila embryo. Nature *374*, 464-467.

Garcia-Martinez, V., and Schoenwolf, G. C. (1993). Primitive-streak origin of the cardiovascular system in avian embryos. Developmental Biology *159*, 706-719.

Garcia, L. R., Mehta, P., and Sternberg, P. W. (2001). Regulation of distinct muscle behaviors controls the *C. elegans* male's copulatory spicules during mating. Cell *107*, 777-788.

Gassmann, M., Casagranda, F., Orioli, D., Simon, H., Lai, C., Klein, R., and Lemke, G. (1995). Aberrant neural and cardiac development in mice lacking the ErbB4 neuregulin receptor. Nature *378*, 390-394.

Gleason, J. E., Korswagen, H. C., and Eisenmann, D. M. (2002). Activation of Wnt signaling bypasses the requirement for RTK/Ras signaling during *C. elegans* vulval induction. Genes & Development *16*, 1281-1290.

Grumolato, L., Liu, G., Mong, P., Mudbhary, R., Biswas, R., Arroyave, R., Vijayakumar, S., Economides, A. N., and Aaronson, S. A. (2010). Canonical and noncanonical Wnts use a common mechanism to activate completely unrelated coreceptors. Genes & Development *24*, 2517-2530.

Gruninger, T. R., Gualberto, D. G., LeBoeuf, B., and Garcia, L. R. (2006). Integration of male mating and feeding behaviors in *Caenorhabditis elegans*. Journal of Neuroscience *26*, 169-179.

Guo, X., Navetta, A., Gualberto, D. G., and Garcia, L. R. (2012). Behavioral decay in aging male *C. elegans* correlates with increased cell excitability. Neurobiology of Aging *33*, 1483 e1485-1423.

Harfe, B. D., Vaz Gomes, A., Kenyon, C., Liu, J., Krause, M., and Fire, A. (1998). Analysis of a *Caenorhabditis elegans* Twist homolog identifies conserved and divergent aspects of mesodermal patterning. Genes & Development *12*, 2623-2635.

Hedgecock, E. M., Culotti, J. G., Hall, D. H., and Stern, B. D. (1987). Genetics of cell and axon migrations in *Caenorhabditis elegans*. Development *100*, 365-382.

Heisenberg, C. P., Tada, M., Rauch, G. J., Saude, L., Concha, M. L., Geisler, R., Stemple, D. L., Smith, J. C., and Wilson, S. W. (2000). Silberblick/Wnt11 mediates convergent extension movements during zebrafish gastrulation. Nature *405*, 76-81.

Herman, M. A., Vassilieva, L. L., Horvitz, H. R., Shaw, J. E., and Herman, R. K. (1995). The *C. elegans* gene *lin-44*, which controls the polarity of certain asymmetric cell divisions, encodes a Wnt protein and acts cell nonautonomously. Cell *83*, 101-110.

Hodgkin, J. (1987). Primary sex determination in the nematode *C. elegans*. Development *101 Suppl*, 5-16.

Hodgkin, J. (1988). Sex determination. Right gene, wrong chromosome. Nature *336*, 712.

Hodgkin, J., Horvitz, H. R., and Brenner, S. (1979). Nondisjunction Mutants of the Nematode *Caenorhabditis elegans*. Genetics *91*, 67-94.

Hogan, P. G., Chen, L., Nardone, J., and Rao, A. (2003). Transcriptional regulation by calcium, calcineurin, and NFAT. Genes & Development *17*, 2205-2232.

Huang, J., and Forsberg, N. E. (1998). Role of calpain in skeletal-muscle protein degradation. Proceedings of the National Academy of Sciences of the United States of America *95*, 12100-12105.

Huang, T., Xie, Z., Wang, J., Li, M., Jing, N., and Li, L. (2011). Nuclear factor of activated T cells (NFAT) proteins repress canonical Wnt signaling via its interaction with Dishevelled (Dvl) protein and participate in regulating neural progenitor cell proliferation and differentiation. The Journal of Biological Chemistry *286*, 37399-37405.

Hunter, C. P., Harris, J. M., Maloof, J. N., and Kenyon, C. (1999). Hox gene expression in a single *Caenorhabditis elegans* cell is regulated by a caudal homolog and intercellular signals that inhibit Wnt signaling. Development *126*, 805-814.

Hunter, C. P., and Wood, W. B. (1990). The *tra-1* gene determines sexual phenotype cell-autonomously in *C. elegans*. Cell *63*, 1193-1204.

Hunter, C. P., and Wood, W. B. (1992). Evidence from mosaic analysis of the masculinizing gene her-1 for cell interactions in *C. elegans* sex determination. Nature *355*, 551-555.

Imbeaud, S., Belville, C., Messika-Zeitoun, L., Rey, R., di Clemente, N., Josso, N., and Picard, J. Y. (1996). A 27 base-pair deletion of the anti-mullerian type II receptor gene is the most common cause of the persistent mullerian duct syndrome. Human Molecular Genetics *5*, 1269-1277.

Inoue, T., Oz, H. S., Wiland, D., Gharib, S., Deshpande, R., Hill, R. J., Katz, W. S., and Sternberg, P. W. (2004). *C. elegans* LIN-18 is a Ryk ortholog and functions in parallel to LIN-17/Frizzled in Wnt signaling. Cell *118*, 795-806.

Ishitani, T., Kishida, S., Hyodo-Miura, J., Ueno, N., Yasuda, J., Waterman, M., Shibuya, H., Moon, R. T., Ninomiya-Tsuji, J., and Matsumoto, K. (2003). The TAK1-NLK mitogen-activated protein kinase cascade functions in the Wnt-5a/Ca(2+) pathway to antagonize Wnt/beta-catenin signaling. Molecular and Cellular Biology *23*, 131-139.

Ishitani, T., Ninomiya-Tsuji, J., Nagai, S., Nishita, M., Meneghini, M., Barker, N., Waterman, M., Bowerman, B., Clevers, H., Shibuya, H., and Matsumoto, K. (1999). The TAK1-NLK-MAPK-related pathway antagonizes signalling between beta-catenin and transcription factor TCF. Nature *399*, 798-802.

Jansen, G., Thijssen, K. L., Werner, P., van der Horst, M., Hazendonk, E., and Plasterk, R. H. (1999). The complete family of genes encoding G proteins of Caenorhabditis elegans. Nature Genetics *21*, 414-419.

Jarrell, T. A., Wang, Y., Bloniarz, A. E., Brittin, C. A., Xu, M., Thomson, J. N., Albertson, D. G., Hall, D. H., and Emmons, S. W. (2012). The connectome of a decision-making neural network. Science *337*, 437-444.

Jones, S. E., and Jomary, C. (2002). Secreted Frizzled-related proteins: Searching for relationships and patterns. Bioessays *24*, 811-820.

Jopling, C., Sleep, E., Raya, M., Marti, M., Raya, A., and Izpisua Belmonte, J. C. (2010). Zebrafish heart regeneration occurs by cardiomyocyte dedifferentiation and proliferation. Nature *464*, 606-609.

Kamath, R. S., Martinez-Campos, M., Zipperlen, P., Fraser, A. G., and Ahringer, J. (2001). Effectiveness of specific RNA-mediated interference through ingested double-stranded RNA in Caenorhabditis elegans. Genome Biology *2*, RESEARCH0002.

Katanaev, V. L., Ponzielli, R., Semeriva, M., and Tomlinson, A. (2005). Trimeric G protein-dependent frizzled signaling in Drosophila. Cell *120*, 111-122.

Kawano, Y., and Kypta, R. (2003). Secreted antagonists of the Wnt signalling pathway. Journal of Cell Science *116*, 2627-2634.

Kenyon, C. (1986). A gene involved in the development of the posterior body region of *C. elegans*. Cell *46*, 477-487.

Khorchid, A., and Ikura, M. (2002). How calpain is activated by calcium. Nature Structural Biology *9*, 239-241.

Kim, E., Sun, L., Gabel, C. V., and Fang-Yen, C. (2013). Long-term imaging of *Caenorhabditis elegans* using nanoparticle-mediated immobilization. PLoS One *8*, e53419.

Klein, P. S., and Melton, D. A. (1996). A molecular mechanism for the effect of lithium on development. Proceedings of the National Academy of Sciences of the United States of America *93*, 8455-8459.

Kohn, A. D., and Moon, R. T. (2005). Wnt and calcium signaling: Beta-catenin-independent pathways. Cell Calcium *38*, 439-446.

Komiya, Y., and Habas, R. (2008). Wnt signal transduction pathways. Organogenesis *4*, 68-75.

Koopman, P., Gubbay, J., Vivian, N., Goodfellow, P., and Lovell-Badge, R. (1991). Male development of chromosomally female mice transgenic for Sry. Nature *351*, 117-121.

Korswagen, H. C., Herman, M. A., and Clevers, H. C. (2000). Distinct beta-catenins mediate adhesion and signalling functions in *C. elegans*. Nature *406*, 527-532.

Kuhl, M., Sheldahl, L. C., Malbon, C. C., and Moon, R. T. (2000). Ca(2+)/calmodulin-dependent protein kinase II is stimulated by Wnt and Frizzled homologs and promotes ventral cell fates in *Xenopus*. The Journal of Biological Chemistry *275*, 12701-12711.

Kuwabara, P. E. (1996). A novel regulatory mutation in the *C. elegans* sex determination gene *tra-2* defines a candidate ligand/receptor interaction site. Development *122*, 2089-2098.

Kuwabara, P. E., and Kimble, J. (1995). A predicted membrane protein, TRA-2A, directs hermaphrodite development in *Caenorhabditis elegans*. Development *121*, 2995-3004.

Kwon, C., Arnold, J., Hsiao, E. C., Taketo, M. M., Conklin, B. R., and Srivastava, D. (2007). Canonical Wnt signaling is a positive regulator of mammalian cardiac progenitors. Proceedings of the National Academy of Sciences of the United States of America *104*, 10894-10899.

Laugwitz, K. L., Moretti, A., Lam, J., Gruber, P., Chen, Y., Woodard, S., Lin, L. Z., Cai, C. L., Lu, M. M., Reth, M., *et al.* (2005). Postnatal isl1+ cardioblasts enter fully differentiated cardiomyocyte lineages. Nature *433*, 647-653.

LeBoeuf, B., Correa, P., Jee, C., and Garcia, L. R. (2014). *Caenorhabditis elegans* male sensory-motor neurons and dopaminergic support cells couple ejaculation and post-ejaculatory behaviors. Elife *3*.

LeBoeuf, B., Gruninger, T. R., and Garcia, L. R. (2007). Food deprivation attenuates seizures through CaMKII and EAG K+ channels. PLoS Genetics *3*, 1622-1632.

LeBoeuf, B., Guo, X., and Garcia, L. R. (2011). The effects of transient starvation persist through direct interactions between CaMKII and ether-a-go-go K+ channels in *C. elegans* males. Neuroscience *175*, 1-17.

Lee, K., and Portman, D. S. (2007). Neural sex modifies the function of a *C. elegans* sensory circuit. Current Biology *17*, 1858-1863.

Lee, K. F., Simon, H., Chen, H., Bates, B., Hung, M. C., and Hauser, C. (1995). Requirement for neuregulin receptor erbB2 in neural and cardiac development. Nature *378*, 394-398.

Lepilina, A., Coon, A. N., Kikuchi, K., Holdway, J. E., Roberts, R. W., Burns, C. G., and Poss, K. D. (2006). A dynamic epicardial injury response supports progenitor cell activity during zebrafish heart regeneration. Cell *127*, 607-619.

Lickert, H., Kutsch, S., Kanzler, B., Tamai, Y., Taketo, M. M., and Kemler, R. (2002). Formation of multiple hearts in mice following deletion of beta-catenin in the embryonic endoderm. Developmental Cell *3*, 171-181.

Lim, X., Tan, S. H., Koh, W. L., Chau, R. M., Yan, K. S., Kuo, C. J., van Amerongen, R., Klein, A. M., and Nusse, R. (2013). Interfollicular epidermal stem cells self-renew via autocrine Wnt signaling. Science *342*, 1226-1230.

Lin, L., Cui, L., Zhou, W., Dufort, D., Zhang, X., Cai, C. L., Bu, L., Yang, L., Martin, J., Kemler, R., *et al.* (2007). Beta-catenin directly regulates Islet1 expression in cardiovascular progenitors and is required for multiple aspects of cardiogenesis. Proceedings of the National Academy of Sciences of the United States of America *104*, 9313-9318.

Lin, R., Hill, R. J., and Priess, J. R. (1998). POP-1 and anterior-posterior fate decisions in *C. elegans* embryos. Cell *92*, 229-239.

Lin, R., Thompson, S., and Priess, J. R. (1995). *pop-1* encodes an HMG box protein required for the specification of a mesoderm precursor in early *C. elegans* embryos. Cell *83*, 599-609.

Liu, K. S., and Sternberg, P. W. (1995). Sensory regulation of male mating behavior in *Caenorhabditis elegans*. Neuron *14*, 79-89.

Liu, Y., LeBeouf, B., Guo, X., Correa, P. A., Gualberto, D. G., Lints, R., and Garcia, L. R. (2011). A cholinergic-regulated circuit coordinates the maintenance and bi-stable states of a sensory-motor behavior during *Caenorhabditis elegans* male copulation. PLoS Genetics *7*, e1001326.

Liu, Y., LeBoeuf, B., and Garcia, L. R. (2007). G alpha(q)-coupled muscarinic acetylcholine receptors enhance nicotinic acetylcholine receptor signaling in *Caenorhabditis elegans* mating behavior. Journal of Neuroscience *27*, 1411-1421.

Logan, C. Y., and Nusse, R. (2004). The Wnt signaling pathway in development and disease. Annual Review of Cell and Developmental Biology *20*, 781-810.

Lum, D. H., Kuwabara, P. E., Zarkower, D., and Spence, A. M. (2000). Direct protein-protein interaction between the intracellular domain of TRA-2 and the transcription factor TRA-1A modulates feminizing activity in *C. elegans*. Genes & Development *14*, 3153-3165.

Luo, J. H., and Weinstein, I. B. (1993). Calcium-dependent activation of protein kinase C. The role of the C2 domain in divalent cation selectivity. The Journal of Biological Chemistry *268*, 23580-23584.

MacDonald, B. T., Tamai, K., and He, X. (2009). Wnt/beta-catenin signaling: Components, mechanisms, and diseases. Developmental Cell *17*, 9-26.

Maloof, J. N., Whangbo, J., Harris, J. M., Jongeward, G. D., and Kenyon, C. (1999). A Wnt signaling pathway controls hox gene expression and neuroblast migration in *C. elegans*. Development *126*, 37-49.

Marvin, M. J., Di Rocco, G., Gardiner, A., Bush, S. M., and Lassar, A. B. (2001). Inhibition of Wnt activity induces heart formation from posterior mesoderm. Genes & Development *15*, 316-327.

Mason, D. A., Rabinowitz, J. S., and Portman, D. S. (2008). *dmd-3*, a doublesex-related gene regulated by *tra-1*, governs sex-specific morphogenesis in *C. elegans*. Development *135*, 2373-2382.

Mattila, P. K., and Lappalainen, P. (2008). Filopodia: Molecular architecture and cellular functions. Nature Review Molecular Cell Biology *9*, 446-454.

McIntire, S. L., Jorgensen, E., and Horvitz, H. R. (1993a). Genes required for GABA function in *Caenorhabditis elegans*. Nature *364*, 334-337.

McIntire, S. L., Jorgensen, E., Kaplan, J., and Horvitz, H. R. (1993b). The GABAergic nervous system of *Caenorhabditis elegans*. Nature *364*, 337-341.

Mehra, A., Gaudet, J., Heck, L., Kuwabara, P. E., and Spence, A. M. (1999). Negative regulation of male development in *Caenorhabditis elegans* by a protein-protein interaction between TRA-2A and FEM-3. Genes & Development *13*, 1453-1463.

Mello, C. C., Kramer, J. M., Stinchcomb, D., and Ambros, V. (1991). Efficient gene transfer in *C.elegans*: Extrachromosomal maintenance and integration of transforming sequences. EMBO Journal *10*, 3959-3970.

Melzer, W., Herrmann-Frank, A., and Luttgau, H. C. (1995). The role of Ca^{2+} ions in excitation-contraction coupling of skeletal muscle fibres. Biochimica et Biophysica Acta *1241*, 59-116.

Mikels, A. J., and Nusse, R. (2006). Wnts as ligands: Processing, secretion and reception. Oncogene *25*, 7461-7468.

Monzen, K., Shiojima, I., Hiroi, Y., Kudoh, S., Oka, T., Takimoto, E., Hayashi, D., Hosoda, T., Habara-Ohkubo, A., Nakaoka, T.*, et al.* (1999). Bone morphogenetic proteins induce cardiomyocyte differentiation through the mitogen-activated protein kinase kinase kinase TAK1 and cardiac transcription factors Csx/Nkx-2.5 and GATA-4. Molecular and Cellular Biology *19*, 7096-7105.

Moon, R. T., Kohn, A. D., De Ferrari, G. V., and Kaykas, A. (2004). WNT and beta-catenin signalling: Diseases and therapies. Nature Review Genetics *5*, 691-701.

Moretti, A., Caron, L., Nakano, A., Lam, J. T., Bernshausen, A., Chen, Y., Qyang, Y., Bu, L., Sasaki, M., Martin-Puig, S.*, et al.* (2006). Multipotent embryonic isl1+ progenitor cells lead to cardiac, smooth muscle, and endothelial cell diversification. Cell *127*, 1151-1165.

Mowrey, W. R., Bennett, J. R., and Portman, D. S. (2014). Distributed effects of biological sex define sex-typical motor behavior in *Caenorhabditis elegans*. Journal of Neuroscience *34*, 1579-1591.

Naito, A. T., Shiojima, I., Akazawa, H., Hidaka, K., Morisaki, T., Kikuchi, A., and Komuro, I. (2006). Developmental stage-specific biphasic roles of Wnt/beta-catenin signaling in cardiomyogenesis and hematopoiesis. Proceedings of the National Academy of Sciences of the United States of America *103*, 19812-19817.

Nguyen, C. Q., Hall, D. H., Yang, Y., and Fitch, D. H. (1999). Morphogenesis of the *Caenorhabditis elegans* male tail tip. Developmental Biology *207*, 86-106.

Niehrs, C. (2012). The complex world of WNT receptor signalling. Nature Reviews Molecular Cell Biology *13*, 767-779.

Pan, C. L., Howell, J. E., Clark, S. G., Hilliard, M., Cordes, S., Bargmann, C. I., and Garriga, G. (2006). Multiple Wnts and frizzled receptors regulate anteriorly directed cell and growth cone migrations in *Caenorhabditis elegans*. Developmental Cell *10*, 367-377.

Pandur, P., Lasche, M., Eisenberg, L. M., and Kuhl, M. (2002). Wnt-11 activation of a non-canonical Wnt signalling pathway is required for cardiogenesis. Nature *418*, 636-641.

Peden, E., Kimberly, E., Gengyo-Ando, K., Mitani, S., and Xue, D. (2007). Control of sex-specific apoptosis in *C. elegans* by the BarH homeodomain protein CEH-30 and the transcriptional repressor UNC-37/Groucho. Genes & Development *21*, 3195-3207.

Perry, M. D., Li, W., Trent, C., Robertson, B., Fire, A., Hageman, J. M., and Wood, W. B. (1993). Molecular characterization of the *her-1* gene suggests a direct role in cell signaling during *Caenorhabditis elegans* sex determination. Genes & Development *7*, 216-228.

Qyang, Y., Martin-Puig, S., Chiravuri, M., Chen, S., Xu, H., Bu, L., Jiang, X., Lin, L., Granger, A., Moretti, A.*, et al.* (2007). The renewal and differentiation of Isl1+ cardiovascular progenitors are controlled by a Wnt/beta-catenin pathway. Cell Stem Cell *1*, 165-179.

Raya, A., Koth, C. M., Buscher, D., Kawakami, Y., Itoh, T., Raya, R. M., Sternik, G., Tsai, H. J., Rodriguez-Esteban, C., and Izpisua-Belmonte, J. C. (2003). Activation of Notch signaling pathway precedes heart regeneration in zebrafish. Proceedings of the National Academy of Sciences of the United States of America *100 Suppl 1*, 11889-11895.

Reiner, D. J., and Thomas, J. H. (1995). Reversal of a muscle response to GABA during *C. elegans* male development. Journal of Neuroscience *15*, 6094-6102.

Reiner, D. J., Weinshenker, D., Tian, H., Thomas, J. H., Nishiwaki, K., Miwa, J., Gruninger, T., Leboeuf, B., and Garcia, L. R. (2006). Behavioral genetics of *Caenorhabditis elegans* unc-103-encoded erg-like K(+) channel. Journal of Neurogenetics *20*, 41-66.

Rocheleau, C. E., Downs, W. D., Lin, R., Wittmann, C., Bei, Y., Cha, Y. H., Ali, M., Priess, J. R., and Mello, C. C. (1997). Wnt signaling and an APC-related gene specify endoderm in early *C. elegans* embryos. Cell *90*, 707-716.

Rocheleau, C. E., Yasuda, J., Shin, T. H., Lin, R., Sawa, H., Okano, H., Priess, J. R., Davis, R. J., and Mello, C. C. (1999). WRM-1 activates the LIT-1 protein kinase to transduce anterior/posterior polarity signals in *C. elegans*. Cell *97*, 717-726.

Ross, J. M., Kalis, A. K., Murphy, M. W., and Zarkower, D. (2005). The DM domain protein MAB-3 promotes sex-specific neurogenesis in *C. elegans* by regulating bHLH proteins. Developmental Cell *8*, 881-892.

Salser, S. J., and Kenyon, C. (1996). A *C. elegans* Hox gene switches on, off, on and off again to regulate proliferation, differentiation and morphogenesis. Development *122*, 1651-1661.

Salser, S. J., Loer, C. M., and Kenyon, C. (1993). Multiple HOM-C gene interactions specify cell fates in the nematode central nervous system. Genes & Development *7*, 1714-1724.

Schlesinger, A., Shelton, C. A., Maloof, J. N., Meneghini, M., and Bowerman, B. (1999). Wnt pathway components orient a mitotic spindle in the early *Caenorhabditis elegans* embryo without requiring gene transcription in the responding cell. Genes & Development *13*, 2028-2038.

Schnabel, H., and Schnabel, R. (1990). An Organ-Specific Differentiation Gene, *pha-1*, from *Caenorhabditis elegans*. Science *250*, 686-688.

Schneider, V. A., and Mercola, M. (2001). Wnt antagonism initiates cardiogenesis in *Xenopus* laevis. Genes & Development *15*, 304-315.

Schultheiss, T. M., Burch, J. B., and Lassar, A. B. (1997). A role for bone morphogenetic proteins in the induction of cardiac myogenesis. Genes & Development *11*, 451-462.

Schultheiss, T. M., Xydas, S., and Lassar, A. B. (1995). Induction of avian cardiac myogenesis by anterior endoderm. Development *121*, 4203-4214.

Schwartz, H. T., and Horvitz, H. R. (2007). The *C. elegans* protein CEH-30 protects male-specific neurons from apoptosis independently of the Bcl-2 homolog CED-9. Genes & Development *21*, 3181-3194.

Seetharaman, A., Selman, G., Puckrin, R., Barbier, L., Wong, E., D'Souza, S. A., and Roy, P. J. (2011). MADD-4 is a secreted cue required for midline-oriented guidance in *Caenorhabditis elegans*. Developmental Cell *21*, 669-680.

Sheldahl, L. C., Park, M., Malbon, C. C., and Moon, R. T. (1999). Protein kinase C is differentially stimulated by Wnt and Frizzled homologs in a G-protein-dependent manner. Current Biology : CB *9*, 695-698.

Shin, T. H., Yasuda, J., Rocheleau, C. E., Lin, R., Soto, M., Bei, Y., Davis, R. J., and Mello, C. C. (1999). MOM-4, a MAP kinase kinase kinase-related protein, activates WRM-1/LIT-1 kinase to transduce anterior/posterior polarity signals in *C. elegans*. Molecular Cell *4*, 275-280.

Slack, J. M., Isaacs, H. V., and Darlington, B. G. (1988). Inductive effects of fibroblast growth factor and lithium ion on *Xenopus* blastula ectoderm. Development *103*, 581-590.

Slusarski, D. C., Corces, V. G., and Moon, R. T. (1997a). Interaction of Wnt and a Frizzled homologue triggers G-protein-linked phosphatidylinositol signalling. Nature *390*, 410-413.

Slusarski, D. C., Yang-Snyder, J., Busa, W. B., and Moon, R. T. (1997b). Modulation of embryonic intracellular Ca^{2+} signaling by Wnt-5A. Developmental Biology *182*, 114-120.

Srivastava, D., Cserjesi, P., and Olson, E. N. (1995). A subclass of bHLH proteins required for cardiac morphogenesis. Science *270*, 1995-1999.

Srivastava, D., Thomas, T., Lin, Q., Kirby, M. L., Brown, D., and Olson, E. N. (1997). Regulation of cardiac mesodermal and neural crest development by the bHLH transcription factor, dHAND. Nature Genetics *16*, 154-160.

Sternberg, P. W., and Horvitz, H. R. (1986). Pattern formation during vulval development in *C. elegans*. Cell *44*, 761-772.

Sulston, J. E., Albertson, D. G., and Thomson, J. N. (1980a). The *Caenorhabditis elegans* male: Postembryonic development of nongonadal structures. Developmental Biology *78*, 542-576.

Sulston, J. E., Albertson, D. G., and Thomson, J. N. (1980b). The *Caenorhabditis elegans* male: Postembryonic development of nongonadal structures. Developmental Biology *78*, 542-576.

Sulston, J. E., and Horvitz, H. R. (1977). Post-embryonic cell lineages of the nematode, *Caenorhabditis elegans*. Developmental Biology *56*, 110-156.

Sulston, J. E., Schierenberg, E., White, J. G., and Thomson, J. N. (1983). The embryonic cell lineage of the nematode *Caenorhabditis elegans*. Developmental Biology *100*, 64-119.

Sulston, J. E., and White, J. G. (1980). Regulation and cell autonomy during postembryonic development of *Caenorhabditis elegans*. Developmental Biology *78*, 577-597.

Takeuchi, J. K., Ohgi, M., Koshiba-Takeuchi, K., Shiratori, H., Sakaki, I., Ogura, K., Saijoh, Y., and Ogura, T. (2003). Tbx5 specifies the left/right ventricles and ventricular septum position during cardiogenesis. Development *130*, 5953-5964.

Tam, P. P., Parameswaran, M., Kinder, S. J., and Weinberger, R. P. (1997). The allocation of epiblast cells to the embryonic heart and other mesodermal lineages: The role of ingression and tissue movement during gastrulation. Development *124*, 1631-1642.

Thomas, J. H. (1990). Genetic analysis of defecation in *Caenorhabditis elegans*. Genetics *124*, 855-872.

Ueno, S., Weidinger, G., Osugi, T., Kohn, A. D., Golob, J. L., Pabon, L., Reinecke, H., Moon, R. T., and Murry, C. E. (2007). Biphasic role for Wnt/beta-catenin signaling in cardiac specification in zebrafish and embryonic stem cells. Proceedings of the National Academy of Sciences of the United States of America *104*, 9685-9690.

Waldo, K. L., Kumiski, D. H., Wallis, K. T., Stadt, H. A., Hutson, M. R., Platt, D. H., and Kirby, M. L. (2001). Conotruncal myocardium arises from a secondary heart field. Development *128*, 3179-3188.

Wang, Y., Macke, J. P., Abella, B. S., Andreasson, K., Worley, P., Gilbert, D. J., Copeland, N. G., Jenkins, N. A., and Nathans, J. (1996). A large family of putative transmembrane receptors homologous to the product of the Drosophila tissue polarity gene frizzled. The Journal of Biological Chemistry *271*, 4468-4476.

Whangbo, J., and Kenyon, C. (1999). A Wnt signaling system that specifies two patterns of cell migration in *C. elegans*. Molecular Cell *4*, 851-858.

White, J. Q., and Jorgensen, E. M. (2012). Sensation in a single neuron pair represses male behavior in hermaphrodites. Neuron *75*, 593-600.

White, J. Q., Nicholas, T. J., Gritton, J., Truong, L., Davidson, E. R., and Jorgensen, E. M. (2007). The sensory circuitry for sexual attraction in *C. elegans* males. Current Biology *17*, 1847-1857.

Wu, D., Katz, A., and Simon, M. I. (1993). Activation of phospholipase C beta 2 by the alpha and beta gamma subunits of trimeric GTP-binding protein. Proceedings of the National Academy of Sciences of the United States of America *90*, 5297-5301.

Wu, M., and Herman, M. A. (2006). A novel noncanonical Wnt pathway is involved in the regulation of the asymmetric B cell division in *C. elegans*. Developmental Biology *293*, 316-329.

Yamagishi, H., Yamagishi, C., Nakagawa, O., Harvey, R. P., Olson, E. N., and Srivastava, D. (2001). The combinatorial activities of Nkx2.5 and dHAND are essential for cardiac ventricle formation. Developmental Biology *239*, 190-203.

Yi, W., Ross, J. M., and Zarkower, D. (2000). Mab-3 is a direct *tra-1* target gene regulating diverse aspects of *C. elegans* male sexual development and behavior. Development *127*, 4469-4480.

Zhang, H., and Bradley, A. (1996). Mice deficient for BMP2 are nonviable and have defects in amnion/chorion and cardiac development. Development *122*, 2977-2986.

APPENDIX A

Supplementary Tables

Supplementary Table 1. SNP mapping to identify the locus of the mutation that is responsible for *rg441* phenotype.

	rg441			Wild type		
	N2	CB	het	N2	CB	het
LGI Center K04F10	15/16 93.75%	1/16 6.25%	0/16 0	13/14 92.86%	0/14 0	1/14 7.14%
LGII Center F45E12	5/16 31.25%	3/16 18.75%	8/16 50%	4/12 33.33%	5/12 41.67%	3/12 25%
LGIII Center R13F6	9/16 56.25%	5/16 31.25%	2/16 12.5%	6/14 42.86%	4/14 28.57%	4/14 28.57%
LGIV Center D2096	8/16 50%	5/16 31.25%	3/16 18.75%	5/14 35.71%	5/14 35.71%	4/14 28.57%
LGV Left end F36F12	16/16 100%	0/16 0	0/16 0	0/14 0	14/14 100%	0/14 0

Supplementary Table 1. Continued

	rg441			Wild type		
	N2	CB	het	N2	CB	het
LGX Left end F53A9	7/16 43.75%	6/16 37.5%	3/16 18.75%	5/14 35.71%	5/14 35.71%	4/14 28.57%